



PHD

Moisture Buffering Capacity of Unfired Clay Masonry

Mcgregor, Fionn

Award date:
2014

Awarding institution:
University of Bath

[Link to publication](#)

Alternative formats

If you require this document in an alternative format, please contact:
openaccess@bath.ac.uk

Copyright of this thesis rests with the author. Access is subject to the above licence, if given. If no licence is specified above, original content in this thesis is licensed under the terms of the Creative Commons Attribution-NonCommercial 4.0 International (CC BY-NC-ND 4.0) Licence (<https://creativecommons.org/licenses/by-nc-nd/4.0/>). Any third-party copyright material present remains the property of its respective owner(s) and is licensed under its existing terms.

Take down policy

If you consider content within Bath's Research Portal to be in breach of UK law, please contact: openaccess@bath.ac.uk with the details. Your claim will be investigated and, where appropriate, the item will be removed from public view as soon as possible.

Moisture buffering capacity of unfired clay masonry

A thesis submitted by

FIONN ALISTER PHILIPP MCGREGOR

for the degree of

Doctor of Philosophy

University of Bath

Department of Architecture and Civil Engineering

October 2014

COPYRIGHT

Attention is drawn to the fact that copyright of this thesis rests with the author. A copy of this thesis has been supplied on conditions that anyone who consults it is understood to recognise that its copyright rests with the author and that they must not copy it or use material from it except as permitted by law or with the consent of the author.

This thesis may be made available for consultation within the University Library and may be photocopied or lent to other libraries for the purposes of consultation with effect from November 2014.

Signed on behalf of the Faculty of:.....



In memory of Enrico Fodde who was the second supervisor of this PhD project until he passed away on the 29th of October 2013.

Acknowledgements

First of all I would like to recognise the incredible work environment that the University of Bath provides. I'm thankful to the University for they have financially supported this work and for the general service and environment that a PhD student can profit from. Equally the Department of Architecture and Civil Engineering has incredibly efficient and competent staff.

I would specially like to thank my supervisors Andrew Heath, Enrico Fodde and Andy Shea who have shown a great support during these three years. I'm also grateful to Pete Walker who has brought support and advice to the project. I would specially like to dedicate this work to Enrico Fodde who passed away on the 29th of October 2013.

These three years have been an amazing experience on the professional side and also on the social side. A great support came from my fellow PhD students in particular Dragos Naicu, Manuel Nuno and Daniel Brandon. However, I would like to thank all my office colleagues as without them I would not have been able to find the motivation and who also provided some incredible source of information, skills and fun.

I'm grateful to Samuel Dubois and Mariana Palumbo who I've met during my study and with who a collaboration was made. I'm grateful to people I've met interested in earth construction with who I could have some enriching conversation, notably Pierre-Antoine Chabriac and Jean-Claude Morel from the ENTPE in France, Paul Jaquin, Michael Lawrence and Daniel Maskell from EBUK in the UK and Marc Goldman from the University of New Mexico/Taos.

Finally, I'm most over all grateful to my life partner, Virginie, for her constant support and for accepting the challenge to live in the UK for three years. Our son, Oscar, who was born five days after I submitted this thesis was my main source of motivation to finish in time and has been since a source of pride.

Abstract

Earth building materials or unfired clay masonry have a strong potential to regulate indoor humidity variations. This was identified through observations of historical buildings where earth was used as a major building material. A stable relative humidity provides many benefits such as a healthier environment for the occupants, a reduced surface condensation or a reduced energy consumption for air conditioning systems.

Building physicists have started to bring attention to this phenomenon called moisture buffering where the building envelope plays a major role in the moisture balance of the building. Yet only a limited amount of research has been done on one of the most promising materials in terms of moisture buffering performance.

This study aimed to characterise the moisture buffering capacity of unfired clay masonry. Steady-state and dynamic hygric properties of 146 samples were measured. A selection of soils were selected to represent the high variability of these building materials and to determine the influence of composition and material properties on moisture buffering.

The moisture buffering test protocol used was primarily based on the Nordtest project yet the influence of boundary conditions and test protocol was investigated to obtain reliable dynamic results. This showed that results from different boundary conditions could be compared as they remained proportional. The surface film resistance showed to have a significant influence. Additional investigations were made on the dynamic adsorption process using a Dynamic vapour sorption (DVS) system which showed the influence of the hysteresis.

Samples were prepared as compressed earth blocks (CEB) or plasters. The CEB and plasters were further investigated with the addition of natural fibres to explore the potential to improve their buffering capacity.

Overall not only was the performance of the materials characterised but it could be identified which properties influence the adsorption capacity also it was pos-

sible to compare the results with existing classifications for buffering materials. It became clear that not only are these materials out performing most of conventional materials but their own performance can also be adjusted and improved for required applications.

Dissemination

Journal articles accepted

- McGregor, F., Heath, A., Fodde, E. and Shea, A. (2014), 'Conditions affecting the moisture buffering measurement performed on compressed earth blocks', *Building and Environment* 75, pp.11-18.
- Dubois, S., McGregor, F., Evrard, A., Heath, A. and Lebeau, F. (2014), 'An inverse modelling approach to estimate the hygric parameters of clay-based masonry during a moisture buffer value test', *Building and Environment* 81(0), pp.192-203.
- McGregor, F., Heath, A., Shea, A., Lawrence, M., (2014), 'The moisture buffering capacity of unfired clay masonry', *Building and Environment* 82, pp.599-607.

Conference papers

- McGregor, F., Heath, A., Ayre, G., Fodde, E. and Walker, P. (2012), The effect of stabilisation on humidity buering of earth walls, in 'Proceedings of LEHM 2012: 6th International Conference on Building with Earth', Dachverband Lehm e.V, Weimar, Germany
- McGregor, F., Heath, A., Fodde, E. (2013), 'Experimentally measured effect of earth building material properties on moisture buffering capacity' in *Proceedings of Earth USA 2013*, Santa Fe, New Mexico, USA

Presentations

- McGregor, F., Heath, A., Fodde, E. (2013), 'The potential of Dynamic Vapour Sorption systems to investigate the moisture buffering of unfired clay masonry', *Earthen Construction Symposium: Durham 2013*, Durham, UK

- McGregor, F., Heath, A., Shea, A. (2014), ‘Optimising the indoor air moisture regulation in earth construction’ EBUK 2014, Norwich, UK (Link: https://www.youtube.com/watch?v=qrYR_Mhj-A4)

Contents

Acknowledgements	I
Abstract	III
Publications	V
Table of Contents	VII
List of Tables	XI
List of Figures	XIII
List of Equations	XVIII
Abbreviations	XX
List of Terms	XXII
1 Introduction	1
1.1 Global context and climate change	1
1.2 Indoor Air Quality	2
1.3 Moisture regulation and earth construction	5
1.4 Scope and structure of the thesis	6
2 Literature review	8
2.1 Earth building materials	8
2.1.1 Definition	8
2.1.2 History and use	9
2.1.3 Building Techniques	10
2.2 Moisture buffering concept	12

2.2.1	Evolution and definition	12
2.2.2	Importance of moisture buffering	13
2.2.3	Experimental testing	13
2.2.3.1	Full scale monitoring	18
2.2.4	Mathematical model	20
2.3	Hygic properties of porous building materials	21
2.3.1	Hygroscopicity and moisture storage	21
2.3.2	Water vapour permeability	26
2.3.3	Surface moisture transfer resistance	29
2.4	Clay minerals and their adsorption properties	31
2.4.1	Clay minerals: a definition	31
2.4.2	Sorption properties	36
2.5	Review on the moisture buffering capacity of unfired clay masonry	37
2.6	Summary	39
3	Materials and methodology	41
3.1	Materials	41
3.1.1	Nature of soils	41
3.1.2	Soils composition	43
3.2	Sample preparation	44
3.2.1	Mixing	44
3.2.2	Size, thickness and compaction	46
3.2.2.1	Large samples	46
3.2.2.2	Small samples	46
3.2.2.3	Plasters	47
3.2.2.4	Thickness	49
3.2.3	Water content	49
3.2.4	Drying	50
3.3	Testing	51
3.3.1	Water vapour permeability	51
3.3.2	Sorption isotherms	52
3.3.2.1	Salt solutions	52
3.3.2.2	Dynamic vapour sorption	53
3.3.3	Moisture buffering test	54

4	Conditions affecting the moisture buffering measurement	59
4.1	Boundary conditions	59
4.1.1	Preconditioning	59
4.1.2	Effect of relative humidity level and time steps	60
4.1.3	Effect of surface film resistance	65
4.1.4	Logging method	67
4.2	Sample parameters	72
4.2.1	Effect of sample thickness	72
4.2.2	Effect of sample size	72
4.3	Summary	76
5	Experimental results	78
5.1	Calculations	78
5.1.1	Water vapour permeability	79
5.1.2	Sorption isotherms	81
5.1.3	Moisture buffering values	82
5.2	Results from parametric study	83
5.2.1	Group I: Stabilisation	83
5.2.2	Group II and III : Initial water content	85
5.2.3	Group IV and V: Apparent density and mixing method	88
5.2.4	Group VI : Mineralogy	93
5.2.5	Group VII : Natural brick soils	95
5.2.6	Group VIII and IX : commercial plasters	99
5.3	Summary	104
6	Discussion	106
6.1	Properties affecting the structural organisation of the material	106
6.1.1	Apparent density	106
6.1.2	Water content	110
6.1.3	Influence of a modified structure on the dynamic adsorption	113
6.2	Properties affecting the internal surface activity of the material	119
6.2.1	Particle size distribution	119
6.2.2	Mineralogy	126
6.2.3	Addition of stabiliser	129

6.2.4	Influence of a modified internal surface activity on the dynamic adsorption	131
6.3	Classification of results	131
6.4	Prediction of MBV based on steady-state properties	137
6.4.1	Penetration depth	141
6.4.2	Prediction of steady-state properties based on the results from the moisture buffering test	143
6.5	Summary	145
7	Further investigation on the sorption properties and the addition of natural fibres	147
7.1	Investigation of dynamic adsorption properties with the DVS equipment.	147
7.1.1	DVS moisture buffering test, influence of hysteresis	147
7.1.2	Variation in adsorption rate	150
7.1.3	Comparison between small and large scale moisture buffering test	152
7.2	Addition of organic fibres	152
7.2.1	Introduction	152
7.2.2	Sample preparation	156
7.2.3	Testing and results	156
7.2.3.1	CEB moisture buffering results	158
7.2.3.2	Plasters moisture buffering results	158
7.2.4	Moisture buffering value	161
7.2.5	Discussion	162
8	Conclusions	164
8.1	Summary	164
8.2	Future work	166
	References	169
	Appendix	178
	Articles published	195

List of Tables

2.1	Results from the Round Robin test of the Nordtest project Rode et al. (2005)	15
2.2	Values for water vapour permeability from the literature	29
2.3	Moisture buffering results from Lustig-Rössler (1992)	38
3.1	Soils used	42
3.2	Overview of sample groups and properties investigated	43
5.1	Symbols and units	78
5.2	Linear correlation coefficients between size fraction and hygric parameters for samples in group VII	96
6.1	Correlation between apparent density and water vapour resistance factor for all groups	107
6.2	Lineat correlation coefficients for water vapour resistance and moisture buffering	115
6.3	Linear correlation coefficients between size fraction and hygric parameters for samples from group I to VII	125
6.4	Proposed extended classification	137
7.1	Sample description	157
7.2	MBV for all tested mixes	161
.1	Group I experimental reults	179
.2	Group II and III experimental results	181
.3	Group IV experimental results	183
.4	Group V experimental results	185
.5	Group VI experimental results	187
.6	Group VII experimental results	190

.7	Group VIII experimental results	192
.8	Group IX experimental results	194

List of Figures

1.1	Influence of relative humidity, modified from Arundel et al. (1986)	4
2.1	Example of soil classification	9
2.2	The flux chamber from Padfield (1998)	16
2.3	Results from the flux chamber Padfield (1998)	17
2.4	Connection between system level and room level (Abadie and Mendonça, 2009)	19
2.5	The penetration depth (Svennberg, 2006)	20
2.6	Psychrometric chart	23
2.7	Soil Water Characteristic Curve from Fredlund (2006))	24
2.8	Types of sorption isotherms from Sing (1985)	25
2.9	Described sorption isotherm from Hall and Allinson (2009)	27
2.10	Transmission electron micrographs of some clay minerals with varied particle morphology: (A) kaolinite from Sasso (Italy) showing typical books of particles; (B) high-quality flint clay from Gasconade County, Missouri, USA; (C) tubular halloysite particles alongside kaolinite plates from Sasso, Italy; (D) smectite or illite/smectite from Sasso, Italy; (E) filamentous illite from sandstones in offshore Netherlands; (F) lath-shaped illite from sandstones in offshore Netherlands; (G) pseudo-hexagonal illite particles from sandstones in offshore Netherlands; (H) fibrous palygorskite from Southern Georgia (USA). These images were taken from Bergaya and Lagaly (2006) who had previously taken them from various authors.	32
2.11	1/1 type clay mineral, from Meunier (2005)	33
2.12	2/1 type clay mineral from Meunier (2005)	34
2.13	Pillared clays modified from Rouquérol et al. (1999)	35

3.1	Small mortar mixer	44
3.2	Large mortar mixer	45
3.3	Hand mixing bowl and pallet knife	45
3.4	Size of samples used	46
3.5	CIV-RAM press	47
3.6	Adapted Wykeham Farrance triaxial frame	48
3.7	Plastic drain pipe used as form	48
3.8	Samples of 70 mm, 50 mm and 30 mm	49
3.9	Sample set up for water vapour permeability test	51
3.10	Salt solution sorption isotherm set up	53
3.11	Example of MB test results	56
4.1	Effect of boundary conditions on moisture adsorbed	61
4.2	Simulated moisture adsorption variation from 6h-16h to 24h-24h cycles from (Roels and Janssen, 2006)	62
4.3	Time step influence on samples of group I	63
4.4	Correlation between MBV obtained from different RH cycles. . . .	64
4.5	Unstabilised sample from group I under different air velocity con- ditions	66
4.6	Raw data from continuous logging without windhsield	67
4.7	Averaged data from continuous logging with windshield	68
4.8	Logging method	69
4.9	Effect of ventilation in the conditioning room on the precision of the results in 50/85% RH cycle	70
4.10	Reduced effect of the ventilation in the conditioning room mea- sured in a 53/75% RH cycle	71
4.11	Different thickness for an unstabilised sample from group I mea- sured in a 50-85% RH cycle	73
4.12	Comparison between two different sample sizes of the unstabilised material from group I measured both without windshield in the same chamber	74
4.13	Comparison between two different sample sizes of the unstabilised material from group I measured in different air velocity conditions	75

5.1	Raw data from the water vapour permeability experiment with three identical samples for each material	80
5.2	Water vapour resistance factor and moisture buffering value for samples in group I	84
5.3	Sorption isotherms for stabilised samples, group I . a. cement sorption isotherms, b. cement hysteresis, c. lime sorption isotherms, d. lime hysteresis, e. geopolymer sorption isotherms, f. geopolymer hysteresis.	86
5.4	Water vapour resistance factor and moisture buffering value for samples in group II and III	87
5.5	Group II compared sorption isotherms	88
5.6	Group III compared sorption isotherms	89
5.7	Water vapour resistance and moisture buffering results for samples in group IV and V	90
5.8	Influence of apparent density on sorption isotherms	91
5.9	Salt solution and DVS sorption isotherms from samples in group IV	92
5.10	Water vapour permeability and moisture buffering results for samples in group VI	93
5.11	Salt solution sorption isotherms for samples 1 to 9 in group VI	94
5.12	Compared sorption isotherms and hysteresis with different Bentonite contents from group VI	95
5.13	Water vapour permeability and moisture buffering results for samples in group VII	97
5.14	Sorption isotherms of different brick soils	98
5.15	Water vapour resistance of plasters from group VIII	100
5.16	Moisture buffering results from plasters in group VIII	101
5.17	Water vapour resistance factor of plaster from group IX	102
5.18	Moisture buffering value of plasters from group IX	103
6.1	Correlation between apparent density and water vapour permeability	108
6.2	Influence of apparent density on the moisture buffering value	109
6.3	Influence of apparent density on water vapour factor in group IV and V	111
6.4	Corrected water vapour resistance values of group II and III	112

6.5	Influence of water content on sorption isotherms	113
6.6	Linear fit between μ factor and MBV	114
6.7	Exponential fit between μ factor and MBV	115
6.8	Power fit between μ factor and MBV	116
6.9	Water vapour resistance factor and moisture buffering value	117
6.10	Experimental results compared with the results from (Rode et al., 2005)	118
6.11	Compared sorption isotherms of Le and St soils	120
6.12	Compared sorption isotherms of Bi and Th soils	121
6.13	The influence of particle size fractions on the water vapour resis- tance factor	122
6.14	The influence of particle size fractions on the moisture buffering value	123
6.15	The influence of particle size fractions on the moisture capacity .	124
6.16	Sorption isotherms of the Kaolinite and the Bentonite used during this study	127
6.17	Schematic representation of a Kaolinite and a Montmorillonite type mineral and the associated porosity	128
6.18	Sorption isotherms comparison of tested mineralogy contents, the pure Kaolinite was tested in the form of a powder as a reference.	129
6.19	FTIR spectra of cement stabilised samples	132
6.20	FTIR spectra of lime stabilised samples	133
6.21	FTIR spectra of geopolymer stabilised sample	134
6.22	Influence of the moisture capacity on the MBV	135
6.23	Water vapour sorption classification from Schroeder (2010)	137
6.24	Experimental results and the German classification limits for earth plasters, WS I between the full line and large dotted line, WS II between the large dotted and small dotted line and WS III is anything above the small dotted line	138
6.25	Proposed classifications subdivisions based on experimental results	139
6.26	Experimental and calculated results compared	140
6.27	Penetration depth values based on DVS or salt solution moisture capacity	142
6.28	Inverse modeling procedure (Dubois et al., 2014)	144

7.1	DVS moisture buffering test	148
7.2	The active moisture capacity during a moisture buffering test . .	149
7.3	Data from sorption isotherm measurement	150
7.4	Variable adsorption rates on the RH range	151
7.5	Relative moisture uptake to mass for small and large scale sample	153
7.6	Chopped Barley straw ($\simeq 2$ cm)	154
7.7	Barley wool	155
7.8	Chopped Corn stalk (0.5 cm max)	155
7.9	Results from the moisture buffering test of CEB with barley straw fibres and CEB without fibres from group V	158
7.10	Results from the moisture buffering test of plasters with fibres . .	159
7.11	Difference of water vapour adsorption compared to 0% fibres . .	160
.1	Moisture buffering test under 53/75 % RH cycle, group I	178
.2	Moisture buffering test 33/75% RH, group II and III	180
.3	Moisture buffering test 33/75% RH, group IV	182
.4	Moisture buffering test 33/75% RH, group V	184
.5	Moisture buffering test 33/75% RH, group VI	186
.6	Moisture buffering test 33/75% RH, group VI	188
.7	Moisture buffering test 33/75% RH, group VII	189
.8	Moisture buffering test 33/75% RH, group VIII	191
.9	Moisture buffering test 33/75% RH, group IX	193

List of Equations

Equation	2.1 : $MBV = \frac{\Delta_m}{A \cdot \Delta RH}$	12
Equation	2.2 : $MBV^* = \alpha \cdot MBV_{8h} + (1 - \alpha) \cdot MBV_{1h}$	18
Equation	2.3 : $b_m = \sqrt{\frac{\delta_p \cdot \rho_0 \cdot \frac{\partial u}{\partial \varphi}}{p_s}}$	20
Equation	2.4 : $RH = \frac{P_w}{P_{ws}} \times 100$	22
Equation	2.5 : $\xi = \frac{\partial u}{\partial \varphi}$	26
Equation	2.6 : $W = \frac{G}{A \cdot \Delta p_v}$	28
Equation	2.7 : $\delta_p = W \cdot d$	28
Equation	2.8 : $\mu = \frac{\delta_a}{\delta_p}$	28
Equation	4.1 : $MBV_{50/85} \simeq MBV_{33/75} \times 0.69$	63
Equation	5.1 : $g = \frac{G}{A}$	79
Equation	5.2 : $W = g_{me} \cdot \Delta p_v$	79
Equation	5.3 : $\delta = W \cdot d$	81
Equation	5.4 : $\mu = \frac{\delta_a}{\delta}$	81
Equation	5.5 : $EMC = \frac{m - m_{ref}}{m_{ref}} \times 100$	81
Equation	5.6 : $MU_t = \frac{m_t - m_0}{A}$	82
Equation	5.7 : $MBV = \frac{MU_t}{\Delta \% RH}$	82
Equation	6.1 : $MBV_{ideal} = 0.00568 \cdot p_s \cdot b_m \cdot \sqrt{t_p}$	140
Equation	6.2 : $\frac{\Delta u_x}{\Delta u_s} = e^{-x \sqrt{\frac{\pi}{D_w t_p}}}$	141

Equation 6.3 :	$d_{1/e} = \sqrt{\frac{D_w t_p}{\pi}}$141
Equation 7.1 :	$MBV = \frac{\Delta_m}{A \cdot \Delta_{RH}}$161

Abbreviations

- CEB : Compressed Earth Block
- CEC : Cationic Exchange Capacity
- DTU : Technical University of Denmark
- DVS : Dynamic Vapour Sorption
- ENTPE : Ecole National des Travaux Publiques d'Etat
- EMC : Equilibrium Moisture Content
- FTIR : Fourier Transform Infrared Spectroscopy
- HVAC : Heating Ventilation Air Conditioning
- IAQ : Indoor Air Quality
- IPCC : International Panel on Climate Change
- LTH : Lund University, Sweden
- MBP : Moisture Buffering Potential
- MBV : Moisture buffering Value
- NBI: The Norwegian Building Research Institute
- PAQ : Perceived Air Quality
- PRM : Passive Removal Material
- RH : Relative Humidity

- SBS : Sick Building Syndrome
- SCEB : Stabilised Compressed Earth Blocks
- SWCC : Soil Water Characteristic Curve
- VOC : Volatile Organic Compound
- VTT : Technical Research Centre of Finland
- WS : Wasserdampf adsorptionsklasse (water vapour adsorption categories)

- WUFI : Wärme und Feuchte instationär

List of Terms

- Absorbent : General description of a material that can store a fluid.
- Absorption : Process where a fluid is taken up by the solid phase not by the surface.
- Adsorption : Process where a fluid is enriching the surface of a solid.
- Apparent Density/Bulk Density : It's the ration between the apparent volume including voids and the dry mass of the sample.
- Capillary condensation : Water molecules condensing in the pores of the soil, this phenomenon is the final stage of water uptake in the hygroscopic domain.
- Dynamic adsorption : Adsorption related to the time cycles of the moisture buffering experiment.
- Equilibrium moisture content : The stable content of water at a given relative humidity.
- Hygric properties : Properties referring to the interaction of the material with water (vapour or liquid).
- Hygroscopic : The ability to attract and store moisture from the air.
- Hysteresis : Difference between the adsorption and desorption curve in a sorption isotherm
- Surface activity : Ability of a material surface to attract water molecules (synonym of hygroscopicity)
- Initial water content : Water mixed to the soil for the preparation of the blocks or plasters which is then dried out.

- Isothermal : Invariable temperature.
- Monolayer adsorption : When one layer of water molecules are attached to the surface of the particles.
- Multilayer adsorption : When several layers of water molecules are attached to the surface of the particles.
- Microporosity : Pores with an internal width smaller than 2 nm.
- Mesoporosity : Pores with an internal width between 2 and 50 nm.
- Macroporosity : Pores with an internal width greater than 50 nm.
- Moisture buffering : The passive regulation of indoor water vapour concentrations.
- Moisture penetration depth : The thickness of the material that is active during a daily moisture buffering cycle.
- Occupants : People living or working in the building affected by and affecting the indoor environment.
- Sorption : Characterises the combined phenomenon of adsorption and absorption.
- Stabilisation : Addition of products to mechanically or chemically stabilise raw earth
- Step response : A method that uses a known change in boundary conditions and measures the response.
- Workability : For plaster this is achieved when they have the right consistency to be applied to a wall surface.

1 Introduction

1.1 Global context and climate change

It is now widely accepted in the scientific community that human societies play a major role in climate change. The newest report of the International Panel on Climate Change (IPCC) is clear on this matter. The report summarises observation made from research around the world about the state of the climate change including eventual risks such as sea level rise, the melting of ice caps and moreover the increased number of extreme weather events. Many of these events are likely to increase during the 21st century. According to the IPCC report the carbon dioxide concentration in the atmosphere has increased by 40% since the pre-industrial age and is for a great part responsible of the climate change. The building sector is partly responsible for some carbon dioxide emissions through the use of fossil fuel in the manufacturing process and during the use of buildings. The global combustion of fossil fuels and the production of cement for the year 2011 released 9.4 Gigatonnes of carbon dioxide into the atmosphere, which represents 54% more than the 1990 level(IPCC, 2013). In the UK, a report from the Government Low Carbon Construction Innovation and Growth Team (IGT, 2010) indicates that the construction sector is responsible for 47% of the total CO₂ emission of the UK. From the 47% of carbon emission that can be saved, 15% can be made during the manufacturing process of building materials and 80% during the use of the buildings. Policy makers have taken the first steps to respond to the observed climate change, by putting legal targets to reduce the impact of human activity. The Climate Change Act of 2008 in the UK targets to reduce residential emissions by 29 % by 2020 and all new homes will have to be “zero carbon” by 2016(IGT, 2010).

A database has been created at the University of Bath which estimates the embodied energy and embodied carbon of various materials(Hammond and Jones, 2008).

Many conventional building materials have a high embodied energy. Cement and fired bricks for example both common building materials have a high energy consumption during their production process, 3MJ/kg for bricks and 0.95MJ/kg for concrete. Policy mainly target energy consumption in the use of the building, some high standards are now more and more applied as for example the “Passivehaus” design in which the energy consumption of the building in use has a zero or positive energy balance. These kind of low impact building designs also takes into account more and more the nature and embodied energy of the building materials used. Materials with a low embodied energy that also have the potential to be recycled should be favoured. There is a regain of interest in recent years for natural building materials (clay, hemp, straw, timber) which in most situations have a very low embodied energy and can easily be reused or just composted. In this context natural building materials will most likely regain a position they had many years ago. Among them, unfired clay masonry is a traditional building material that can be sourced locally and usually has a small embodied energy. This material presents therefore a sustainable alternative to replace high embodied energy materials in many situation.

1.2 Indoor Air Quality

One of the main purposes of buildings is to shelter man from exterior climatic conditions, providing a more comfortable “artificial” indoor climate. From providing a basic shelter from rain and wind, houses evolved to offer a comfortable indoor temperature using heating, in the past different regions had a particular architecture, vernacular, related to the outdoor climate, this was influenced by whether the indoor climate needed to be cooled or heated. This is commonly referred to as environmental design (Mahdavi and Kumar, 1996)

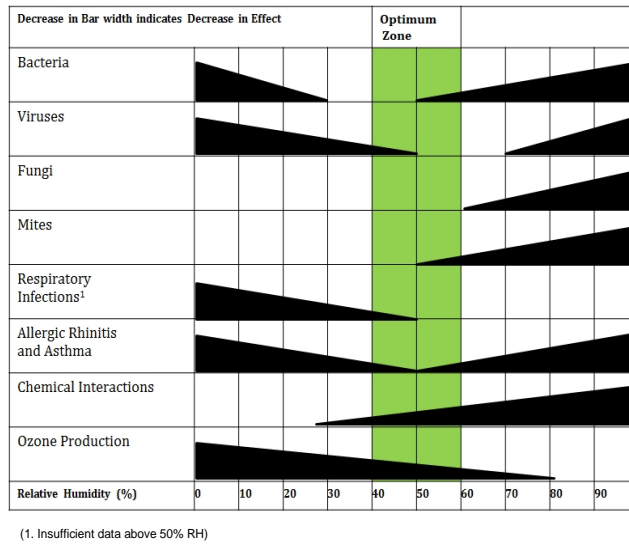
Starting with the industrial revolution new materials and new building methods did not consider the long established relation between outdoor climate, building materials and architecture. New homes were built with the idea that indoor climate can be artificially maintained whatever the outdoor conditions, by using a newly available source of energy (fossil fuel). An “industry-based” approach to control indoor climate was adopted and existing passive methods were discarded in modern architecture (Mahdavi and Kumar, 1996). Starting with the first oil-

crisis in the 1970s an increasing concern appeared towards this type of approach which relied on energy consuming systems to control the internal environment. It became clear that energy is a precious resource which needs to be used with consideration. The industry response was to improve the thermal efficiency of buildings. New insulation technologies were designed, and the natural air exchange rate was reduced to up to 0.2 or 0.3 air exchanges per hour. The reduced air exchange rate had a direct consequence to the increase of indoor trapped humidity and air pollution, which was at that time not taken into account (Jones, 1998; Trechsel, 1994). This resulted in a major increase in health issues such as asthma and respiratory allergies which has been related to the Sick Building Syndrome (SBS) (Redlich et al., 1997). In the UK, 15% of the population is now suffering from asthma (Braman, 2006).

From the middle of the 19th century, during the “hygienic revolution”, indoor pollution was believed to be a major concern until the 1960’s where the outdoor pollution started to receive an increasing attention and became a dominant concern (Sundell, 2004). It was considered that outdoor pollution may be the principal environmental factor causing an increase of health issues in the late decades of the 20th century (Jones, 1998). In fact, there is more and more evidence for indoor pollution being a main cause and the increase of indoor pollution coincided with the changes made to houses for improved thermal efficiency (more insulation, less air exchange), a greater use of synthetic building materials and an increased share of people’s time spend indoors, reaching an average of 95% (Jones, 1998). There was also an increase in sources of indoor pollutants. These sources have increased due to occupant’s behavior (tobacco smoke, burning of biomass, pesticides, solvents...) or are also linked to the nature of building materials (paint, insulation materials, asbestos...). Often less considered is pollution due to microorganisms, as fungi, bacteria or arthropods (mainly Mites in the UK).

Indoor pollution is related to relative humidity (RH) levels in the buildings. High humidity levels increase the emission of Volatile Organic Compounds from materials and provides ideal conditions for microorganisms to proliferate (Fang et al., 1999). Whereas a too dry RH directly affects human health by drying the mucus (Minke, 2012). It is now considered that a RH between 40% and 60% is the optimal zone for an improved Indoor Air Quality (IAQ), see Figure 1 (Arundel et al., 1986).

Figure 1.1: Influence of relative humidity, modified from Arundel et al. (1986)



Therefore, the control of humidity is essential for a healthy environment but this is rarely taking into account in residential buildings (Padfield, 1998). The approach of controlling the interior climate with energy consuming equipments is still most often the solution put into place. Mahdavi and Kumar (1996) critically discuss the mechanically controlled environment, the viability and consistence of a believed ideal indoor environment regardless of the exterior climate and human adaptivity. From their conclusion, the use of HVAC systems are rather unsatisfactory in many respects. The technology is nearly exclusively focused on thermal control; the systems are often unreliable and fail to deliver the set of environmental conditions they were designed for. The systems demand a regular maintenance which is not systematically done, therefore creating poor performance (Mahdavi and Kumar, 1996). On the contrary, a passive control, does not depend on an energy input and therefore represents a more sustainable option. It can be integrated into the design of the building and adapted to local climate. This can be achieved by using specific building materials that present advantages such as thermal mass, moisture buffering and also include natural ventilation, shading in the design process. This makes the whole building more resilient. For

passive control, the nature and hygrothermal behaviour of buildings materials are of a major importance, as the whole building envelope participates in indoor climate control. For example the use of wood as a hygroscopic building material has been shown to reduce the indoor Relative Humidity (RH) peaks by up to 35% in some examples(Rode et al., 2005).

1.3 Moisture regulation and earth construction

One of the big disadvantages of clay as a building material is its sensitivity to water. When in contact with liquid water, or in a saturated state, the cohesion strength of earth as a building material is greatly reduced(Heath et al., 2009). This sensitivity also induces the material to be highly hygroscopic and therefore the materials disadvantage becomes one of the materials greatest advantages. It has been observed in buildings that clay can stabilize the humidity levels even in a very moist environment such as in a shower room(Morton et al., 2005). It has been shown through observation that clay has a particular behavior towards moisture. Some of the first academic work was done in Germany, by Ursula Lustig Rossler, under the supervision of Gernot Minke and published in 1992 (Lustig-Rössler, 1992). They used a dynamic laboratory test to estimate the interaction between indoor vapour and clay building materials. At the Technical University of Denmark, Padfield (1998) has compared different materials using an experimental flux chamber. The best performing materials to lower RH peaks were end grain wood and a mixture of clay with Perlite. Based on this research and empirical observations, commercial plaster companies now sell earth plasters claiming the benefits to the indoor climate these can provide.

Dynamic vapour sorption is a parameter that is not systematically measured in building materials unlike steady state hygrothermal properties such as vapour permeability. Overall, there is little information that exists in the literature and there is yet not a recognised standard value to express this dynamic property, even though the Moisture Buffering Value (MBV) from a Nordtest project seems to take a lead. Commercial plasters from Germany provide dynamic sorption values in g/m^2 for 1 h and 12h adsorption times. But such values are dependant on the testing conditions and therefore these would need to be provided. This

will be described in detail in the next chapter describing the different measuring methods. Overall, the potential of these materials to be used as a building envelope that provides a passive moisture control is still not well understood due to a lack of experimental data and academic research into the mechanism of moisture buffering and the benefits it can provide.

1.4 Scope and structure of the thesis

A literature review on dynamic moisture adsorption and soils is given in Chapter 2. The ability of earth materials to adsorb moisture has been demonstrated in the past, so therefore the aim of this work is to understand the material properties affecting behaviour. Through the systematic measurements of dynamic and static hygroscopic properties, the influence of a variety of parameters can be investigated. This work has never been done in the past, it will provide the tools for soil materials to be engineered in order to provide the required dynamic properties.

Compressed earth blocks and plasters were used for the study as the properties of these are easy to control. As described in the next chapter, there are a variety of earth building techniques, looking at the materials properties directly allows a comparison between these different techniques and it is expected that for example, properties such as the bulk density of the material will have a similar effect for cob and rammed earth. The studied material properties and how the samples are prepared are described in Chapter 3.

The main experimental work for this study involved acquiring reliable dynamic adsorption data. This initially consisted of establishing the reliability of the test method and the obtained values, which are described in Chapter 4. The second stage consisted of preparing series of samples applying different material properties and following the previously described test protocols, these results are presented in Chapter 5. An overview and a discussion of these results are developed in Chapter 6. Additional work was undertaken on the addition of different fibres, which is often done in practice. This work was done in collaboration with Mariana Palumbo and is presented in Chapter 7. A conclusion will be drawn in Chapter 8.

2 Literature review

2.1 Earth building materials

2.1.1 Definition

“Earth building materials” is the term frequently used in the literature to refer to building components composed of a soil rich in clay. The soil is the upper layer forming the lithosphere and is an active boundary between the mineral and the organic world. This interface is formed by the weathering of parent rocks lying underneath and the organic activity above. The soil type depends on the nature of the parent rock, the type of vegetation, climatic and hydric conditions and more recently, the action of man. Soils can be divided into horizontal layers called “horizons” because of their variable composition. The top horizon is most often rich in organic matter and typically not suitable for earth construction. The “subsoil” horizon usually has the most appropriate composition for construction purposes. The solid portion of subsoils is composed of mineral particles with a large variation in size and nature, the fluid part is mainly composed of air and water. The classification of soils depends for a great part on their particle size distribution (Houben and Guillaud, 1994). Figure 2.1 shows an example of a typical triplot which classifies a soil depending on its particle size distribution.

The mineral particles can be divided into different size categories. In Europe these are gravels (over 2 mm), sand (between 2 mm and 63 μm), silt (between 63 μm and 2 μm) and clay (<2 μm) but different boundaries are used in different countries as in Figure 2.1. The clay fraction is responsible for the cohesive force acting as a cement between the coarser particles and is mostly composed of clay minerals. These silicate minerals present a particular layered crystal structure (phyllosilicates) and surface charges that make them a highly hydrophilic material responsible for many of the adsorption characteristics of earth building materials

as described in the clay minerals section.

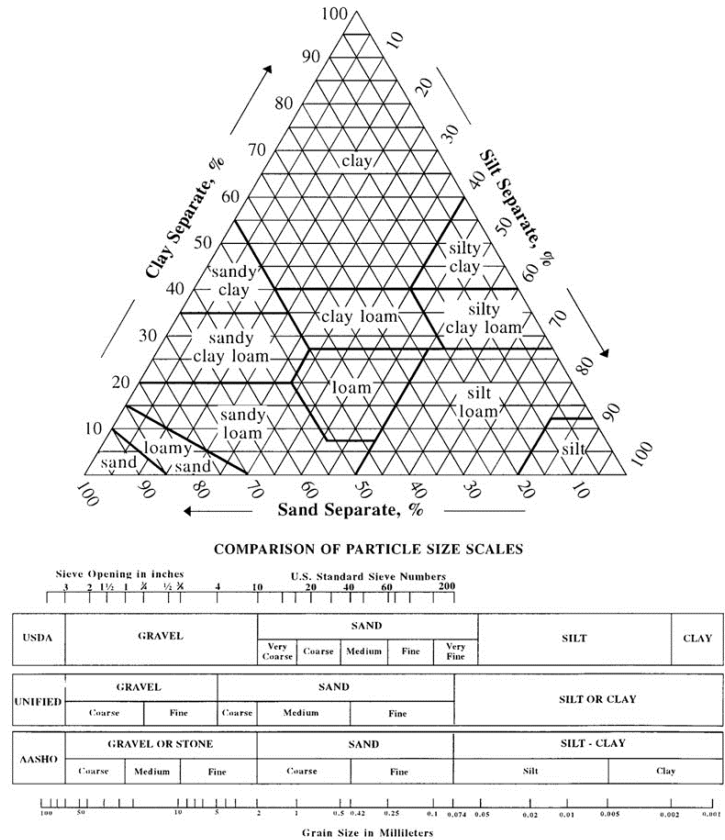


Figure 2.1: Example of soil classification

2.1.2 History and use

Through history humans have always used material available on site to build their homes and shelters. One of these materials nearly universally available around the world was the underlying earth. Every inhabited continent has its heritage of earth buildings with their specific techniques associated and adapted to a type of environment. Building with earth can be traced back to the first settlements of hunter-gatherers into a sedentary living mode (Houben and Guillaud, 1994). It has been used throughout history and has remained a principal building material in many countries, principally in rural areas. In 1982, it was estimated around

40% of the world population lived in earth buildings Houben and Guillaud (1994) this number might have changed significantly in recent years, no exact estimation has been made in recent years.

The fortified city in the Draa valley in Morocco, the city of Bam in Iran, sections of the great wall of China, the great Mosque of Djenne in Mali, the town of Shibam in Yemen are examples of outstanding historical earthen architecture (Minke, 2012). Great civilisations including the Egyptians and the Persians mastered the earth and incorporated high ceilings with vaults and domes in their buildings. A recent project “Terra InCognita” aimed to produce an inventory of earthen architecture in Europe and a book with many illustrations of architectural styles was published. In the more industrialised countries, commercially manufactured materials such as fired bricks and cement replaced earth and other traditional materials as mainstream construction materials. Consequently, the use of earth as a building material declined and it became perceived as unreliable and primitive.

In recent years, environmental awareness has become a priority and the use of earth re-emerged and was modernised. Institutes like Craterre in France or the Earth Institute in India have been created to gather existing traditional knowledge and develop new knowledge (Houben and Guillaud, 1994). In developing countries, the main argument for using earth is the need to house an increasing population with low cost and available materials even in remote regions. In the last few years “earth” has re-emerged as a credible building material, research programs are being launched in many universities and industries have started to see a strong development potential in it. Moreover, the mentality of the public is changing. For example cob houses in California are becoming a trend with their potential for organic forms. Many fired brick manufacturers have invested and developed unfired brick technologies. However, one of the main limitations in many countries remains the need to establish standards and regulations for earth construction.

2.1.3 Building Techniques

Earth building construction techniques have been evolving for several hundreds of years and therefore a very large variety exists. Composition, compaction, initial moisture content and drying method vary between each technique, therefore each technique needs to be considered as a unique system when considering moisture

buffering. In modern earth buildings, these main techniques are principally used:

- Rammed earth is directly compacted on site in between temporary formwork. The walls are typically 300-450 mm thick. The moist soil is compacted in layers, therefore the walls present a characteristic layered appearance often used for aesthetic purpose, therefore plaster or render is usually not applied (Walker, 2005). In order to reduce cracking, the soil must have low shrinkage and have a low compaction water content.
- Earth blocks exist under a variety of forms. Traditionally the blocks are made manually and sun dried (adobe or mud brick) which is still the case in many countries. These bricks can be mixed with organic fibres such as straw. Nowadays, industries are producing machines to produce compressed earth blocks (CEB) or extruded earth blocks. Earth brick buildings are usually covered by earth rendering or can be smoothed with some additional moisture (Minke, 2012). A shrinkage occurs before construction, they can have a higher clay content and compaction water content.
- Cob building is a method which uses a wet soil with organic fibers to directly shape the walls by hand. This method is much appreciated for its artistic potential creating sculptures a round shapes incorporated into the walls (Minke, 2012). A low compaction energy can result in low density.
- Infill of timber structures by earth is a common practice that is still visible in many places in Europe along with wattle and daub seen in South America, Africa and Asia. There is a large variation of these techniques (Minke, 2012) but as the earth is not load-bearing, more variable soils can be used.
- Earth is also used for renders, final coatings. A few companies sell earth plasters with a large variety of colours and textures. A special investigation will be dedicated on renders as these are always in contact with the indoor humidity and may either take up most of the buffering or strongly affect the buffering capacity of the wall system depending on moisture penetration depth.

2.2 Moisture buffering concept

2.2.1 Evolution and definition

Moisture buffering refers to the potential of materials to regulate indoor humidity levels. The first reference to the concept of moisture buffering in the built environment can be found in Kunzel (1965), where some work was done on the potential of interior surfaces to adsorb moisture.

Eshoj and Padfield (1993) related the stable climate provided by the building materials in a historical church. Padfield (1998) published his PhD thesis on the “role of absorbent building materials in moderating changes of relative humidity”. Rode, Holm and Padfield (2004), published the outcomes of a workshop where it was agreed that a formal definition of Moisture Buffer Capacity was needed and this work was part of a Nordtest project first initiated in 2003 to determine a Nordtest protocol for moisture buffering. Soon after this project, publications appeared using the concept of moisture buffering (Hameury, 2005; Harderup, 2005; Mortensen et al., 2005; Rode et al., 2005; Salonvaara et al., 2004). A technical report (Rode et al., 2005) was then published proposing a unique value and a method to describe the moisture buffering capacity of building materials. The unique value was named the Moisture Buffering Value and could be obtained experimentally (MBV_{practical}) or numerically (MBV_{ideal}). The given definition was : “The practical Moisture Buffer Value (MBV_{practical}) indicates the amount of water that is transported in or out of a material per open surface area, during a certain period of time, when it is subjected to variations in relative humidity of the surrounding air. When the moisture exchange during the period is reported per open surface area and per % RH variation, the result is the MBV_{practical}. The unit for MBV_{practical} is $g/(m^2 \cdot \%RH)$.” Rode et al. (2005).

The MBV is calculated from the experimental results by the equation 2.1:

$$MBV = \frac{\Delta_m}{A \cdot \Delta RH} \quad (2.1)$$

Where Δ_m is the mass difference of the material exposed to a cyclic variation of moisture levels, A is the surface exposed and ΔRH is the variation of moisture levels. The obtained MBV is dependend on the boundary conditions, therefore results for different materials can only be compared if the same boundary condi-

tions were used.

2.2.2 Importance of moisture buffering

The relation between the indoor humidity levels and the health of the occupants was described in Chapter 1. There are also many other situation in which a passive humidity regulation can be beneficial.

The durability of building materials is influenced by high humidity levels as there is an increase in chemical interactions with building materials at higher RH levels (Arundel et al., 1986). The use of buffering materials in the building envelope increases the surface area where water vapour can condense and be stored and released when RH decreases. This avoids the extreme condensation that occurs at some vapour impermeable surfaces such as on paints with a cold underlying surface. This presence of liquid water damages the surface and creates the ideal environment for mould growth.

Padfield (1998) undertook some case studies of moisture buffering in historical buildings or archive storages. He underlined the potential of the building envelope to actively regulate the indoor climate. Archive storage or museum storage where the indoor climate (humidity and temperature) needs to be constantly maintained and where there is a low air exchange rate are examples where the moisture buffering of the building envelopes can have a great impact on energy savings.

2.2.3 Experimental testing

Either laboratory tests where the performance of a material is tested or full scale room buffering tests where the buffering capacity of a whole room is measured can be used. The main focus will be on the laboratory tests to characterise the performance of a material as quantifying material performance is an aim of this research .

In 1965, H. Kunzel (Kunzel, 1965) compared the moisture sorption of indoor surfaces with a dynamic experiment, using the “step response” method. The step-response method corresponds to a high relative humidity cycle characterising the adsorption followed by a low humidity cycle to characterise desorption, the mass change of the sample being monitored during the process. This type of experiment was continued by several authors as reported by Svennberg et al.

(2007). A Japanese Industrial Standard (JIS-A1470, 2002) test uses the same principle and the outcome of the Nordtest project on humidity buffering for proposed the same type of testing for moisture buffering evaluation. A comparison of the two test was performed by Roels and Janssen (2006). The main difference are time steps, RH gradients and specimen thickness between the two last methods. An ISO standard was also published in 2008 (ISO-24353, 2008), although the Nordtest method is currently the most used. It follows a cycle of 8h high RH levels and a cycle of 16h of low RH. The RH levels may vary, although the Nordtest protocol suggests using levels easily achievable with saturated salt solutions. A Round Robin test was done by several universities for this test method. The results were all comparable even with varying experimental set-ups. Table 2.1 shows the results obtained by different laboratories, DTU (Technical University of Denmark), NBI (The Norwegian Building Research Institute), VTT (Technical Research Centre of Finland), LTH (Lund University, Sweden) with different experimental set-ups.

In general there is a good agreement between the results, but it is clear that particular attention needs to be given to the experimental set up.

A different type of testing that also describes the moisture buffering was proposed by Padfield (1998) using a flux chamber. The flux chamber creates sinusoidal cycles of moisture added and therefore a change in RH in the chamber. The building materials are placed in the flux chamber and sensors monitor how these influence the change in relative humidity generated by the added moisture. To be able to compare the building materials, the same surface area must be used for each sample. The results are presented as relative humidity change over time as compared to an empty chamber, see Figure 2.3. The measurement realised in an empty chamber determine the boundary conditions. There is however a limitation to this test as it does not quantify the amount of moisture adsorbed by the material even though it quantifies the effect. The flux chamber is a very specific equipment, see Figure 2.2 which does not exist as a standard tool, every new flux chamber may therefore generate different RH levels and response of the material which would make the comparison in between laboratories difficult. Whereas the Nordtest protocol can easily be reproduced.

Table 2.1: Results from the Round Robin test of the Nordtest project Rode et al. (2005)

	Laboratory	MBV _{practical} (g/m ² %RH)		
		Average	Standard Deviation	% Deviation
Spruce boards	DTU	1.22	0.04	3
	NBI	1.12	0.09	8
	VTT	1.15	0.05	4
Concrete	DTU	0.42	0.11	26
	NBI	0.35	0.18	51
	LTH	0.37	0.04	10
Gypsum	NBI	0.69	0.13	19
	LTH	0.57	0.01	1
	VTT	0.65	0.02	3
Laminated wood with vanish	DTU	0.46	0.07	16
	NBI	0.39	0.06	14
	VTT	0.54	0.05	9
Lightweight aggregate concrete with stucco	DTU	0.74	0.08	10
	NBI	0.81	0.10	12
	LTH	0.72	0.08	11
Cellular concrete	DTU	1.05	0.07	6
	LTH	0.96	0.06	6
	VTT	1.11	0.04	4
Brick	DTU	0.39	0.06	16
	LTH	0.35	0.02	5
	VTT	0.69	0.11	17
Birch panels	NBI	0.91	0.16	18
	LTH	0.61	0.05	8
	VTT	1.03	0.06	6

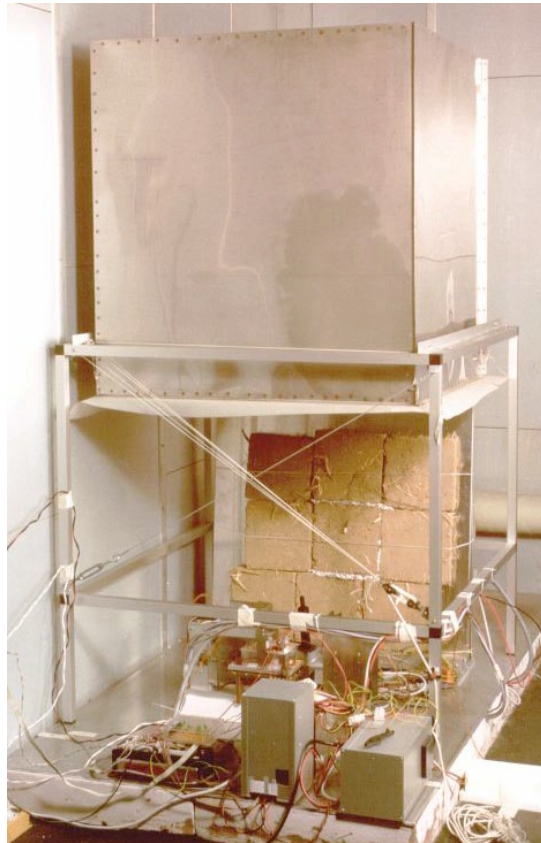


Figure 2.2: The flux chamber from Padfield (1998)

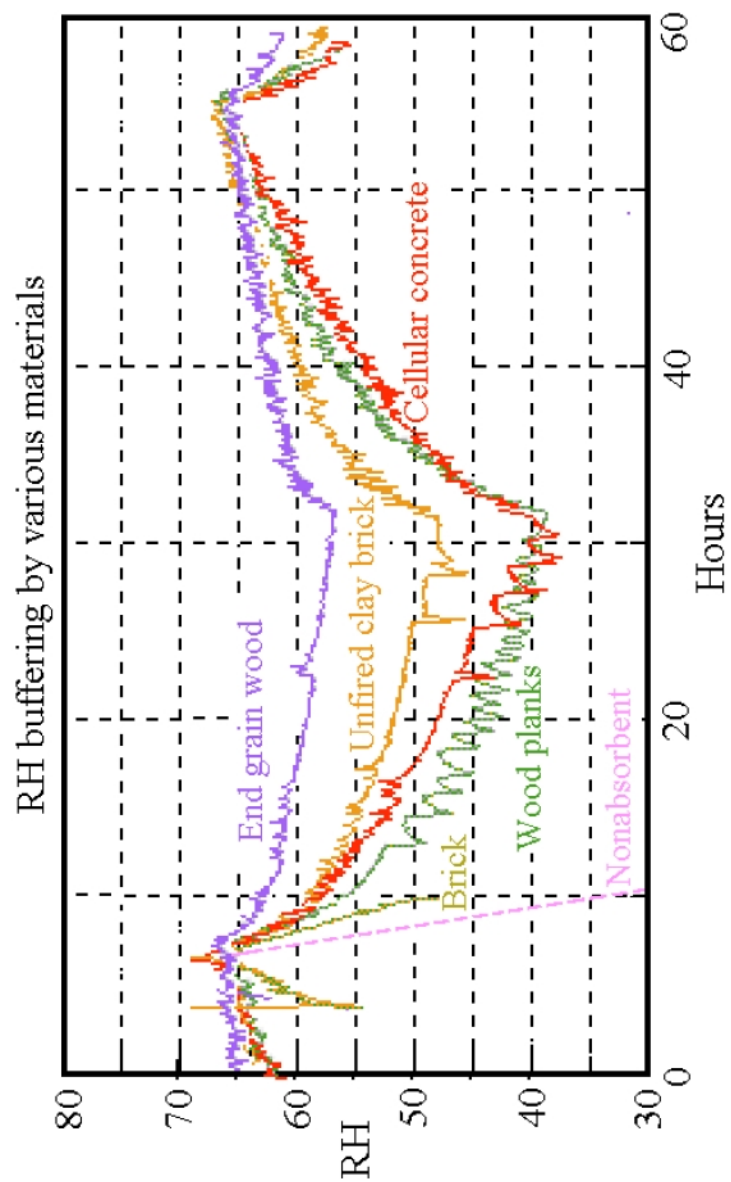


Figure 2.3: Results from the flux chamber Padfield (1998)

2.2.3.1 Full scale monitoring

The limitation of the moisture buffering test remains on to how to link the results of test with the performance in a full room and this is still being investigated (Abadie and Mendonça, 2009), see Figure 2.4. For the purpose of this work it is not considered as an issue as the aim was mainly to characterise the material properties and determine important factors. A few experiments have been conducted to quantify the buffering potential in a real building situation through full scale experiments (Mortensen et al., 2005; Holm et al., 2003; Vereecken et al., 2011; Likos and Lu, 2002).

Some tested the moisture buffering in a real building situation with earth materials Allinson and Hall (2010). This paper compared the RH levels measured in a stabilised rammed earth building with simulated values through the WUFI program using the hygric properties of the rammed earth material. The boundary conditions for the simulation were taken from an adjoining room. A rather good agreement was found between simulated and measured results. Hygric properties were also directly measured by placing sensors in rammed earth walls of a real building (Chabriac et al., 2014).

It was shown by Janssen and Roels (2009), that on a large scale the moisture buffering potential (MBP) of a room can be estimated by combining the MBP of the different interior elements. They modified the original MBV time schemes to fit those measured in a study on different rooms including bathroom and living room. To do this they proposed typical moisture cycles as long, short and peak and have introduced the weighted-average MBP to take shorter cycles into account, see equation 2.2:

$$MBV^* = \alpha \cdot MBV_{8h} + (1 - \alpha) \cdot MBV_{1h} \quad (2.2)$$

This modified version showed a close relationship to the RH variation in all types of cycles and based on their results, a MBV above 1,5 maintained a RH variation below 10%.

Therefore it can be considered that if the MBV for all interior elements and their surface area is known, the MBP of a room can be estimated which can give an indication of the RH variation that will be observed in real building situations.

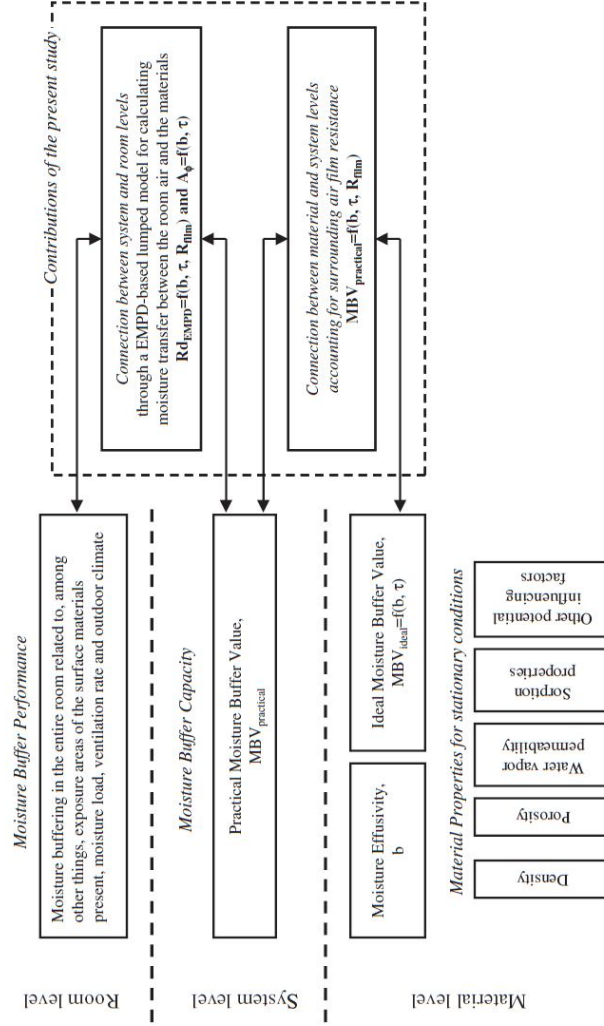


Figure 2.4: Connection between system level and room level (Abadie and Mendonça, 2009)

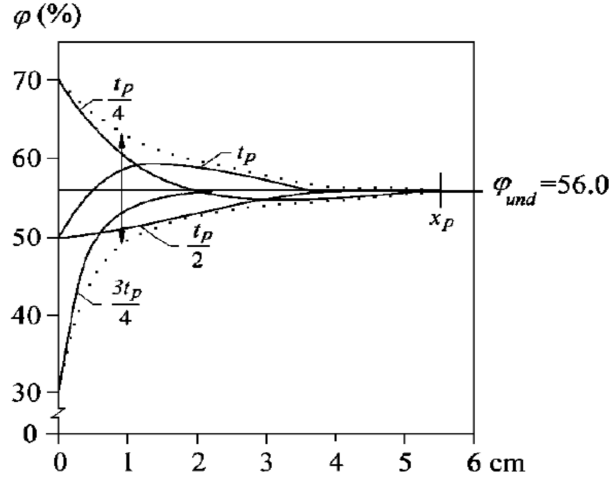


Figure 2.5: The penetration depth (Svennberg, 2006)

2.2.4 Mathematical model

A simplified isothermal theoretical description of moisture buffering is given in Rode et al. (2005), the MBVideal. It uses an analogy to thermal effusivity, the moisture effusivity, b_m ($kg/m^2 Pa s^{\frac{1}{2}}$), which expresses the rate of moisture adsorbed by a material:

$$b_m = \sqrt{\frac{\delta_p \cdot \rho_0 \cdot \frac{\partial u}{\partial \varphi}}{p_s}} \quad (2.3)$$

Where δ_p is the water vapour permeability, ρ_0 is the materials dry density, $\frac{\partial u}{\partial \varphi}$ is the slope of the sorption curve where u is the moisture content and φ is the relative humidity and p_s is the saturation vapour pressure. The function $\frac{\partial u}{\partial \varphi}$ is the slope of the sorption isotherm also defined as the moisture capacity, ξ see equation 2.5.

This model is simplified for isothermal conditions, but the storage capacity is influenced by the temperature which also has a direct influence on the RH. The phenomenon of hysteresis which is very common for clay materials is also not represented in the expression of the moisture capacity. The water vapour permeability is not constant but varies according to the RH (Roels and Janssen, 2006). While assuming it is constant is a limitation, it can however still be used for a simple estimation (Peuhkuri, 2003).

Figure 2.5 illustrates this mathematical problem, where x_p defines the penetra-

tion depth as the point where the variations are less than 1% of the outer surface variation and is therefore referred to as $dp_{1\%}$. Another limit used to describe penetration depth is the $1/e$ value, according to Roels and Janssen (2006) this is a more realistic estimation of the penetration depth. The mean relative humidity within the sample that is not affected by the external variation is defined as the undisturbed relative humidity, φ_{und} .

2.3 Hygric properties of porous building materials

The research in this thesis relates to water in the form of vapour. The interaction between water vapour and a material is called the hygroscopicity.

The conventional background in geotechnical engineering that deals with the interaction between water and a soil is unsaturated soil mechanics. Unsaturated soil mechanics does not accurately represent the hygroscopic domain, it was therefore not considered appropriate for the purposes of this research. More information was found in the science of colloids and interfaces.

This section of the literature review provides some background knowledge on properties that characterise the hygroscopicity of a material and the dynamic interaction between water vapour and a porous material.

2.3.1 Hygroscopicity and moisture storage

The hygroscopicity refers to the interaction between water vapour in the surrounding air and the surface of a solid. Hygroscopic materials respond to a change of relative humidity (RH) and accordingly adsorbing or desorbing moisture.

There is a distinction between adsorption and absorption. The term adsorption describes the enrichment of a material on the interface layer by a fluid or gas as the fluid or gas is attracted to the surface. In the case of moisture buffering the enrichment occurs on the interlayer between the solid soil particle surfaces and water vapour in the air. The term absorption corresponds to the penetration of a fluid into the solid or liquid phase as for example a sponge absorbs water, or water absorbs oxygen. Adsorption generally includes a reduction of surface energy, it is an exothermic process. Heat is released when water molecules are adsorbed on the surface of the particles, this is called the latent heat of condensation (Rouquérol

et al., 1999). Materials that are highly hygroscopic can be referred to as phase change materials as water molecules change phase to a solid after being adsorbed (Morony, 2005). The term absorption being a more generic term is often used instead of adsorption. In the context of this study, the term adsorption will be used. The term adsorbate is the material adsorbed and the adsorbent is the material that is enriched (Novikov, 2003).

The relative humidity (RH), is the most common term used in building physics to express partial water vapour pressure from air. It corresponds to the ratio of partial water vapour pressure over the saturation water vapour pressure for a given temperature, see equation 2.4.

$$RH = \frac{P_w}{P_{ws}} \times 100 \quad (2.4)$$

Where P_w is the partial pressure of water vapour, P_{ws} is the saturation pressure of water vapour at a given temperature. The dew point which appears at 100% RH can vary locally as P_{ws} depends on temperature, therefore in badly insulated buildings condensation can appear on surfaces where the temperature is lower than the surrounding air, at for example cold bridges. If the temperature increases, the saturation pressure increases and therefore the RH decreases. This can visualised on a psychrometric chart, see Figure 2.6.

The psychrometric chart shows the relationship between dry bulb temperature and wet bulb temperature. From these two temperatures the RH can be calculated. Many climatic chambers use a dry and wet bulb to control the RH. When the RH changes, a difference in the vapour partial pressure leads a hygroscopic material to approach equilibrium therefore adsorbing or desorbing moisture. Most materials are to a certain extend hygroscopic but this ability can vary to a great extent in building materials and is related to the available surface area, the surface energy (or affinity to water molecules) of the material and the pore size distribution. There is no unique value to express hygroscopicity.

Sorption isotherms are commonly used to characterise the hygroscopic behaviour of a material. They express the equilibrium moisture content (EMC) for a given RH at constant temperature in the hygroscopic domain. This differs from the soil water characteristic curve (SWCC) from traditional unsaturated soil mechanics, see Figure 2.7. The SWCC also indicates the EMC but for a

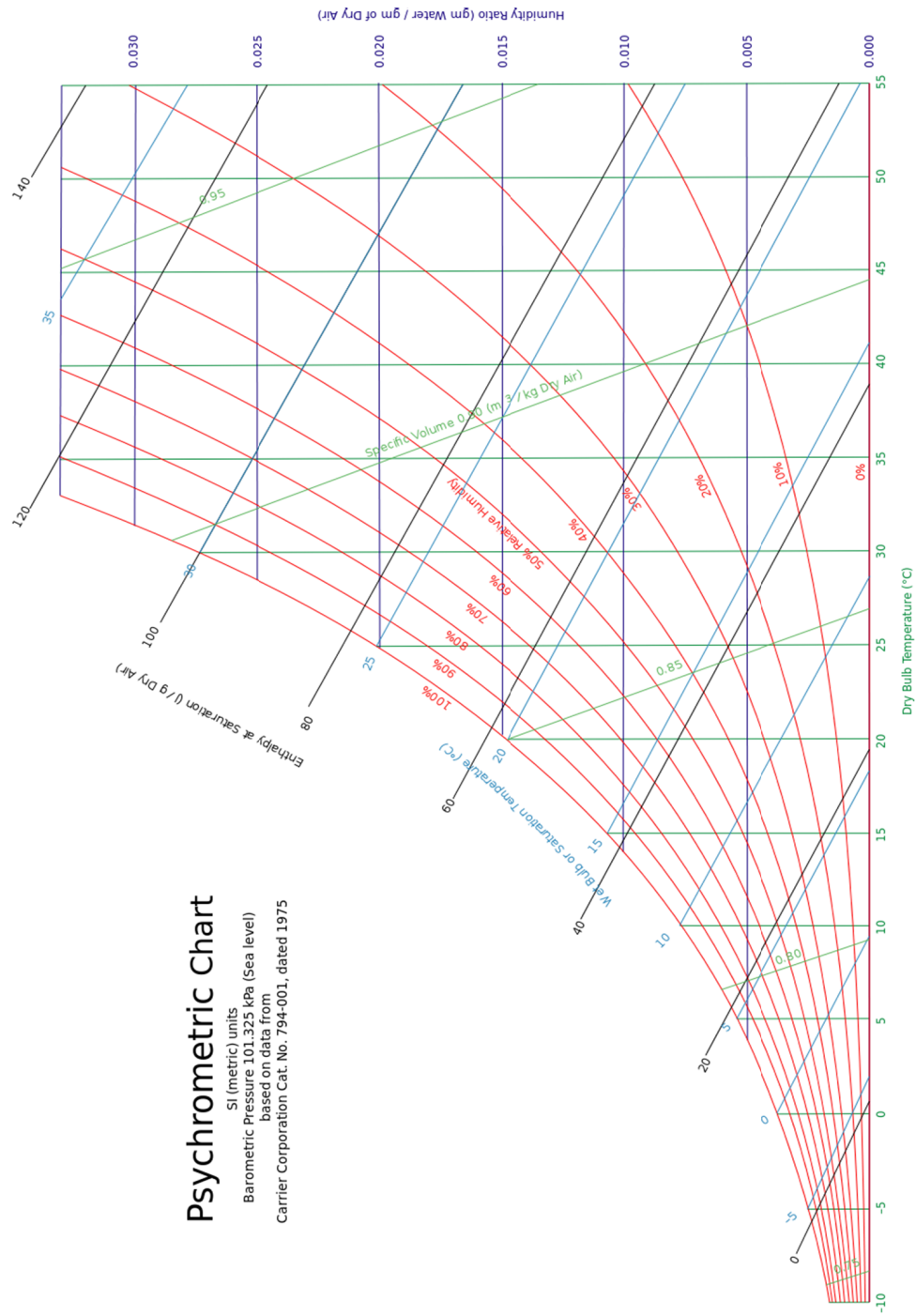


Figure 2.6: Psychrometric chart

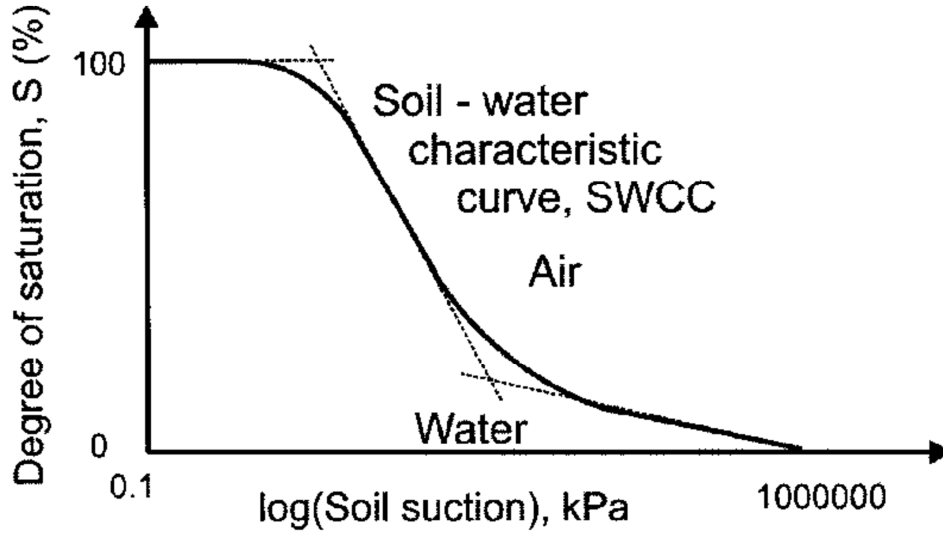


Figure 2.7: Soil Water Characteristic Curve from Fredlund (2006))

given suction pressure or matric suction which corresponds mainly to liquid water retained in the pores of the material and does not give precise information about the hygroscopic domain. The hygroscopic domain corresponds to a very low degree of saturation or moisture content at high suction pressure. For most soils the hygroscopic domain starts at a volumetric water content below 10% which is not well represented on the SWCC as it is difficult to measure suction accurately. Therefore the moisture storage capacity in this work will always refer to the hygroscopic water given by the sorption isotherms.

Sorption isotherms can be classified in different groups, Figure 2.8 shows the 6 main groups. Most soils or aggregates of plate like particles will have a type IIb isotherm with a hysteresis loop. The hysteresis represents the difference between the adsorption path and the desorption path. Hysteresis loops usually appear at higher RH and are associated with capillary condensation. Their exact interpretation is still debated but it certainly involves metastable states of the adsorbate (Rouquérol et al., 1999).

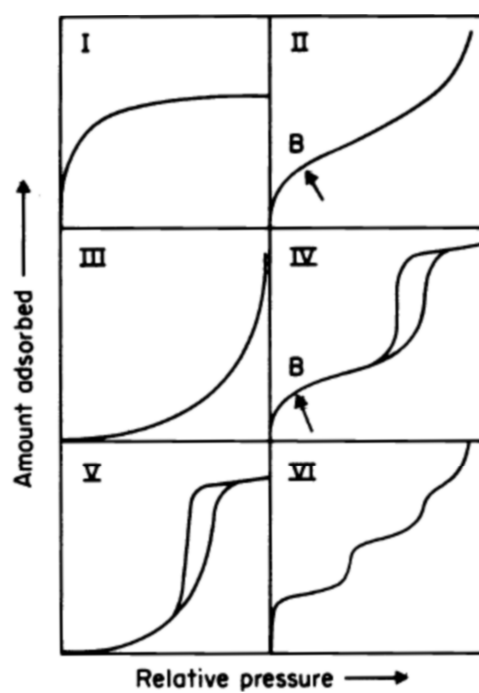


Figure 2.8: Types of sorption isotherms from Sing (1985)

The nature of the process corresponding to each section of the sorption isotherm is well understood. Figure 2.9 describes these processes for water by clay and soil with a simplified representation of soil particles where adsorption is ignored. The initial sharp increase corresponds to the adsorption of one layer of water molecules on the clay minerals. The linear section at mid RH levels corresponds to the adsorption of multiple layers of water molecules. The limit between multilayer adsorption and capillary condensation is not a fixed limit, it usually corresponds to the beginning of the sharp increase of water content towards higher RH. This is the beginning of the capillary domain where the unsaturated soil mechanics background can be applied.

The temperature does influence the adsorption characteristic of the material. Ashour et al. (2011) have measured equilibrium moisture content (EMC) for clay plasters at different temperatures, between 10°C to 40°C. Their results showed a decrease in EMC for an increase of temperature, however the difference was relatively small compared to a change in RH. Künzle (1995) also reports in his thesis that in terms of building physics, the effect of temperature on the EMC can be disregarded between 5°C to 70°C. The effect of temperature on the storage capacity of the material will therefore be disregarded for the purpose of this study and all tests will be described under isothermal conditions.

From the sorption isotherms the moisture capacity, ξ , is obtained, which is given by equation 2.5.

$$\xi = \frac{\partial u}{\partial \varphi} \quad (2.5)$$

Where u is the moisture content in kg/kg and φ is the RH.

In the literature many sorption isotherms can be found for clays used in industry, but not many can be found for soils used for earth building.

2.3.2 Water vapour permeability

The water vapour permeability, also loosely called “breathability”, quantifies the rate of water vapour diffusion through a porous material. The experimental set up and the associated calculations can be found in the EN ISO 12572:2001 Standard for vapour permeability of building products. The water vapour permeability, δ_p (kg/(m.s.Pa)), is measured as the “mass of water vapour transferred through the specimen per area and per time” (ISO-12572, 2001). The experimental tests are

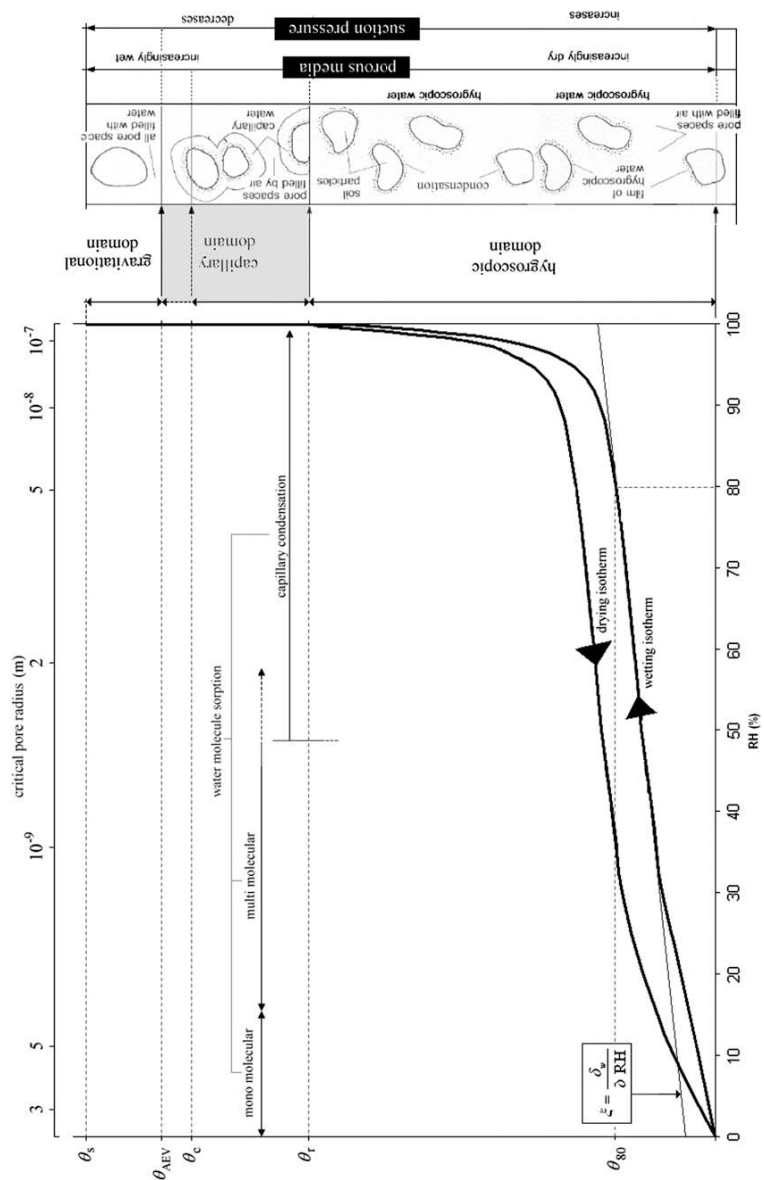


Figure 2.9: Described sorption isotherm from Hall and Allinson (2009)

called “wet cup” or “dry cup” depending on the levels of RH used. To obtain δ_p (kg/(m.s.Pa)), first the water vapour permeance is calculated, W (kg/(m².s.Pa)), which is given by equation 2.6 :

$$W = \frac{G}{A.\Delta p_v} \quad (2.6)$$

Where G (kg/s) is the slope of the regression line obtained from the experimental measurements of the change of mass over time, A (m²) is the cross-section area of the sample and Δp_v (Pa) is the water vapour pressure difference across the sample.

The water vapour permeability is given by equation 2.7:

$$\delta_p = W.d \quad (2.7)$$

where d (m) is the mean thickness of the specimen. Even by following the ISO standard, the measurement of the water vapour permeability can present a large variability. In an “interlaboratory comparison of hygric properties of porous building materials” made by Roels and co-workers (Roels et al., 2004) the water vapour permeability was shown to have significant variations between each laboratory.

Most often the water vapour permeability is expressed through the water vapour resistance factor, μ , which is the default value that will also be used in this work, see equation 2.8.

$$\mu = \frac{\delta_a}{\delta_p} \quad (2.8)$$

Where δ_a is the water vapour permeability of air. A material with a water vapour resistance factor of 10 is 10 times more vapour resistance than air. Table 2.2 provides typical values found in the literature, of the water vapour resistance of earth building materials.

Padfield noted that for a material to improve dynamic moisture buffering the vapour resistance needs to be low (Padfield, 1998). The vapour resistance of a material depends on its porosity and how this porosity is interconnected, its tortuosity. For example, wood has a low vapour resistance in the direction of the end grain because of its tube shaped porosity, but a much higher resistance in

Table 2.2: Values for water vapour permeability from the literature

References	Type of sample	Number of samples	Dry Density (kg/m ³)	Clay content (%)	Vapour resistance factor (μ)
Lustig-Rössler (1992)	Adobe, Silt Clay	5	1780-1820	12	8-9
Lustig-Rössler (1992)	Adobe, Fat Clay	5	1900-1960	28	9-12
Allinson and Hall (2010)	Rammed Earth	3	1980-2120	10	4.6-7.8
Liuzzi et al. (2012)	Rammed Earth	6	1829-2046	-	8.10-11.10
Hansen and Hansen (2002)	Unfired Clay Brick	3	2000	10-20	12.5
Hansen and Hansen (2002)	Unfired Clay Brick	3	2100	10-20	13.1

the traversal direction to the end grain. This allows end grain wood to rapidly adsorb moisture and therefore efficiently buffer RH even though the isotherm is independent of direction.

2.3.3 Surface moisture transfer resistance

The surface film is considered as a static layer of air at the surface of the material and therefore offering a resistance to the inflow of water vapour into the porous material. There is little information in the literature about the impact of surface film resistance on moisture transfer although it is mentioned in Rode et al. (2005) that it should be kept constant to a certain value. The JIS standard (JIS-A1470, 2002) proposes a method to calibrate the surface film resistance in the test apparatus, but since most of climate chambers don't have an adjustable ventilation, this would in most cases be set by using windshields.

The surface moisture transfer resistance can be estimated using the Lewis relation described in Rode et al. (2005). For interior conditions with typical air velocity around 0.1 m/s it can be assumed to be $5 \cdot 10^7 \text{ m}^2 \text{ s Pa} / \text{kg}$.

The surface resistance is considered as negligible for most conditions compared with the internal resistance of the material. However, some authors suggest it must be taken in consideration and may have a more important role than expected.

ted, especially for materials with low resistance.

Gómez et al. (2011) tested the influence of the surface film resistance during a dynamic moisture adsorption test. To do this they created a experimental set up where the air speed could be adjusted. For the materials they have tested, the maximum MBV was obtained with an air velocity over 0.2m/s, the change was significant with 55 g/m² adsorption for a 0.3 m/s air velocity and 36 g/m² adsorption for 0 m/s air velocity. This represents a loss of 35 % of its adsorption capacity.

Allinson and Hall (2012) also identified the surface resistance as playing a major part to the deviation observed between numerical calculation of MBV and experimental results.

Worch (2004) investigated the vapour transfer resistance of building materials. He mentioned that the mass transfer of vapour at the surface under natural convective conditions was greater for some porous building materials than liquid water. Liquid water was always assumed to have the greatest evaporation potential (Worch, 2004), this helps to understand why the surface resistance can have such considerable reduction of the adsorption potential.

During the Round Robin test realised in the Nordtest project (Rode et al., 2005) different air velocities were measured due to the different experimental setups, however no systematic evidence of the effect of the air velocity on the dynamic adsorption properties was observed.

A numerical investigation of the influence of surface film resistance was performed by Roels and Janssen (2006). For 4 different materials, wood fiberboard, plywood, aerated cellular concrete and gypsum plaster. The results showed the surface film resistance has a variable influence depending on the material, e.g. when increasing the surface resistance from a negligible value to $5 \cdot 10^7 \text{ m}^2 \text{ s Pa} / \text{ kg}$, the moisture buffering value decreased by 20 % for a wood fiberboard and only 9% for the gypsum plaster. It was also stated that the surface resistance is influenced by the geometry and size of the sample.

2.4 Clay minerals and their adsorption properties

2.4.1 Clay minerals: a definition

Clay minerals are hydrous layer silicates formed by the weathering of rock. Their crystallography is complex, and often referred to as a solid solution. Most often the crystals present structural defects and isomorphic substitutions.

A common feature is the stacking of tetrahedron (T) and octahedron (O) layers as T-O-T or T-O structures are also named 2/1 structures and 1/1 structure. Fig 2.10 illustrates the complex shapes that clay minerals can have. These shapes are not as well defined in soils where the weathering and erosion decreases the crystallinity of individual platelets.

A 1/1 structure where a tetrahedral sheet is bonded to an octahedral sheet is typically a Kaolinite, see Fig2.11. A 2/1 structure is a octahedral sheet in between two tetrahedral sheets, this being typically a smectite or illite (Meunier, 2005), see Fig 2.12.

The chemistry of 2/1 clay minerals is variable and is often considered unique to each soil or deposit. The cations in the centre of the tetrahedron are most often Si^{4+} and then Al^{3+} or Fe^{2+} , whereas the octahedron cation is mainly Al^{3+} , Mg^{2+} , Fe^{3+} or Fe^{2+} . Isomorphic substitution in the tetrahedron and octahedron layers creates negative surface charges which are compensated by interlayer cations.

These interlayer cations can hydrate in certain conditions and create an increase in volume during hydration or decrease during dehydration, this is the swelling or shrinkage characteristic of 2/1 clay minerals. This is the case with 2/1 minerals whereas the 1/1 minerals have a very low surface charge and therefore have no interlayered cations and typically lower shrinkage. The main adsorption sites by kaolinite type clay minerals are located on the edges due to OH groups completing the sectioned tetrahedrons or octahedrons.

Sorption isotherms can be found in the literature but they are not systematically tested with air and water vapour, most often other gases such as nitrogen are used. Each gas will have different sorption behaviour; therefore a nitrogen sorption isotherm must not be used instead of water vapour isotherm when studying the water vapour sorption behaviour. In the book of Rouquérol et al. (1999) a chapter is specifically dedicated to the adsorption of clays and modified clays.

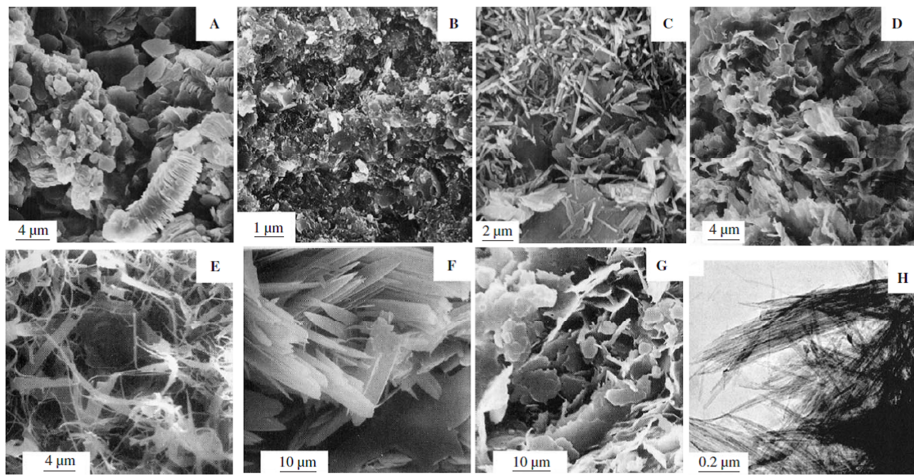


Figure 2.10: Transmission electron micrographs of some clay minerals with varied particle morphology: (A) kaolinite from Sasso (Italy) showing typical books of particles; (B) high-quality flint clay from Gasconade County, Missouri, USA; (C) tubular halloysite particles alongside kaolinite plates from Sasso, Italy; (D) smectite or illite/smectite from Sasso, Italy; (E) filamentous illite from sandstones in offshore Netherlands; (F) lath-shaped illite from sandstones in offshore Netherlands; (G) pseudo-hexagonal illite particles from sandstones in offshore Netherlands; (H) fibrous palygorskite from Southern Georgia (USA). These images were taken from Bergaya and Lagaly (2006) who had previously taken them from various authors.



Figure 2.11: 1/1 type clay mineral, from Meunier (2005)

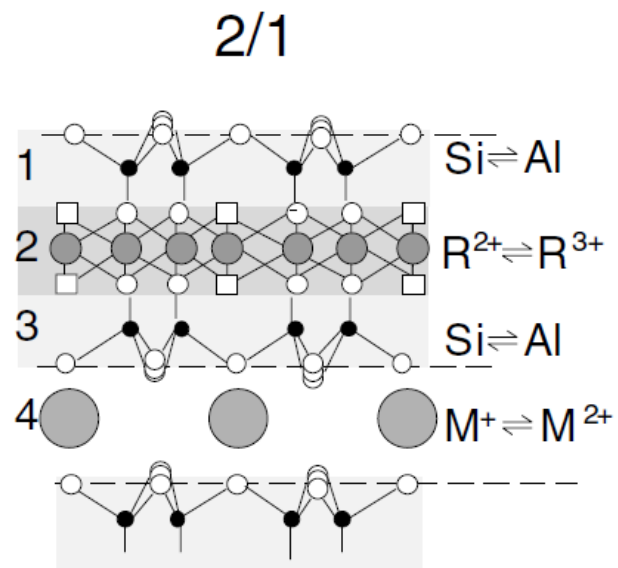
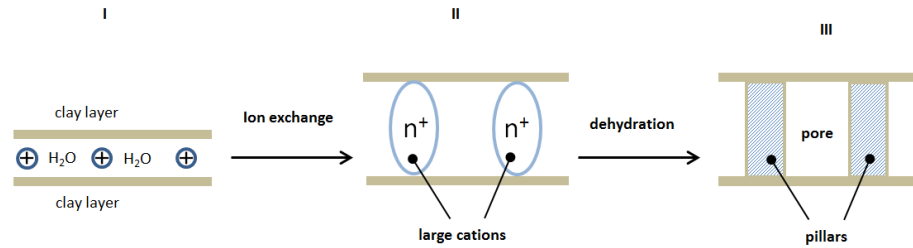


Figure 2.12: 2/1 type clay mineral from Meunier (2005)



is

Figure 2.13: Pillared clays modified from Rouquérol et al. (1999)

Studies have shown that the nature of the compensating cations will have an impact on the sorption behaviour of the clay mineral (Dontsova et al., 2004).

Each clay mineral has a specific amount of cations it can release and exchange, this is called the Cationic Exchange Capacity (CEC). The higher the CEC the more cations can be exchanged. Cations have by their nature variable hydration potentials and therefore influence the sorption characteristics. “Modified clays”, for example pillared clays, which have an artificially increased interlayer adsorption capacity have been developed in recent years by research for the catalytic industry, see Fig2.13.

An example is given in Rouquerol et al. of a pillared Montmorillonite which shows nitrogen adsorption values 4 times higher than a normal Montmorillonite and even 6 times higher with additional heat treatment. It also appears that this may considerably reduce the shrinkage and swelling of Smectite types of minerals. These types of technologies open a wide range of application in building materials to design materials with specific characteristics as both increased adsorption and

reduced swelling could be desirable.

A further interesting aspect of clay minerals is their ability to adsorb organic compounds. Theng (1979) produced a monograph on these interactions. This phenomenon is extensively studied by soil scientists due to the formation of humus in soils which are clay polymer complexes. These studies lead to the engineering of new nanocomposites termed “organoclays” or “Bentones” which are used in many industries (Ruiz-Hitzky and Van Meerbeek, 2006).

Recently some authors investigated the possible reduction of organic pollutants in the indoor environment by the presence of a clay plaster (Darling et al., 2012). Darling et al. (2012) measured a decrease of pollutant concentrations with the presence of clay plaster and an increased perceived air quality (PAQ), which was determined by a panel of 24 human subjects. They categorise clay plaster as a passive removal material (PRM), which can remove indoor pollutants without the formation of by-products (Darling et al., 2012). This is directly linked to the ability of clays to bind molecules to their surface.

A study was conducted by Ruiz et al. (1998) to quantify the adsorption of Volatile Organic Compounds (VOCs) from gases onto different soil particles. Sand, limestone and clay gave clearly distinct results, the clay adsorbed one order of magnitude more than sand and two orders of magnitude more than limestone (Ruiz et al., 1998), which indicates clay should have greater benefits for indoor air quality than just passive humidity regulation. Clay minerals will also interact with the pollutants such as ozone.

2.4.2 Sorption properties

The adsorption capacity of soils containing a high clay fraction has been known for a long time and this property was traditionally used to remove fat from animal wool using a process called “fulling”. Therefore the term “Fuller’s earth” emerged. Clay has been used to refine vegetable oils and even stabilize beer or improve the taste and quality of juices and cheap wines. It has also been used as soap (Harvey and Lagaly, 2006).

The adsorption capacity of soils is largely due to charged colloidal particles being clay minerals. The high surface area of colloidal particles can reach values of close to 1000m^2 per gram. This received increasing attention in the 20th century when clay science developed as a discipline. Interface and colloid science

explores the interactions occurring at particles interfaces, opening a whole new field of engineering. Adsorption properties of clay materials, in particular Bentonites, are increasingly used in the Chemical industry, Environmental technology, Agriculture, Food industry, cosmetics, pharmaceuticals and others.

However, Bentonites are usually avoided in earth building because of their swelling properties, and research is therefore needed before they are used for moisture buffering.

2.5 Review on the moisture buffering capacity of unfired clay masonry

The previous sections have shown that earth building has a long history and that earth can buffer humidity and this can benefit occupant health, energy use and durability. A reasonable amount of work was done in building physics on the importance of an envelope participating in the hygric balance of a building. However, there has been only limited research into humidity buffering by earth. The main research on the moisture buffering capacity of unfired clay masonry was undertaken in Germany in the early 1990's by Lustig-Rössler for a thesis under the supervision of Gernot Minke (Lustig-Rössler, 1992). In this work, they measured the water vapour permeability, sorption isotherms and dynamic adsorption of three different soil compositions. The three tested soils were as follows:

- “Mortar-Clay”, 14% of clay, 24% of silt, 57% of sand and 5% of gravel
- “Silt Clay”, 12% of clay, 75% of silt, 11% of sand and 2% of gravel
- “fat Clay”, 28% of clay, 33% of silt, 37% of sand and 3% of gravel

The dynamic moisture buffering test consisted of stabilising the samples for about 8 weeks at 35% RH in a climate chamber until the samples had reached equilibrium moisture content. The RH in the chamber was then increased to 75% RH and lowered back down to 35% RH for a 24h cycle and an 8h cycle. Tests were then run for 8 consecutive cycles. The results are presented as bar graphics showing the final mass change in g/m^2 after each 24h or 8h period.

During this study these three soils were used as a base to further investigate different samples thickness of 1, 2, 3 and 4 cm, different waterproofing coats

and different plaster formulations. Soil samples were also compared with other building materials such as gypsum, lime, cement plasters or treated and untreated wood.

The average moisture uptake for 8h periods for each soil and conventional materials at 1 cm thickness is provided in table 2.3.

Table 2.3: Moisture buffering results from Lustig-Rössler (1992)

sample	8h moisture uptake (g/m ²)	Equivalent MBV (g/m ² .%RH)
Mortar-clay (1cm)	45	1.12
Silt clay (1cm)	65	1.62
Fat clay (1cm)	60	1.5
Cellular concrete (1cm)	78	1.95
Fired Brick (1cm)	1	0.025
Plasterboard (1cm)	1	0.025
Wood (1cm)	25	0.625

The samples were prepared as 10x10 cm cubes, 5 faces were sealed for the moisture buffering test with chlorinated rubber paint and paraffin.

The experimental set up for the moisture buffering test is not described, neither is the sample preparation. There is no mention of surface film resistance or air velocity in the climate chamber and the results are therefore not comparable with other research.

Experimental measurement of moisture buffering were performed on Stabilised Rammed Earth in Allinson and Hall (2012). Three different particle size distributions were tested, the proportions are given per dry mass and no information on clay mineralogy was provided:

- “613” mix, which represents a mixture of 60% of sand, 10% of gravel and 30% of silt and clay
- “433” mix, 40% of sand, 30% of gravel and 30% of silt and clay
- “703” mix, 70% of sand, 0% of gravel and 30% of silt and clay

These mixes were stabilised with 10% per dry mass of Portland cement. The MBV was obtained from the 33%/75% cycles used in the Nordtest project with the time period of 8h and 16h. The MBVpractical varied between 0.68 and 1.29 g/m²%RH with the highest value for the “703” mix with no gravel.

2.6 Summary

The idea that porous building materials participate to the internal air moisture balance of buildings has become wide spread and has widely been implemented in studies and heat and mass transfer models. Clay has become a reference in terms of moisture buffering. Commercial unfired clay products are always presented as having this highly attractive capability of regulating the indoor air quality. However there has been only a few research projects where clay was investigated and each one using different methods. These mainly presented clay as a good buffering material when compared to other materials but did not reach into further detail on the variability of clay and its influence on moisture buffering.

This research was therefore directly focused on two aspects:

- using a test method also used by other laboratories and characterising the potential influence of this method on the results to obtain reliable data.
- Investigate the soil properties and in which way their variability may influence the moisture buffering. Based on the described sorption properties it seems likely that clay minerals have an important effect on the moisture buffering this is why these are an important section in this research.

Characterising the influence of earth building materials on a room level is out of scope for this research project. The outcome should allow to choose material properties in order to optimise its moisture buffering capacity.

3 Materials and methodology

This chapter describes the materials and test methods used to achieve the aims of the research.

3.1 Materials

Samples were prepared with variable composition (particle size distribution, mineralogy), physical properties (apparent density which directly influences the pore size distribution). Properties such as initial water content for compaction and the mixing method used were varied as these could affect the structure. In order to obtain variable material composition, natural and artificial soils were used. The aim is to obtain set of samples with known properties to understand how these can impact the hygric properties.

3.1.1 Nature of soils

The natural soils were sourced in the UK from brick manufacturing companies, and one was sourced in France provided by the ENTPE in Lyon which has been used for the construction of a rammed earth house. The brick soils from the UK were coded as follows : (Gr, Ib, Al, Bi, Ch, Le and Th). The soil from France was named St.

To understand the influence of the nature of the clay minerals, artificially composed soils were prepared with a systematic variation of their composition. Individual ingredients such as clay, silt and sand which are the main components of natural soils were used in determined proportions. The clay minerals used in the artificial soils were a 99 % pure Kaolinite sourced from IMERYS in Cornwall, a commercial Bentonite (Ca Montmorillonite) and a pillared Bentonite both sourced from OLMYX in France. The main clay mineralogy and particle size distribution of soils used are presented in table 3.1.

Table 3.1: Soils used

Soil	Main clay mineralogy	Clay: <2 μm (%)	Silt: 2-63 μm (%)	Sand: 63 μm -2 mm (%)	Gravel: >2 mm (%)
Gr	Illite/Smectite	18	24	58	-
Ib	-	25	33.8	31.7	-
Al	Kaolinite, Illite/Mica	25.4	50	24.6	-
Bi	Kaolinite, Illite/Mica	50.1	39.5	10.5	-
Ch	Kaolinite, Illite/Mica	38.6	57.3	4.1	-
Le	Illite/Mica	14.8	66.7	17.2	-
St		16	10.3	26.3	44.4
Th	Kaolinite, Illite/Mica	5.5	25.1	25.4	-
Artificial soil 1	Kaolinite	20	20	60	-
Artificial soil 2	Kaolinite, Bentonite	25	20	55	-
Artificial soil 3	Kaolinite, Pillared Bentonite	25	20	55	-
Plaster 1		1.4		96.6	2
Plaster 2		10		84	6

The clay mineralogy of natural soils was determined by X-ray diffraction from a previous study (Maskell et al., 2014).

A total of 24 100 mm \varnothing test specimens of earth plasters were prepared from both UK (Plaster 2) and German (Plaster 1) suppliers. For each supplier, 12 samples, including three of a 12 mm undercoat, three of a 20 mm undercoat, three of 12 mm undercoat with 3mm finishing coat and three of 20 mm with a 3 mm finishing coat. The exact nature of additives and mineralogical composition of the plasters was not provided by the manufactures.

Table 3.2: Overview of sample groups and properties investigated				
Group	Type	Soils used	Modified parameters	Number of samples
I	SCEB	Gr	addition of stabiliser	18
II	CEB	Gr	initial water content	9
III	CEB	Ib	initial water content	9
IV	CEB	Artificial soil 1	apparent density	9
V	CEB	Artificial soil 2	mixing method	9
VI	CEB	Artificial soil 3	Bentonite content	18
VII	CEB	Al, Bi, Ch, Le, Th and St	Mineralogy, particle size distribution	18
VIII	Plasters	plaster 1	thickness and finishing coat	12
IX	Plasters	plaster 2	thickness and finishing coat	12
X	Results from Lustig-Rössler (Lustig-Rössler, 1992)			

3.1.2 Soils composition

Samples were prepared to represent the variability in composition and preparation methods of unfired clay masonry and to recognise the properties influencing the moisture buffering. Table 3.2 presents the different group of samples, each group was prepared in order to vary a single property if possible in the material. It was not always possible to prepare the samples with only one variable, for example the groups II and III were prepared to investigate the influence of the initial water content but the increase of water content also increased the shrinkage during drying which then also increased the desired apparent density. For this study samples were compacted to the required apparent density rather than compacting to the maximum apparent density what would normally be the case.



Figure 3.1: Small mortar mixer

3.2 Sample preparation

3.2.1 Mixing

For all small samples a small laboratory mixer was used which was most effective for the quantities that had to be prepared. For samples in group V, one material was used with different mixing methods to see if this would have any influence on hygric properties as this could have an impact on the internal structure. The difference in mixing method mainly consisted in using different mixers. The results are presented in Chapter 4 but the different mixing processes are described here.

- Small laboratory mixer, Figure 3.1
- Large laboratory mixer, Figure 3.2
- Hand mixing, Figure 3.3

The plasters were always mixed by hand using a pallet knife and a plastic bowl until the right workability was achieved and following the recommendation from the manufacturer.



Figure 3.2: Large mortar mixer



Figure 3.3: Hand mixing bowl and pallet knife

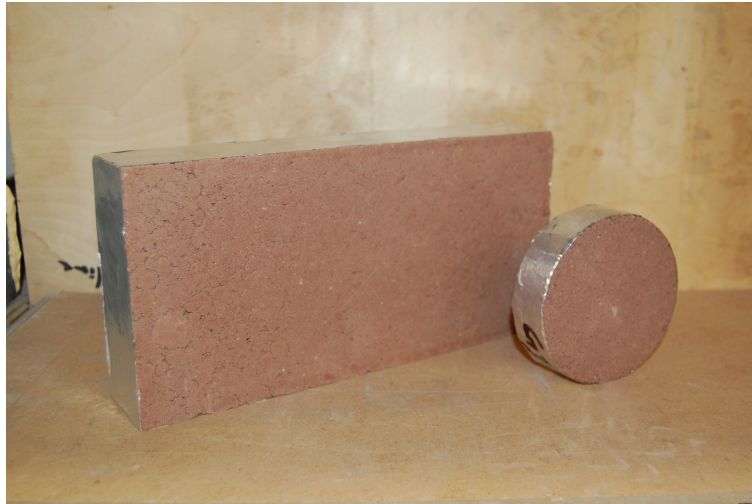


Figure 3.4: Size of samples used

3.2.2 Size, thickness and compaction

3.2.2.1 Large samples

The initial tests were done for group I (see section 2.0) with full sized bricks of 288 mm x 140 mm x 48 mm, see Figure 3.4. This size was problematic because of the precision of the scales, these samples could only be weighed on scales with a precision of 0.1g or less. Furthermore, insufficient source material was available to prepare large samples for all groups. The larger samples were prepared with a CIV-RAM manual press. The disadvantage of using the CIV-RAM press is that it was not possible to control the apparent density as required.

The large samples were prepared using a traditional CIV-RAM manual press, see Figure 3.5.

3.2.2.2 Small samples

As large samples were an issue for the moisture buffering test and for the water vapour permeability test were the samples had to be sealed air-tight on containers, smaller cylindrical shape samples were prepared, see Figure 3.4. The smaller cylindrical shape presented advantages for the water vapour permeability test and the moisture buffering test. The cylindrical shape was easier and faster to seal to a round plastic cup then it would have been for a large rectangular shape. The smaller size allowed a larger number of samples to fit into the climate



Figure 3.5: CIV-RAM press

chamber allowing entire groups to be measured at the same time.

The cylindrical samples were prepared with an adapted Wykeham Farrance 50kN triaxial frame, see Figure 3.6, and a proctor mould used with a 100mm plastic sewage pipe as a form see Figure 3.7. The samples were compacted to a constant size rather than to a constant compaction force.

3.2.2.3 Plasters

The two commercial plasters, from the UK and from Germany were prepared to two different thicknesses, three samples of 12 mm and three samples of 20 mm for each in the shape of a disc of 100 mm in diameter. In addition, the same number of samples was prepared including the finishing coat from each brand with a thickness of 3 mm. The exact nature of additives and mineralogical composition of the plasters was unknown. The 12 mm thickness is the recommended thickness by the manufacturer and 20 mm was prepared to check if it would improve the sorption capacity.

Plasters were also prepared with different contents of fibers to determine their effect on moisture buffering. The commercial product comes with fibers and these were removed and replaced with fibers of different nature to ensure consistent fibers between mixes. The fibers used were corn stem, barley straw and barley

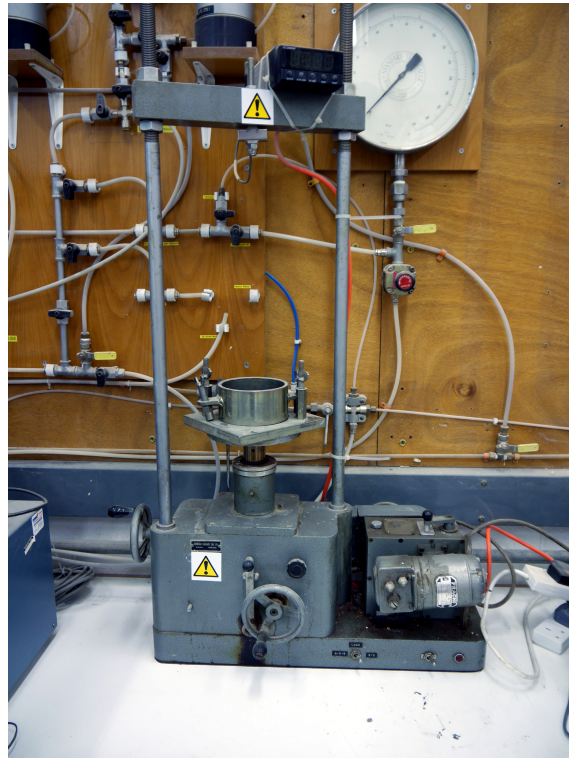


Figure 3.6: Adapted Wykeham Farrance triaxial frame

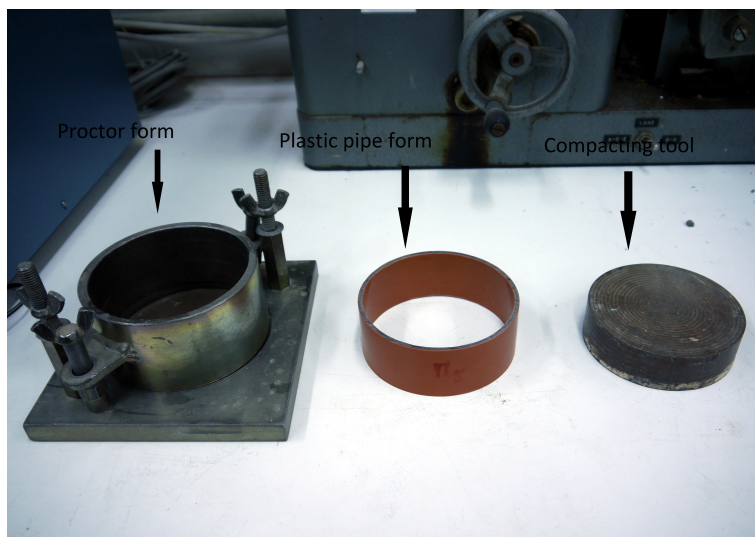


Figure 3.7: Plastic drain pipe used as form



Figure 3.8: Samples of 70 mm, 50 mm and 30 mm

wool. This will be described in detail in Chapter 6.

The plaster samples did not require any compaction and the soil was applied into the form as it would be done on a wall using a plastering trowel.

3.2.2.4 Thickness

The thickness was experimentally determined, the soil from the group I and a soil available in the laboratory (Ib) was used to prepare six samples, three for each soil with a thickness of 30mm, 50mm and 70mm, see Figure 3.8. The moisture buffering test was performed on these samples and the results are presented in Chapter 4. No significant difference in the sorption behaviour between the different thicknesses could be observed. This was further confirmed in the literature, where the penetration depth for clay materials was found to be below 16mm (Padfield, 1998). The final size of the samples were therefore chosen to be discs with a diameter of 100mm and a thickness of 30mm as shown in Figure 3.8 by the last sample on the right.

3.2.3 Water content

The water content is the water mixed with the soil to give it a sufficient workability in order to be able to compact it. The water content at which the highest density is achieved through a standard compaction method is called the optimum water

content. The optimum water content is variable and depends on the nature of the material and the compaction method. The classical method to determine the optimum water content is the proctor test. The proctor test consists of dynamically compacting the soil at different water contents using a standard compaction energy and determining the relation between dry density and water content.

Some authors (P'KLA, 2002) have suggested this method is not suitable for compressed earth blocks in which the compaction is static and not dynamic. Therefore the water content was determined similarly to the drop test described by Minke (2012) based on the texture of the mix.

In this work samples are compacted (see section 2.3) with a hydraulic ram in order to achieve a known apparent density. Therefore the water content was determined arbitrarily during the mixing stage to obtain sufficient workability of the material. It needed to be sufficiently humid to allow compaction but dry enough to reduce shrinkage to a minimum. This is achieved when the dry soil (powder) starts to aggregate without forming clumps bigger than 5 mm. A precise determination of the water content was then achieved by using the Standard BS1377-2 (1990) which requires drying the soil at 105°C.

Samples in group 4 were prepared to determine the influence of a varying initial water content on adsorption properties. The water content at compaction was gradually modified.

3.2.4 Drying

All samples were dried in a room with constant humidity and temperature conditions. The RH was maintained at 60 % +/- 5 % RH and at 20°C +/- 1%. The samples were allowed to dry for at least a month.

Only samples stabilised with a geopolymer had to be dried differently, this process is further explained in the section relevant for this group.

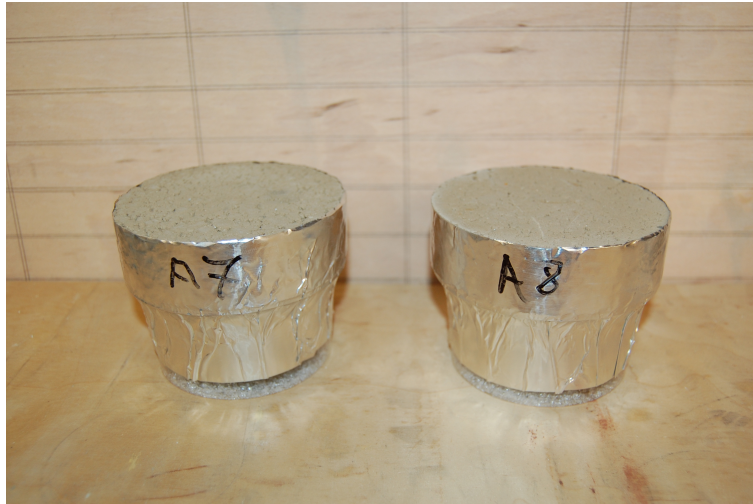


Figure 3.9: Sample set up for water vapour permeability test

3.3 Testing

3.3.1 Water vapour permeability

Water vapour permeability was tested in accordance with the ISO 12572:2001 standard (2001); using the wet cup method. The wet cup method was preferred as the RH levels used are closer to the ones used during the moisture buffering test. The sample was sealed to the top of a plastic container which contained a saturated salt solution of potassium nitrate to maintain a RH level of 94 %, see Figure 3.9.

The container was then stored in a TAS[®] environmental chamber maintained at 50 % RH and 23° C. To provide a vapour-tight seal around the samples aluminium tape was used as this provided suitable performance in previous tests (Svennberg, 2006). Additionally, a thin bed of silicone was applied to seal the sample to the plastic cup. The water vapour resistance factor was determined from the water vapour permeability of the sample compared to the water vapour permeability of air, see Chapter 2. All measurements including MB were performed in the same climate chamber. Measurements taken in the chamber using a hot wire anemometer indicate an average air velocity of 0.65 m/s.

According to previous studies, the water vapour permeability test is prone to errors. In Roels et al. (2004) a round robin test was undertaken to determine the hygric properties of some building materials, and the water vapour permeability

had the widest deviation. Recommendations from the standard could actually be the source of error. The standard recommends only up to 15 mm of air gap between the sample and the top of salt solution level. When manipulating the samples, this solution can easily be put in contact with the sample, thereby affecting the results.

To overcome this potential experimental error, a test was undertaken to check if the distance of 15 mm was actually necessary or if it could be larger. Samples from group V which all had similar vapour permeability were used to obtain results with different salt solution levels. These results are presented in Chapter 4 and did not show any significant difference for an air gap of 15, 25 and 35 mm. The salt solutions for the following tests were therefore prepared with a 35 mm air gap as this avoided too close contact to the sample and was more economic in quantity of salt.

3.3.2 Sorption isotherms

To determine the sorption isotherms, two tests were followed, one using the salt solution method and the other one the DVS equipment. The advantage of the salt solution method was that larger samples and a greater number could be measured at the same time, the disadvantage was the lack of precision and the time needed for the test. The DVS method had the advantage of a much greater precision as it uses a microscale, but the disadvantage of only being able to measure up to 1 g of material, the time was also a problem with this method.

3.3.2.1 Salt solutions

The method proposed by the standard ISO-12571 (2000) was followed with some modifications. Samples of a minimum of 10 g were placed in increasing RH levels. At first the samples were oven dried at 105 °C to start the test from the dry mass. They were then placed in levels of 22, 33, 53, 75 and 94 % RH using an air tight plastic container, see Figure 3.10. A RH and temperature sensor was placed in the container to verify the levels.

The samples were weighed every 5 days and if no more than 0.02 g variation was observed between two measurement, then it was considered to have achieved the equilibrium moisture content for this RH level and then placed at the next

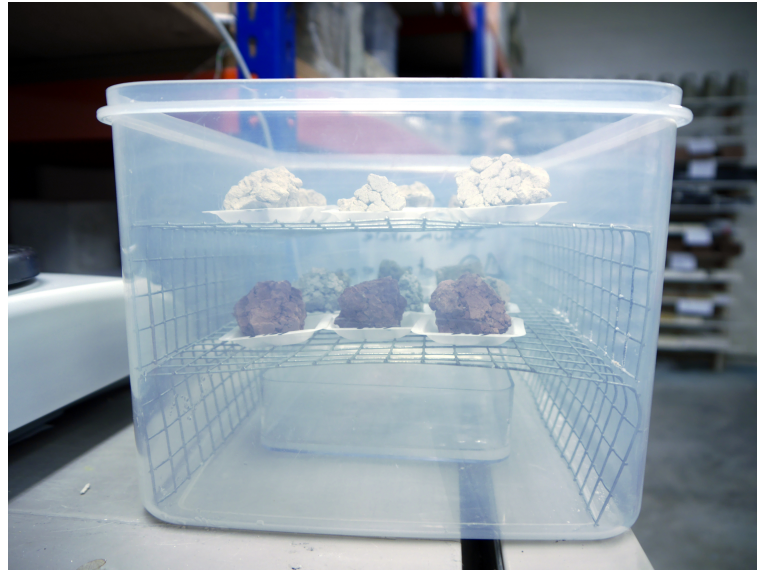


Figure 3.10: Salt solution sorption isotherm set up

RH level. The RH within the box was monitored using a Tynitag temperature and humidity sensor.

It was rapidly shown that the DVS test presents a much greater precision to measure the sorption isotherms (McGregor et al., 2014), therefore this method was preferred.

3.3.2.2 Dynamic vapour sorption

Dynamic Vapour Sorption (DVS) testing using the “Intrinsic” model was undertaken to determine the sorption isotherms of the material. Unlike the other test where three samples were tested per material, only one sample was measured per material using the DVS method. The main reason being the time necessary for each measurement. The adsorption and desorption curves could be obtained within 10 days for each material, but only one sample could be tested at a time.

The following assumptions were made for the measurement of sorption isotherms:

1. For a hygroscopic material with particle size smaller than 2 mm and a homogenous distribution, a sample of less than 1g is representative of the adsorption process on the particles (Engelund et al., 2010).
2. The precision of the instrument makes the repetition for each sample as with the MB test and water vapour permeability test unnecessary.

3. The adsorption at very high RH (above 90 %) may be underestimated because total equilibrium could not be reached in the specified maximum time allocated, but this is not considered a problem as these high humidity levels are unlikely to be achieved for an extended period in a real building. This assumption was expected to slightly reduce the hysteresis because the maximum EMC at high RH is lower.

Each step in RH during the DVS measurement was incremented either when a stable mass was achieved with less than 0.0001 % mass change per minute or a maximum time interval of 360 min was reached for each RH step.

3.3.3 Moisture buffering test

Moisture buffering was measured in terms of water vapour adsorption in response to cyclic humidity variations. This was according to the recently published ISO 24353 standard ISO-24353 (2008) and the Nordtest protocol (Rode et al., 2005). Both of the methods use gravimetric measurements and they mainly vary in the procedure of the test, the time-steps used, the humidity levels, and the sample sizes. There are various sets of RH levels proposed by both methods and the soil samples were therefore tested using different RH cycles and with varying time steps to compare the results from different tests.

For the moisture buffering test the samples were sealed on all but one side with aluminium tape which is completely water vapour impermeable and does not adsorb a significant quantity of moisture itself. The choice of aluminium tape was based on previous study where different sealing materials were compared (Svennberg, 2006).

Although both test methods were used, the Nordtest method was predominantly used as there is more data for this method in the literature.

- Initial testing

Initial tests were undertaken to determine the effect of sample thickness, sample size, logging method, surface film resistance, RH levels and time steps. This was to determine the importance of the boundary conditions in the moisture buffering test.

Experiments were performed using three different RH cycles, 33% to 75% RH, 53% to 75% and 50% to 85%. The recommended cycle by the Nordtest project

was of 33% to 75%. Initially 50% to 85% was chosen as the available climate chamber could not reach levels below 50% and these values are more realistic for humidity conditions in the UK. However, with the later addition of a climate chamber capable of reaching levels of 33% RH, the levels of 33% to 75% RH were preferred so the materials MBV could be compared with MBV of conventional materials available in the literature.

Comparison was made between the results at 53% to 75% and 50% to 85% in McGregor et al. (2014), and it was concluded that for the measured materials the variation of the material from one cycle to another remains proportional. These results will be presented in further detail in Chapter 4 along with comparison of results from 33%/75% cycles and 50%/85% cycles.

Equally two different time steps exist in the currently proposed methods, a 12h/12h cycle with a equal time allocated for adsorption and desorption and a 8h/16h cycle with 8h allocated for the adsorption phase (high RH levels) and 16h for the desorption phase. The 8h/16h cycle was chosen as this would correspond to the typical usage of an office or a bedroom and is easier to test manually as it corresponds to changing humidity levels during a normal working day.

In the office, a high RH is create by the emission of humans in the room for 8h during the day, whereas in a bedroom the same happens at night time. The 16h period corresponds to the time where the room remains empty.

The results are presented as the MBV obtained from the measurement in Chapter 4 whereas the measurement for each individual sample is given in Annex I. The measurement for each individual sample is graphically plotted as g/m^2 over time, this typically gives a curve such as in Figure 3.11. The MBV is calculated as change in mass over change in RH. In the Figure 3.11 the results for the Lime 4%, Lime 8% and Geopolymer samples do not reach a complete desorption of all the moisture that was adsorbed during the cycle, which indicates that these samples have not reached dynamic equilibrium.

Initial test were done with two different climate chambers, and an additional windshield in a further case. This allowed the measurement of the same samples under different air velocities.

Several parameters were identified to have an influence on the moistue buffering test and were published in McGregor et al. (2014). These observations are detailed in chapter 4.

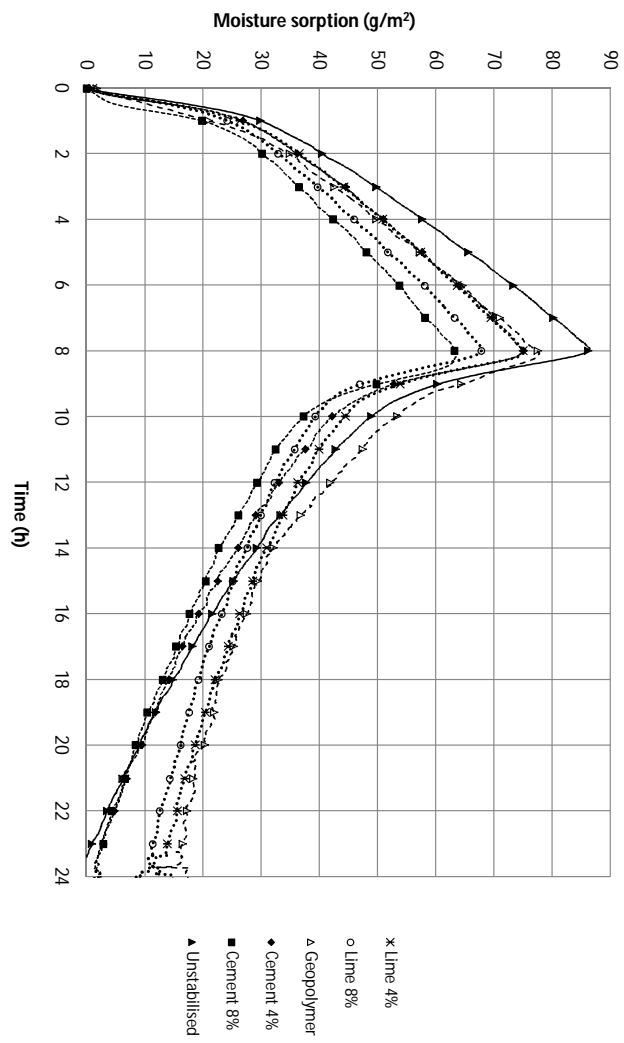


Figure 3.11: Example of MB test results

- Final test protocol

The final test protocol adopted after investigation of different boundary conditions was to use cycles of 33% to 75% with time steps of 8h at high humidity and 16h at low humidity. The samples were measured per group, therefore 9 samples were placed at the same time in the chamber. The surface resistance was chosen to be as low as possible therefore a high ventilation rate was maintained in the chamber (average of 0.65m/s). The mass was recorded on a scale with a accuracy of 0.01g placed outside of the chamber, it was measured at set intervals at 0, 1h, 3h, 5h, 7h, 8h, 9h and 24h. The measurements were performed after the samples were left at least 5 cycles to stabilised in the alternating RH cycles, which meant that the initial was close to equilibrium and that the final moisture content varied by less than 5% of the initial moisture content.

The weighing process for a group of 9 samples was achieved in less than three minutes and was initially compared with a continuous logging process (McGregor et al., 2014) to check if there would be any consequences on the results. The results were not affected by the weighing being done outside of the set environment.

4 Conditions affecting the moisture buffering measurement

The conditions affecting the results of the experimental set up described in Chapter 3 were investigated using the samples from group I, with the addition of samples with varying thickness and size.

4.1 Boundary conditions

4.1.1 Preconditioning

The Nordtest recommends an initial conditioning at $50 \pm 5\%$ RH and $23 \pm 5^\circ\text{C}$. The initial conditioning does have an effect on the measurement of the moisture buffering as most samples that were measured continuously over several cycles showed either an increase or a decrease in its average weight. The conditioning was done in the conditioning room available at the University of Bath, the room temperature was set to $20^\circ\text{C} \pm 1^\circ\text{C}$ and the RH was on average at 60%. The RH was in the room very unstable and considerable variations were observed. This was overcome by measuring the moisture buffering at dynamic equilibrium. As for most measurements, a shift of the average weight during the dynamic test was observed, it has been decided to leave the samples run in the dynamic condition until they reached a stable average weight between adsorption and desorption phase. It has been shown in the Nordtest project (Rode et al., 2005) that the materials reach a “quasi-steady” state after 4 cycles. In general the same number of cycles, about 4 to 5 was needed for the material used in this study to reach dynamic equilibrium. The dynamic equilibrium is reached faster if the preconditioning RH is set close to the average RH of the moisture buffering test.

The peak adsorption during steady cycles was then used to determine the MBV

of the material.

4.1.2 Effect of relative humidity level and time steps

Among the methods existing to measure the moisture buffering capacity several RH cycles are proposed. As shown in Chapter 3 Cycles that are proposed from the Nordtest project, the ISO standard or the JIS standard (ISO-24353, 2008; JIS-A1470, 2002; Rode et al., 2005) include either 33% RH to 75% RH, 53% to 75% RH and time steps of 8h-16h, 12h-12h or 24h-24h (high/low). A further cycle was added to this study, 50% RH to 85% RH because of the limitations of the climate chamber initially available. This conveniently gave more suitable RH levels for climatic conditions in the UK. Various cycle combinations were compared through experimental measurements, on all samples from group I. Figure 4.1 gives results obtained for the average of all unstabilised (US) samples for different time and RH cycles. Through these results it was clear that an increase in peak relative humidity from 75 to 85% has a large effect on moisture adsorption with a maximum adsorption nearly doubled whereas the actual absolute humidity available in the air increased by only 13%.

Concerning the time step, the only previous work found in the literature on the influence of time steps was undertaken by Roels and Janssen (2006), during this work they simulated the influence of time variation from an 8/16 h cycle to a 24/24 h cycle for a Wood fibreboard and a Gypsum plaster, see Figure 4.2. The simulation predicted the same adsorption rate for both time steps, with an increased maximum adsorption reached. The changes observed through experimental results obtained are similar, with the short cycle having a slightly high rate of adsorption during the first 8 hours, but the longer time period leading to increased adsorption after 8 hours.

The Figure 4.3 resumes the influence of a different time step for all samples in group I under a moisture cycle of 53% RH to 75% RH. The effect of the time steps remains proportional for all samples. The solid line is to indicate the line of equal values. Measuring samples in the same RH levels with an adsorption phase of 8h or 12h has only a little influence on the results. The adsorption rate at the end of the high RH phase is rapidly decreasing as the sample approaches equilibrium moisture content and therefore the additional time only has a small effect on the maximum adsorbed moisture. The correlation coefficient between

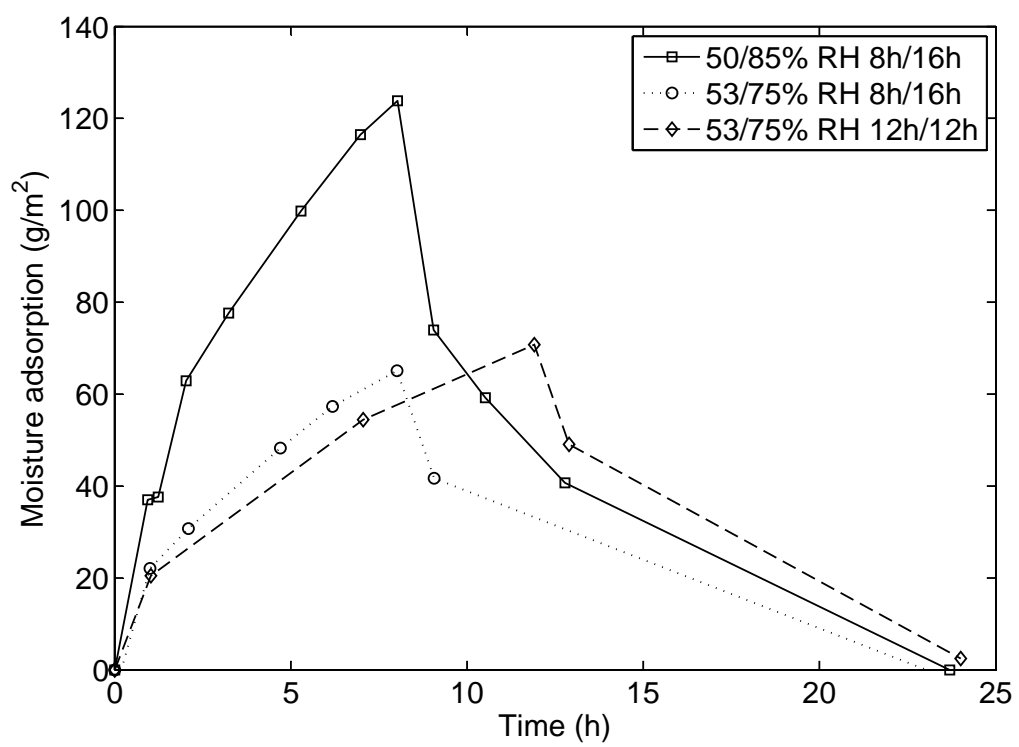


Figure 4.1: Effect of boundary conditions on moisture adsorbed

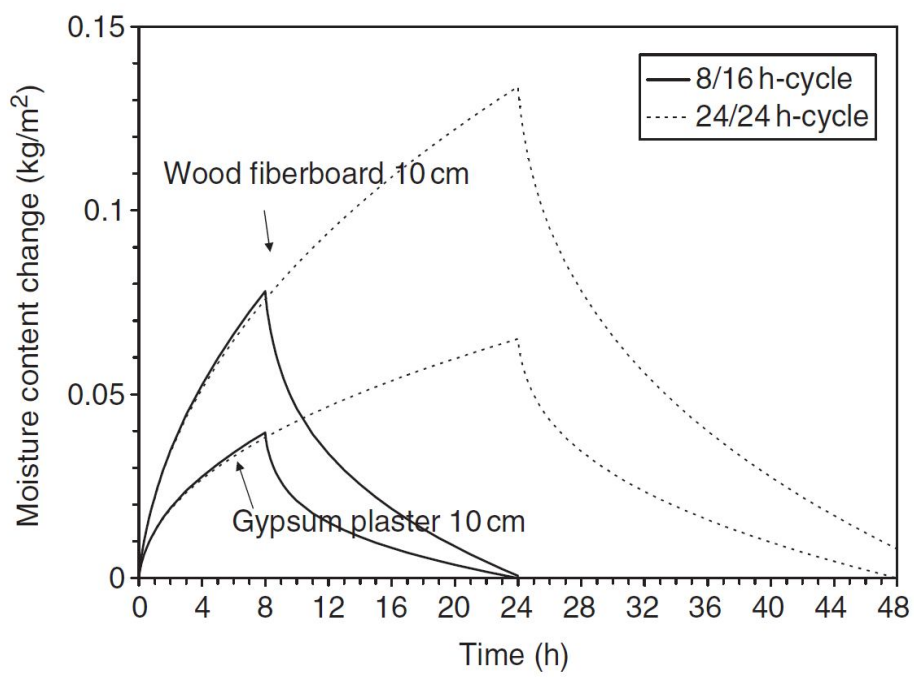


Figure 4.2: Simulated moisture adsorption variation from 6h-16h to 24h-24h cycles from (Roels and Janssen, 2006)

the two sets of values equals 1.

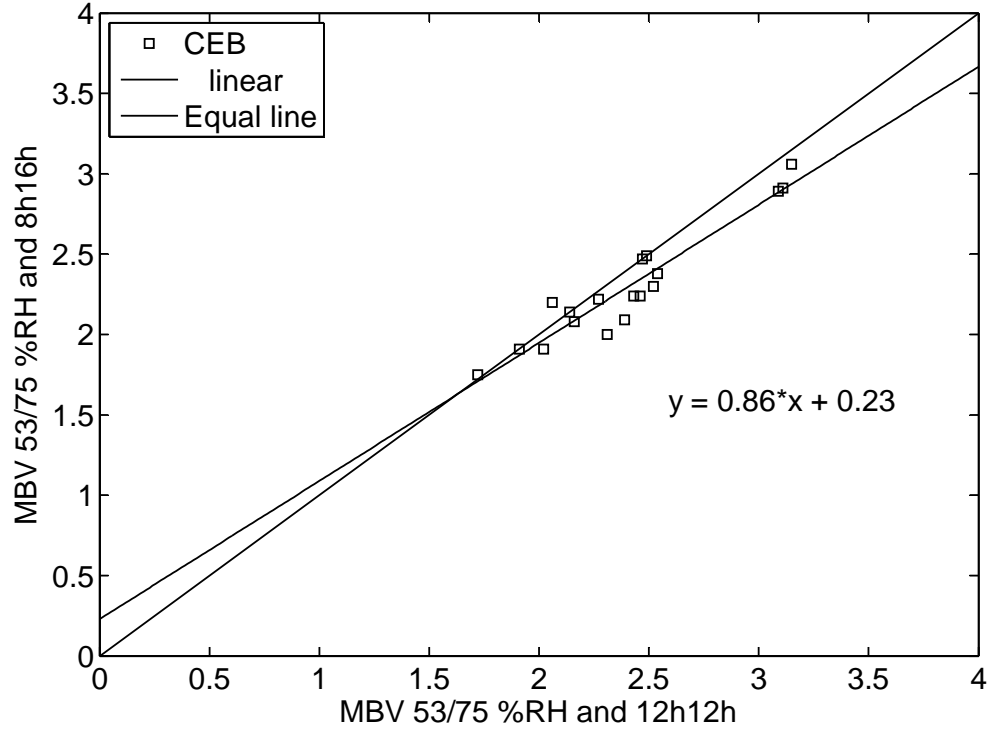


Figure 4.3: Time step influence on samples of group I

The influence of the RH levels is by far the most important especially when the RH is increased to higher levels which is seen in Figure 4.1. A good correlation coefficient of 0.97 was calculate between the results of all samples measured in different RH levels as shown in Figure 4.4.

The MBVs obtained from different cycles cannot be compared as such, they would need to be adjusted by a factor that can be obtained in this case from the slope of the correlation line. If this relation is known, the performance of a sample in a certain cycle can easily be estimated from a measurement on a different cycle. In this case, the MBV from one cycle to another can be approximated using the slope of the trend-line with equation 4.1:

$$MBV_{50/85} \simeq MBV_{33/75} \times 0.69 \quad (4.1)$$

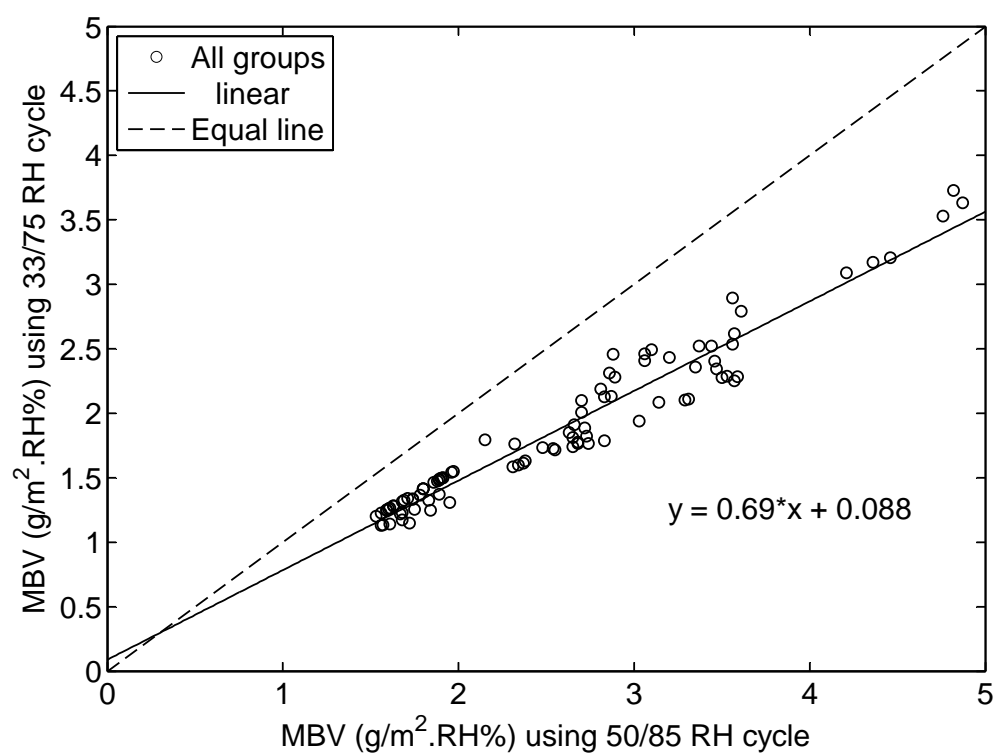


Figure 4.4: Correlation between MBV obtained from different RH cycles.

4.1.3 Effect of surface film resistance

The surface film resistance has more effect than initially anticipated. Roels and Janssen (2006) through numerical simulation have tested the effect of several values of water vapour resistance, from very high to very low, between $3.3 \times 10^4 m^2 s Pa / kg$ to $3.3 \times 10^8 m^2 s Pa / kg$. They made it clear that the surface film resistance can have a great influence on the results and this was further confirmed by the experimental tests by Gómez et al. (2011). The surface film resistance is related to the air velocity above the specimen and the geometry of the specimen, according to Roels and Janssen (2006). This could explain the difference in results observed between small and large compressed earth blocks in the section 4.2.2. The influence of the surface film resistance was investigated here experimentally by using two different chambers which both had a different air velocity and a windshield was used to even further reduce the air velocity. Figure 4.5 shows the results for an unstabilised sample from group I, the corresponding air velocity for each set up was measured with a hot wire anemometer. The values given of the air velocity are the average of 20 readings throughout the chamber, ten in a horizontal position and ten in a vertical position. The greater the air velocity, the greater the moisture adsorption. The relation between air velocity and surface film resistance can not be exactly determined. It can only be assumed that if all samples are measured in same conditions the surface film resistance will be the same. All the subsequent groups were measured in the big chamber without any windscreen in order to reduce to a minimum the surface film resistance effect, hence characterising solely the dynamic adsorption properties.

Through the experimental results observed in Figure 4.5 it can be estimated that there is a difference of about 20% between the maximum performance and the minimum. The Nordtest project recommends a surface film resistance of about $5 \times 10^7 m^2 s Pa / kg$ which is supposed to correspond to an air velocity of about 0.1 m/s, which is closer to the minimum value from this study. So the measurements performed would probably need to be reduced by 20% to compare them to a standard Nordtest measurement.

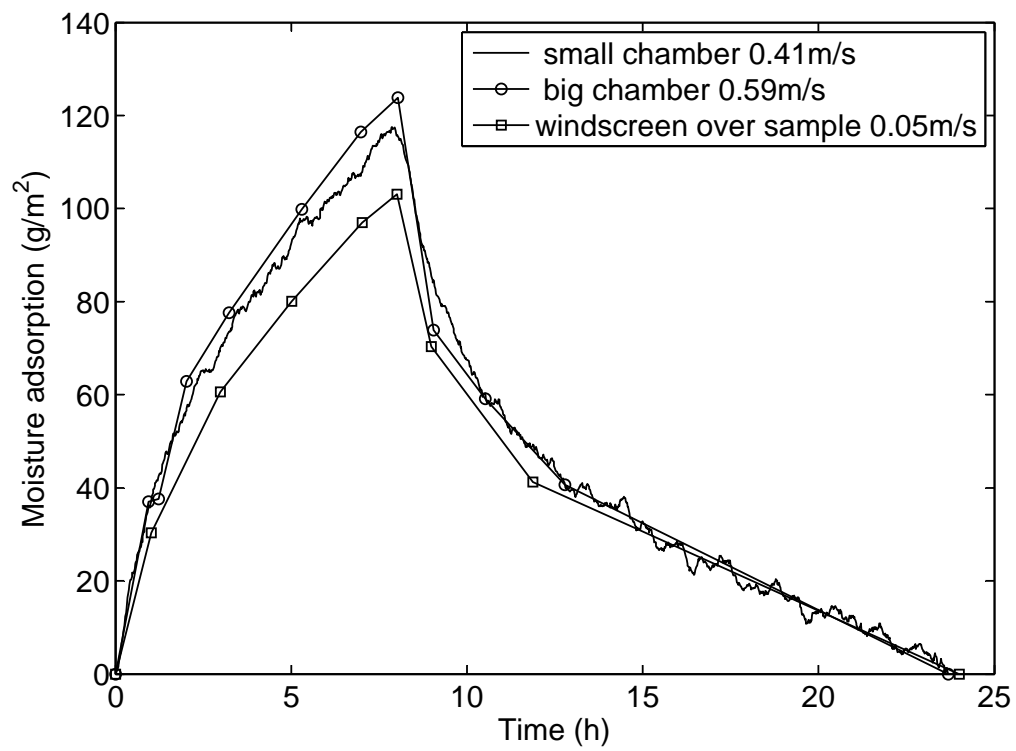


Figure 4.5: Unstabilised sample from group I under different air velocity conditions

4.1.4 Logging method

The original method from the Nordtest project suggests a continuous logging within climate chamber or if not continuously logged it should be weighed at least 5 times during the 8 hour high RH phase. The first tests undertaken for this study were made with a continuous logging within the chamber. Several limitations to this method rapidly appeared:

- The number of samples that can be measured at the same time is very limited, due to the size of the chamber and balance only one sample could be measured.
- The vibration from the ventilation system of the chamber creates a strong background noise on the results, the raw data as it was obtained is shown in Figure 4.6. To obtain better readings from these results the data was processed to obtain a moving average, see Figure 4.7.

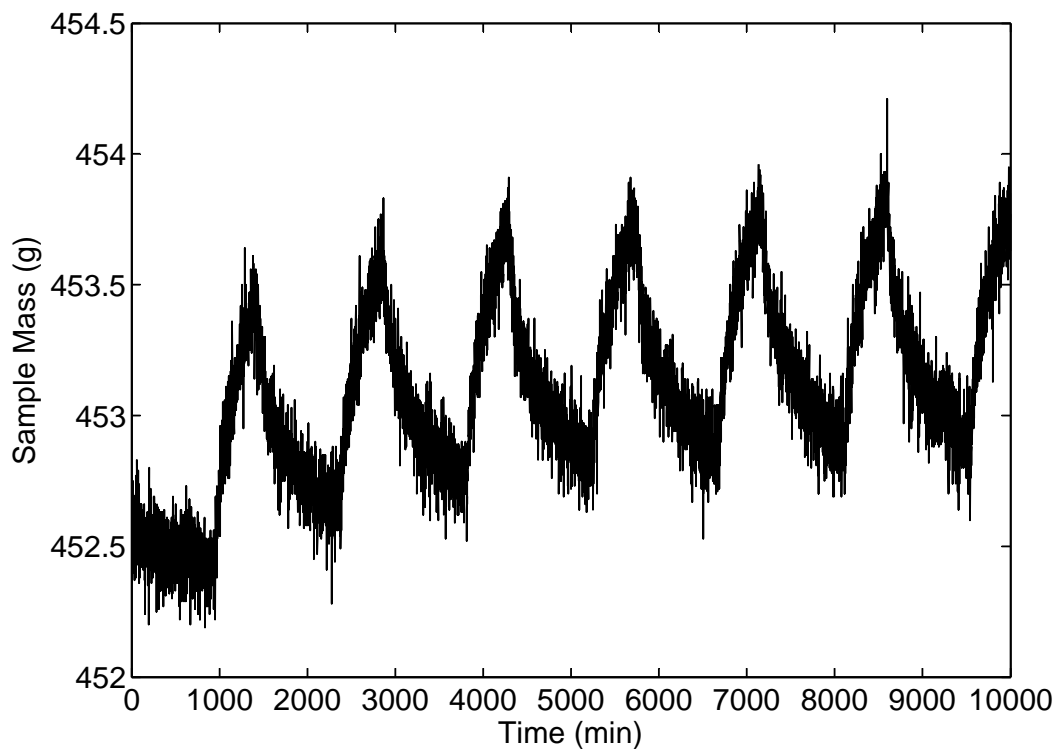


Figure 4.6: Raw data from continuous logging without windshield

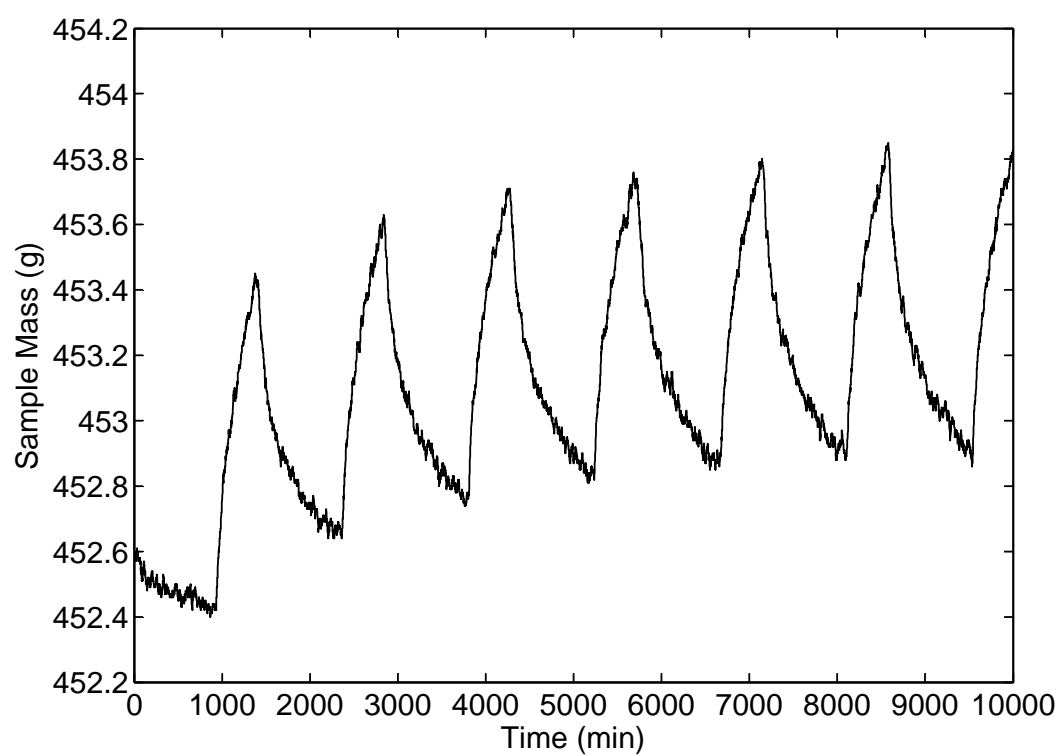


Figure 4.7: Averaged data from continuous logging with windshield

To overcome these issues and to be able to test multiple samples at the same time, the samples were weighed manually outside of the chamber. The mass was recorded at 0, 1, 2, 4, 6, 7, 8, 9 and 24h during the whole cycle. The same sample was measured with both methods and the results shown in Figure 4.8 confirm there is no major difference of the obtained results. Care had to be taken to be as fast as possible during the weighing processes and the opening and closing of the chamber to minimise the effect of the different weighing environment.

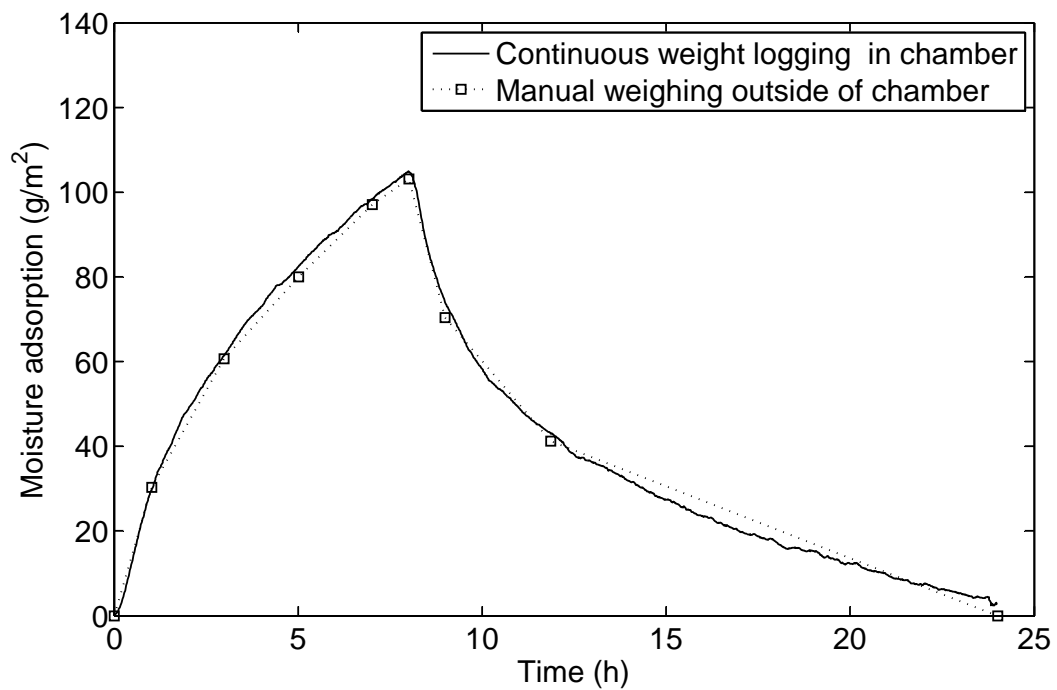


Figure 4.8: Logging method

The scale used for the measurements had a precision of 0.01g, this was necessary as the variation of mass during a typical cycle for small samples was about 1 g (see subsection 4.2.2). Even outside of the chamber the scale was sensitive to the ventilation system in the conditioning room which affected the results of some samples. These could be typically identified by the shape of the curve being irregular to the typical shape normally observed, see Figure 4.9.

The same samples gave a much smoother results as they were measured a second time in a different cycle, see Figure 4.10. It was noticed late in the study

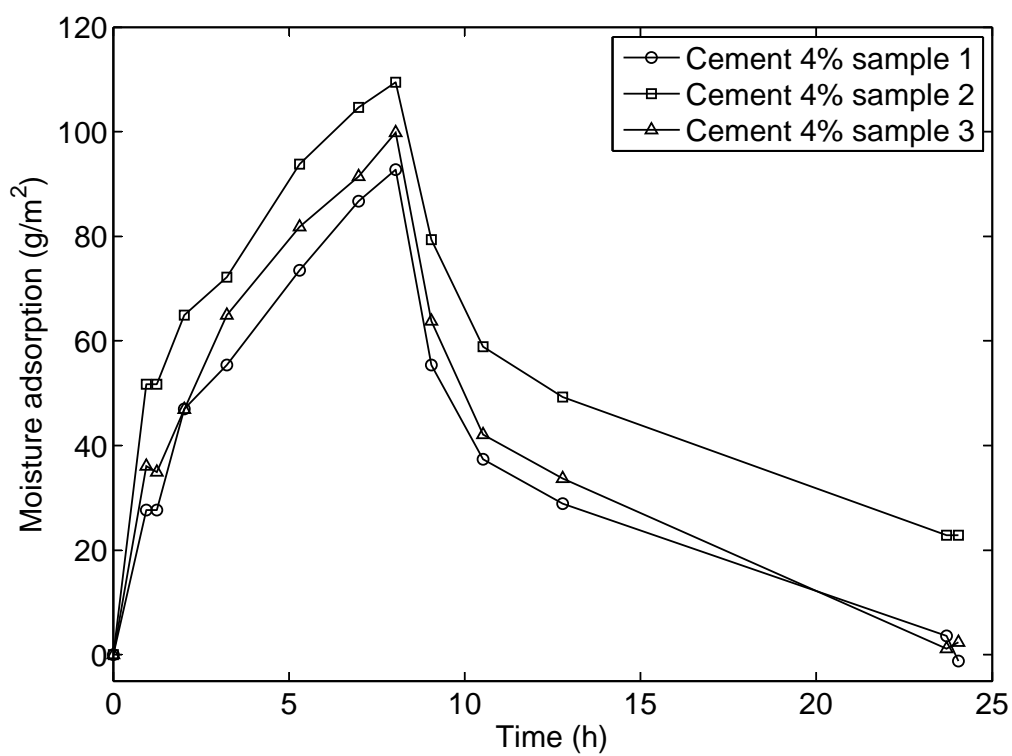


Figure 4.9: Effect of ventilation in the conditioning room on the precision of the results in 50/85% RH cycle

that the origin of this variation was due to the air conditioning in the conditioning room creating vibrations on the shelf where the scales were standing.

The noise of the vibration could be avoided by turning the air conditioning system off during the measurements. This measure improved the accuracy of the measurement back to 0.01 g as with the vibration the accuracy was approximately 0.05 g. However, averaging the results from three samples even with the ventilation system on still allowed to observe the difference in the performance of the sample due to the addition of stabiliser to be accurately quantified.

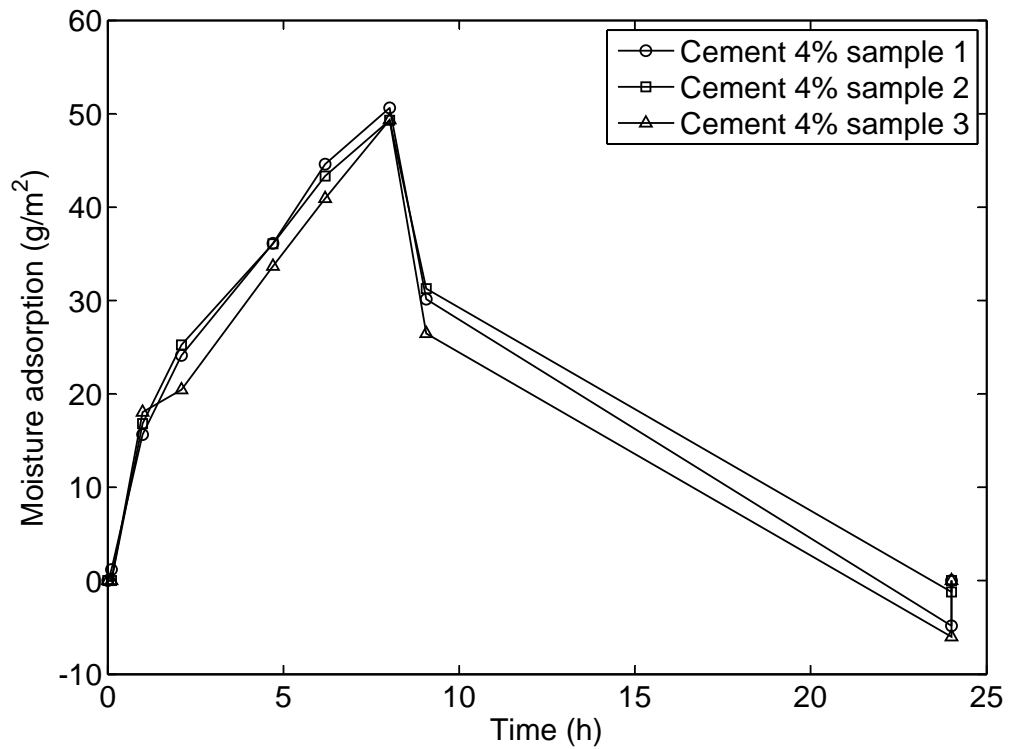


Figure 4.10: Reduced effect of the ventilation in the conditioning room measured in a 53/75% RH cycle

4.2 Sample parameters

4.2.1 Effect of sample thickness

For given boundary conditions, once the sample has reached equilibrium during repeated cycles, a given thickness layer of the sample is active. As seen in chapter 2, the depth of this layer is called the penetration depth which can be calculated. Two limits are used in the literature to determine this value, either defined as the depth where the variation is 1% of the boundary variation or defined as $1/e$ variation of the boundary condition. As mentioned by Roels and Janssen (2006), the $1/e$ limit seems to be more realistic.

The calculations of the penetration depth when using the $1/e$ limit gives values from 3.4 mm to 6.9 mm and this will be discussed further in chapter 6. To confirm that the chosen sample thickness of 30 mm was larger than the penetration depth and therefore has no impact on the MBV, additional samples were prepared with varying thickness.

The Gr and Ib soil were used to prepare unstabilised samples of 30 mm, 50 mm and 70 mm and the results are shown in Figure 4.11.

As shown there is no significant adsorption difference between the 30 mm, 50 mm and 70 mm samples which is unsurprising with a maximum penetration depth of 6.9 mm. It was therefore considered that the 30mm sample thickness is sufficient to characterise the adsorption for the boundary conditions used in this study. Furthermore making unstabilised earth samples less than 30 mm thick would not be practical.

4.2.2 Effect of sample size

Preliminary tests were conducted with samples prepared with the CINVA-RAM brick press. The typical size of the bricks was 293 mm x 140 mm x 48 mm, while the rest of the samples were prepared as described in chapter 2 as 100 mm in diameter, 30 mm thick samples. The group I samples were prepared in both sizes. There is a significant difference in the performance of the material, see Figure 4.12. The results in Figure 4.12 were obtained in the small air conditioning chamber under 50-85% RH cycles. The small sample was measured with a scale having an accuracy of 0.01g and a maximum weighing capacity of 2kg whereas

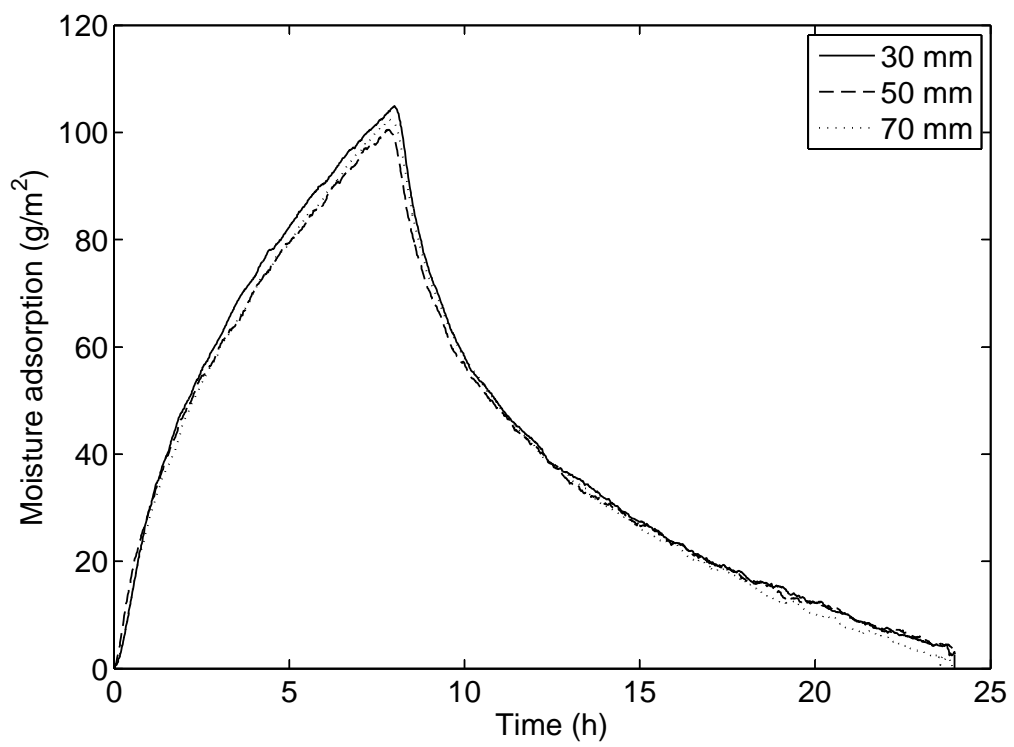


Figure 4.11: Different thickness for an unstabilised sample from group I measured in a 50-85% RH cycle

the big sample with a weight of 3.3 kg had to be weight on a bigger scale with an accuracy of 0.1g. The mass variation of the small sample during an adsorption/desorption phase was about 1 g therefore a weighing accuracy of 0.01 g was the minimum required. As shown in Chapter 5 the difference in performance can not be explained through a difference in the material properties. It is however likely that the size of the sample has an impact on the surface film resistance and therefore affects the amount adsorbed. This is illustrated in Figure 4.13 where the performance of the unstabilised big sample is close to the small unstabilised sample measured under a windshield as shown in subsection 4.1.3.

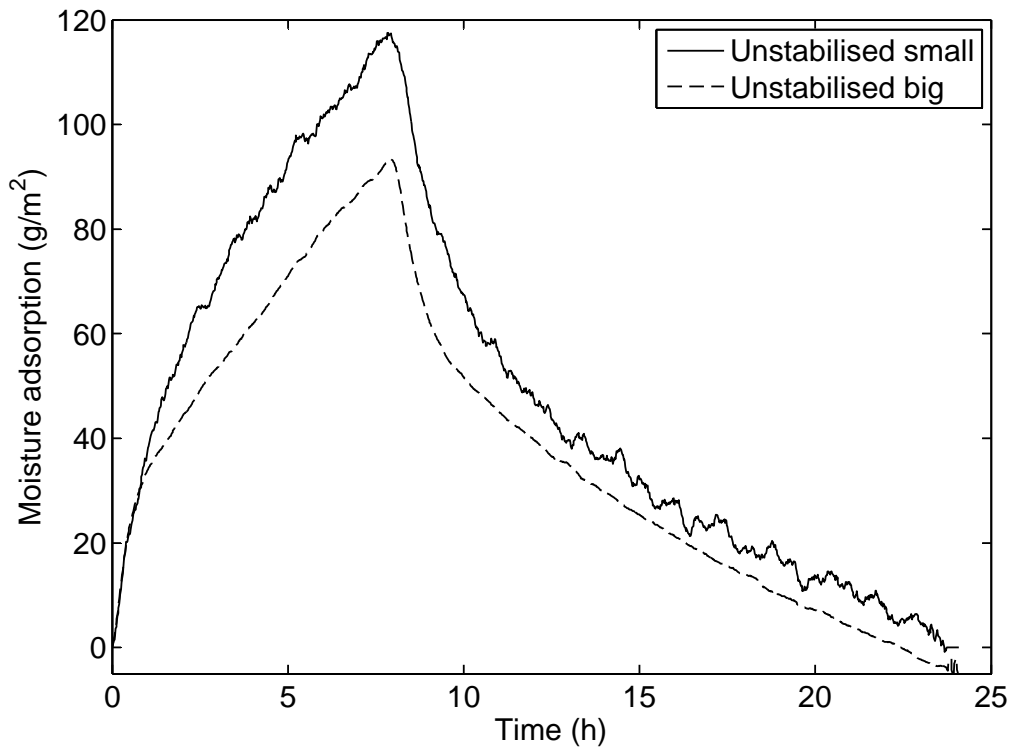


Figure 4.12: Comparison between two different sample sizes of the unstabilised material from group I measured both without windshield in the same chamber

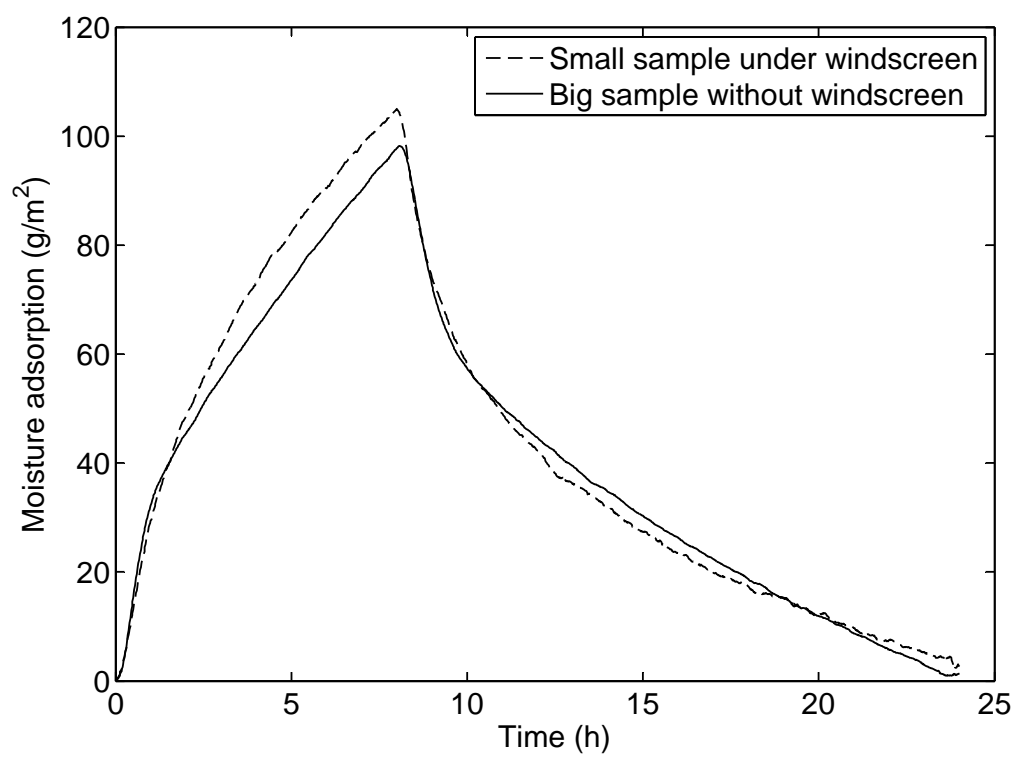


Figure 4.13: Comparison between two different sample sizes of the unstabilised material from group I measured in different air velocity conditions

4.3 Summary

The information presented in this chapter has shown that the chosen humidity levels and timesteps can influence the outcome of the tests, but that the sample thickness and measuring method do not significantly affect the measured MBV. The issue of the surface film resistance is complex and it was decided that minimising this effect by having a high air velocity is preferred, even if this means the measured results will be slightly higher than those using the Nordtest standard.

As a result, all further MBV testing was performed on samples 100 mm diameter, 30 mm thickness using a 33/75% RH step for 16/8 h.

5 Experimental results

5.1 Calculations

Table 5.1: Symbols and units

Symbol	Quantity	Unit
A	area of specimen	m ²
G	water vapour flow rate through specimen	kg/s
T	thermodynamic temperature	K
Wp	water vapour permeance with respect to partial vapour pressure	kg/(m ² .s.Pa)
d	mean thickness of specimen	m
g	density of water vapour flow rate	kg/(m ² .s)
l	diameter of circle	m
m	mass of specimen and cup assembly	kg
p	barometric pressure	hPa
p ₀	standard barometric pressure =1013.25	hPa
t	time	s
Δp_v	water vapour pressure difference across specimen	Pa
δ_p	water vapour permeability with respect to partial vapour pressure	kg/(m.s.Pa)
δ_a	water vapour permeability of air with respect to partial vapour pressure	kg/(m.s.Pa)
μ	water vapour resistance factor	-
φ	relative humidity	-
MU_t	Moisture uptake	g/m ²

5.1.1 Water vapour permeability

The experimental data obtained from the water vapour permeability test is the total of the mass of the sample and plastic cup recorded over time and any change in mass is due to water vapour moving through the sample. Calculations were performed following the EN ISO 12572:2001 Standard (ISO-12572, 2001). The symbols used were according to the standard, see Table 5.1. The mass was recorded every two days and results were plotted as mass versus time. Linear relations were obtained after an initial non linear section. This linear section was then used to determine G , the slope of the line, in kg/s. The raw data obtained is illustrated in Figure 5.1. According to the standard there is usually an initial section of the line that is not linear which should not be taken into account to calculate the slope, this represents the time until the samples moisture content reaches equilibrium with the RH levels it is exposed to. This effect was not pronounced during these experiments. The results for each individual sample are given in Annex I while key data and data analysis is present in this chapter.

After the slope of the regression line, G , is determined from the linear section, the density of water vapour flow rate (g) can be calculated following equation 5.1

$$g = \frac{G}{A} \quad (5.1)$$

The density of water vapour flow rate needs to be corrected for the effect of the masked edge of the specimens. The plastic cup has a diameter of 100 mm but this includes an edge of 3 mm. The equation to obtain the corrected vapour transmission rate taking into account this edge, g_{me} can be found in Annex I in the standard.

The corrected g_{me} value is then used to calculate the permeance, W , with equation 5.2:

$$W = g_{me} \cdot \Delta p_v \quad (5.2)$$

The permeance calculated is therefore directly related to the transmission rate as the water vapour pressure difference used for all experiments was the same.

The permeance can be corrected for the resistance of the air layer within the cup, this is recommended for materials with an equivalent air layer thickness less

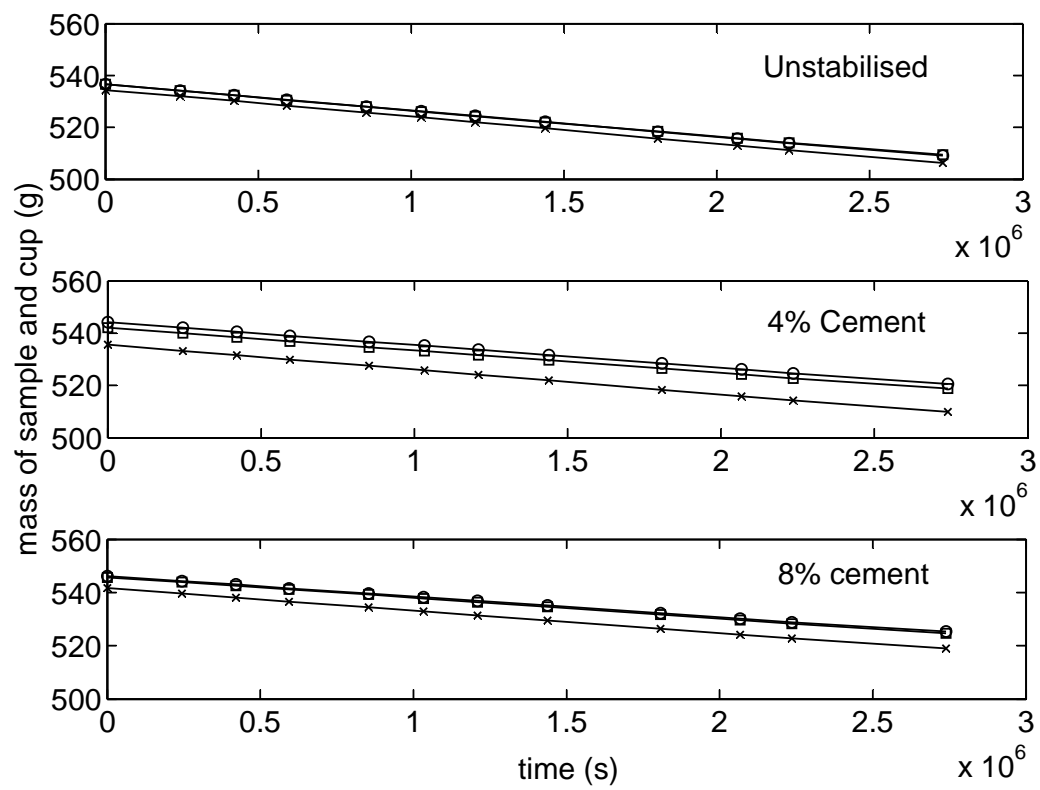


Figure 5.1: Raw data from the water vapour permeability experiment with three identical samples for each material

than 0.2 m. As most of the samples had an equivalent air layer thickness over 0.2 m, it was assumed that the resistance of the air layer in the cup was insignificant compared to the resistance of the material for this study. In addition the air layer was the same for all samples hence it was unlikely to cause a major influence on the results. To verify this assumption a test was performed with the samples from group V as they had similar water vapour resistance properties, air layer thicknesses of 35 mm, 25 mm and 15 mm were used in the plastic cup whereas all the other test conditions remained the same. The results suggest that there is no significant difference between the different levels of air the cups.

The water vapour permeability can be calculated based on the thickness of the material and its permeance and is calculated using equation 5.3.

$$\delta = W \cdot d \quad (5.3)$$

In literature a more convenient descriptive parameter of the water vapour permeability is used, the water vapour resistance factor, μ . It compares the water vapour permeability of the material to the water vapour permeability of the air and is calculated using equation 5.4. The water vapour resistance factor gives numbers that are easier to visualise and the results from this experiment will therefore be presented in this form.

$$\mu = \frac{\delta_a}{\delta} \quad (5.4)$$

5.1.2 Sorption isotherms

Sorption isotherms obtained with the DVS can be directly calculated using the software supplied that can be used in Microsoft Excel[®]. It calculates the sorption isotherms based on the ratio of $\frac{\partial m}{\partial t}$. Equilibrium moisture content is considered achieved when the mass variation is less than 0.0001% of mass per minute or when a maximum time span of 360 minutes per RH level is reached. The equilibrium moisture content is then calculated in percentage by mass using the reference dry mass of the sample which was obtained during the 0% RH stage. Therefore the following equation 5.5 is used:

$$EMC = \frac{m - m_{ref}}{m_{ref}} \times 100 \quad (5.5)$$

Where m_{ref} , is the reference mass of the specimen in dry condition and m is the mass of the sample at a given RH.

The same equation 5.5 is used for the salt solution method. For this method the dry mass of the samples was obtained after placing them in the oven at 105°C for at least 24h. The recommended accuracy of the scale in the standard is of 0.01% of the mass of the sample. Therefore with the salt solution method and a 10 g sample, the scale should have had an accuracy of at least $10 \times \frac{0.01}{100} = 0.001g$. This accuracy was not met during this test as the scales used had an accuracy of 0.01g. Scales with a precision of 0.001 were available but too far from the test and these could not be moved, this was at first considered as a greater source of error if the samples had to be moved every time for the measurement during the test.

Hence both test were used to increase the reliability of the results and both results are presented in this Chapter for comparison

5.1.3 Moisture buffering values

The method to measure the moisture buffering was described in Chapter 3. The data obtained corresponds to mass measures over a 24 h period. As they were measured in quasi steady cycles, the mass at time zero of the stage is used as the reference mass, m_0 . For each reading the scales recorded the time, therefore the first reading at the beginning of the cycle is used as the reference time, t_0 . The moisture uptake per area at a given time, MU_t , can be calculated with equation 5.6:

$$MU_t = \frac{m_t - m_0}{A} \quad (5.6)$$

The value of MU_t at 8 h, at the end of the adsorption cycle is then used to calculate the moisture buffering value, MBV :

$$MBV = \frac{MU_t}{\Delta\%RH} \quad (5.7)$$

This is the $MBV_{practical}$ from the Nordtest project and is the main result from this test. The complete data is presented in Annexe.I.

5.2 Results from parametric study

The results are presented per group to visualise the influence of the modified properties for each group. The influence of the initially modified parameters must be analysed with attention as the modified parameters may affect some other material properties that in turn affect the hygric properties of the sample.

5.2.1 Group I: Stabilisation

In spite of numerous earth buildings surviving thousands of years, there are concerns in the mainstream construction industry that earth has poor durability and stabilisers are sometimes used with earth materials for increasing strength and durability. Cement and lime are the most common stabilisers with less than 10% per weight of cement or lime normally sufficient to provide a significant gain in strength and durability. More specifically, they play an important role in resisting water erosion. A further increase of stabiliser to higher percentages would increase embodied energy, to a point where it is reaching levels of conventional concrete blocks.

With an increasing interest in the use of geopolymers as a low embodied carbon form of stabilisation for earth construction, methods used for this study therefore also included geopolymer stabilisation through the use of 3% NaOH. Geopolymers are inorganic polymeric materials obtained from “the chemical reaction of aluminosilicate oxides (Al^{3+} in IV-fold coordination) with alkali polysilicates yielding polymeric Si-O-Al bonds” Davidovits (1991).

It is a common belief among some practitioners that stabilisation inhibits moisture buffering capacity and that this would have a detrimental effect on indoor air quality.

Group I was tested to investigate the influence of the addition of stabiliser. The results presented in Figure 5.2 show a trend that confirms the influence of stabiliser on the moisture buffering capacity. Materials have a higher water vapour resistance and in return the buffering capacity is decreased.

The first results on the effect of stabilisation on large compressed earth blocks was published in a conference paper for Lehm2012 conference (Mcgregor et al., 2012). The results presented were from testing with the same material used to obtain the following results but on larger compressed earth blocks.

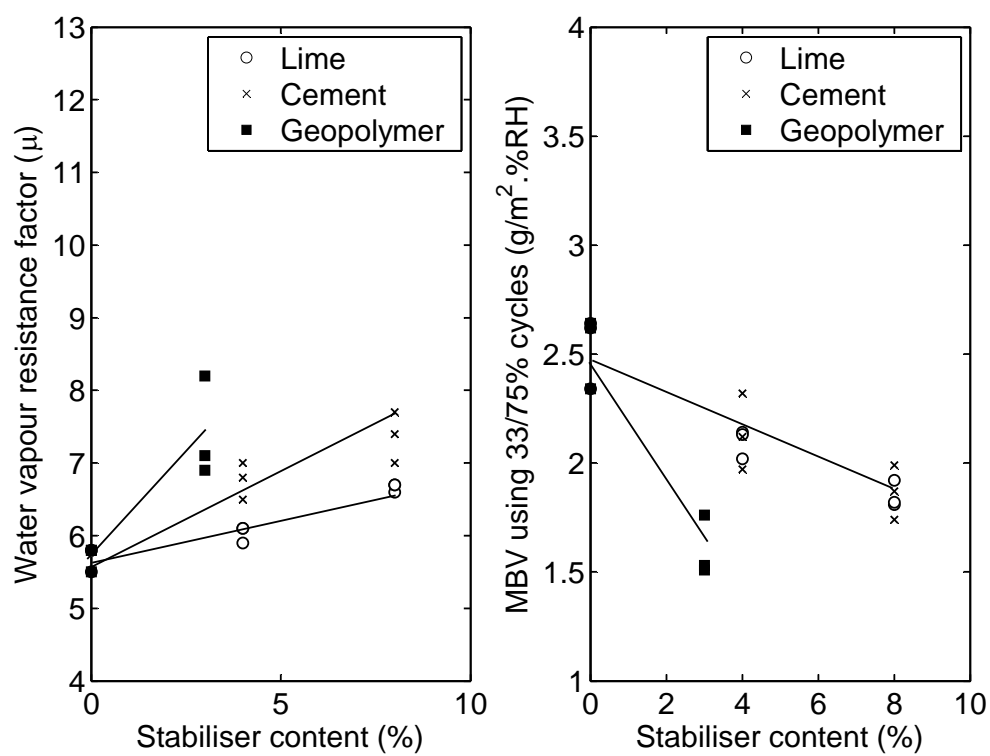


Figure 5.2: Water vapour resistance factor and moisture buffering value for samples in group I

There is, however, a difference depending on the nature of the stabiliser, cement and geopolymer stabilisation have a stronger effect on the vapour permeability than the addition of lime.

Results show that the water vapour resistance ranges from 5.5 for an unstabilised sample to 8.2 for a geopolymer sample. There seems to be a linear relationship between the amount of cement and lime and the steady-state and dynamic hygric performance of the material. The MBV varies from 2.64 g/m² .%RH for an unstabilised sample to 1.51 g/m² .%RH for a geopolymer samples which represents a reduction of about 42 % of the dynamic performance.

The moisture storage capacity is also affected by the addition of stabiliser, Figure 5.3 shows a gradual reduction of the equilibrium moisture content with an increase of stabiliser. Cement and lime stabilisation affects the sorption isotherm after about 20% RH and has greater effect at high RH levels. Cement stabilisation does not seem to affect hysteresis which remains about the same, whereas the lime stabilisation does seem to reduce the hysteresis.

A major influence on the sorption isotherm can be observed on the result of the geopolymer stabilisation. The EMC is reduced until about 80% RH where it then suddenly increases. This final stage of the sorption isotherm is known to be related to the capillary condensation and therefore to the pore size Rouquérol et al. (1999). The observed results could indicate a reduction of the average pore size. As the increase only occurs after 80% RH it is likely not to affect the moisture buffering reading obtained from a 33% to 75% cycle.

5.2.2 Group II and III : Initial water content

The initial moisture content is the moisture added to the soil when preparing the blocks. For a particular type of soil the optimal moisture content is the one that gives the highest dry density after compaction. Compaction at water contents above or below the optimum can influence the orientation of clay particles which in turn affects the shrinkage, permeability and strength characteristics of clay soils (Seed and Chan, 1959). This is because clays compacted at lower water contents have a more randomly orientated structure than those compacted at higher water contents. A more randomly orientated structure can result in a significant increase in saturated permeability, but no research has been conducted on the effect of water vapour permeability. In general it can be considered that

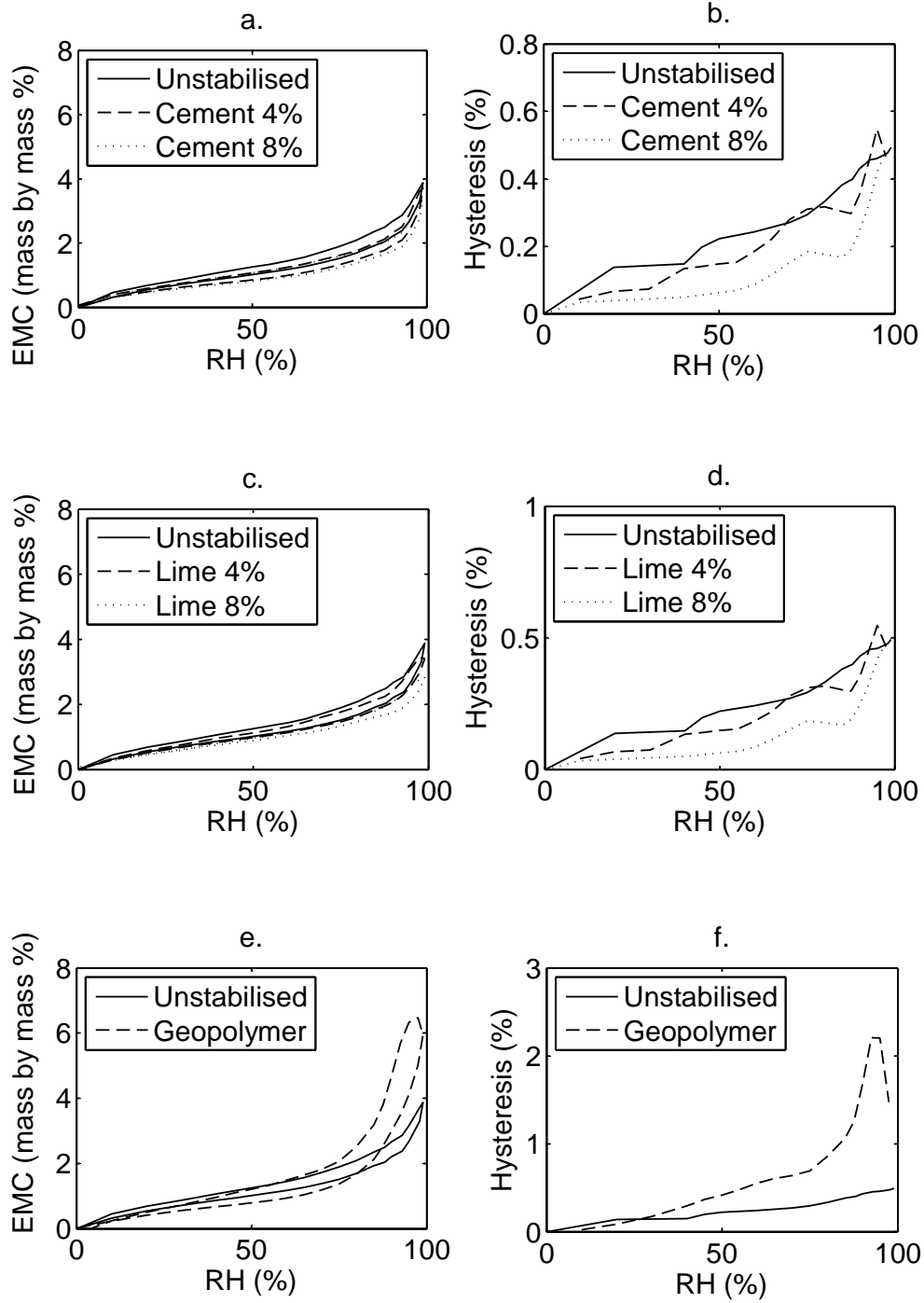


Figure 5.3: Sorption isotherms for stabilised samples, group I . a. cement sorption isotherms, b. cement hysteresis, c. lime sorption isotherms, d. lime hysteresis, e. geopolymer sorption isotherms, f. geopolymer hysteresis.

materials prepared on site have a high variability of initial moisture content as this may not be precisely controlled during preparation of samples.

The results obtained on the two soils (Gr and Ib) show an increase in the resistance to the diffusion of water vapour through the sample with increasing compaction moisture content from a factor of about 6 to 9, as shown in Figure 5.4. The MBV decreases from 2.5 to 1.7 g/m² .%RH, the results for both groups II and III are similar.

The interpretation of this effect is complicated because a further investigation of the material properties also shows an increase in apparent density even though the samples were compacted in order to have same dry density. A higher water content at compaction increases the shrinkage during drying and in consequence the wetter samples were slightly smaller during testing, increasing the apparent density.

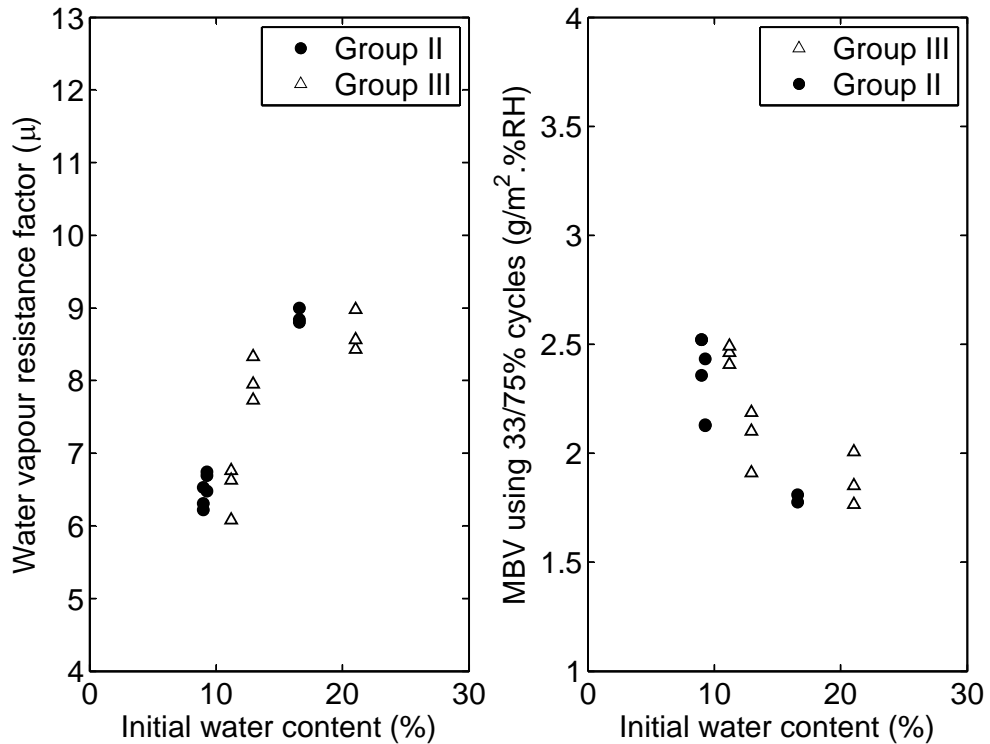


Figure 5.4: Water vapour resistance factor and moisture buffering value for samples in group II and III

The sorption isotherms acquired with the salt solution method for samples in

group II are shown in Figure 5.5. A distinction of the sample due to a higher water content cannot be observed through this data. The same observation is made on the sorption isotherms obtained for group III, see Figure 5.6. The sorption isotherms acquired through the salt solution method because of a low accuracy present a difference between the triplicates. Yet they remain similar compared with the sorption isotherm obtained from the DVS method. The fact that the sorption isotherms are not affected indicates that the change in performance of hygric properties is due to the change in apparent density. A further analysis is done in Chapter 6.

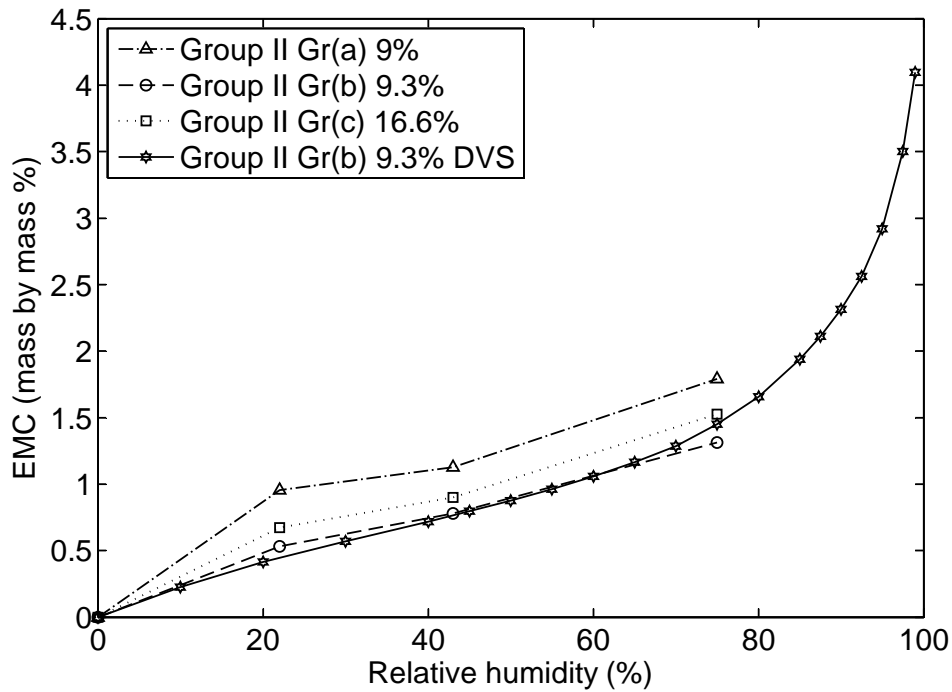


Figure 5.5: Group II compared sorption isotherms

5.2.3 Group IV and V: Apparent density and mixing method

Group IV and V were not prepared for the same purposes yet the materials are nearly the same and the results are very close which is why they are presented together. Group IV was prepared with different apparent densities, whereas group

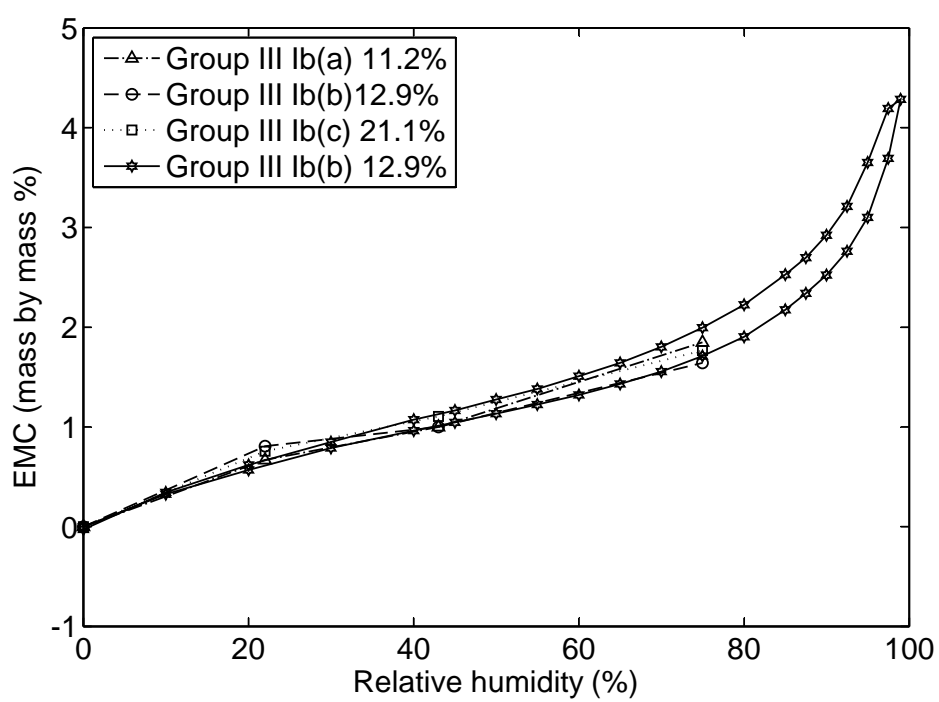


Figure 5.6: Group III compared sorption isotherms

V was prepared with different mixing methods. No variation due to the mixing method could be observed, and all variation in the water vapour resistance or moisture buffering was linked to the variation of the apparent density. Figure 5.7 presents the results of the water vapour resistance and the moisture buffering value plotted against the apparent density. Even though samples in group V were prepared with 5% more clay, the results are very similar. A linear correlation exists between water vapour resistance and apparent density, and a similar correlation is visible for moisture buffering values and apparent density.

The μ factor varies between 6.8 and 13 and the MBV ranges from 1.8 to 1.1 $\text{g/m}^2 \cdot \% \text{RH}$. These results for the dynamic adsorption are amongst the lowest observed for all samples. The clay for these samples was exclusively composed of a 1:1 Kaolinite clay mineral, the same material was used in group VI where 2:1 clays were added.

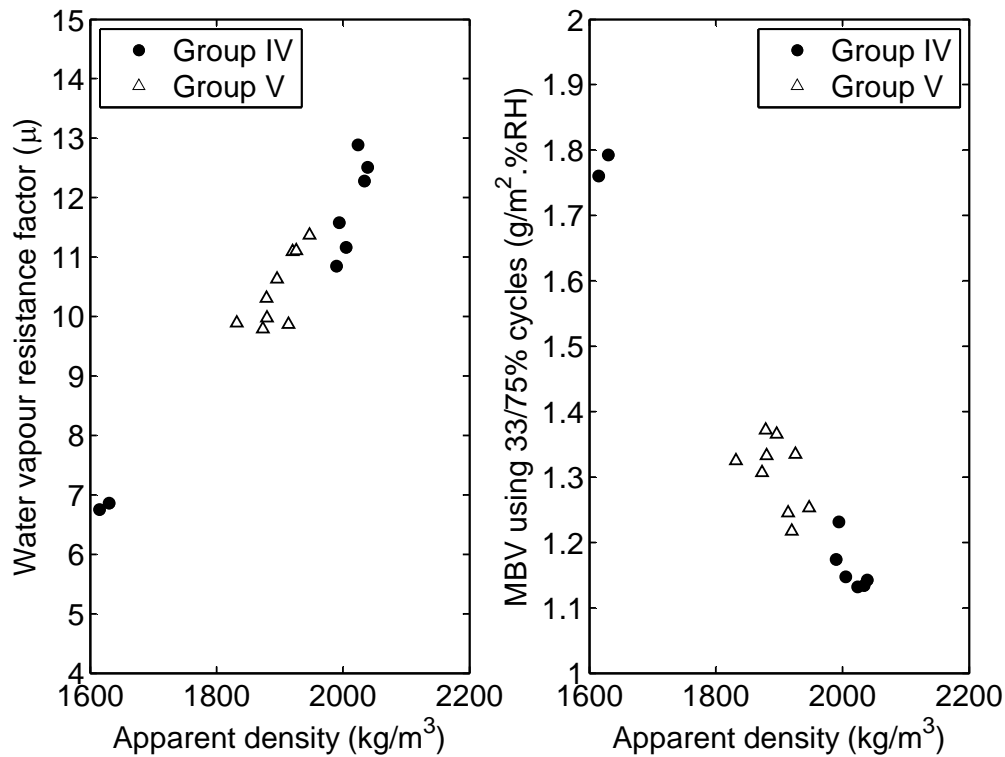


Figure 5.7: Water vapour resistance and moisture buffering results for samples in group IV and V

The sorption isotherms measurement obtained with the DVS are sufficiently

precise to determine a difference due to a change in apparent density from 1615 kg/m³ to 2039 kg/m³, see Figure 5.8. It can be qualified as a minor change to the sorption isotherm and the change only occurs towards higher RH levels, starting around 60% RH.

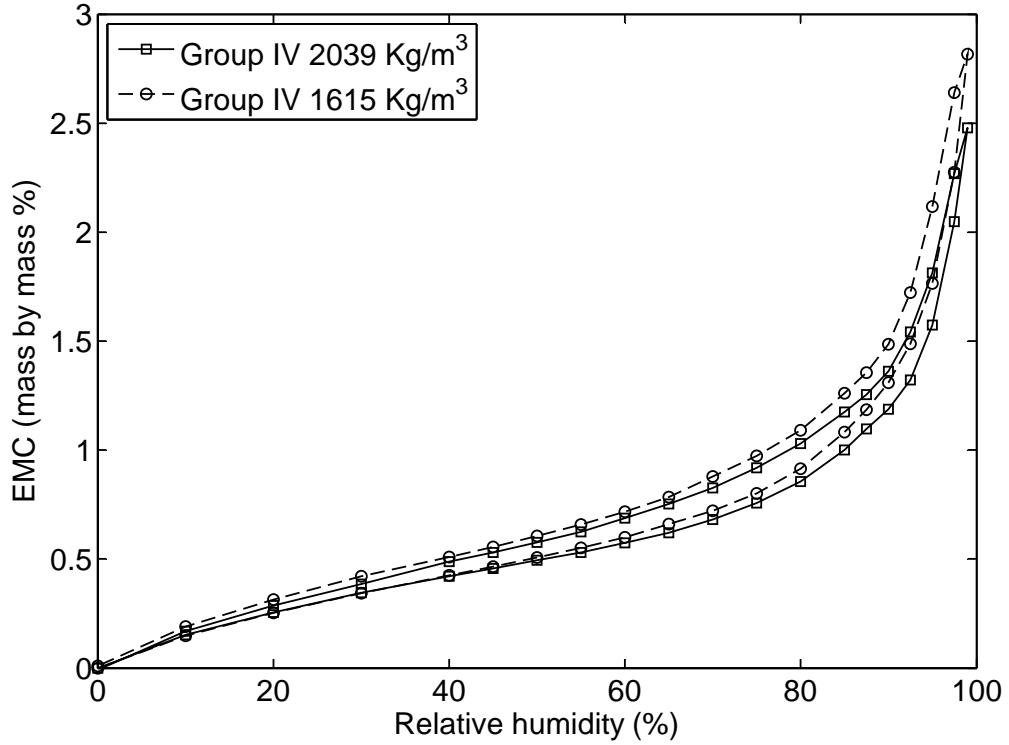


Figure 5.8: Influence of apparent density on sorption isotherms

In Figure 5.9 the average of sample 2 and 3, the average of sample 4 and 6 and the results for sample 7 from group IV obtained through the salt solution method is compared to the sample 2 obtained with the DVS. The results from both methods are relatively close, yet once again the accuracy of the salt solution method is too low to visualise the difference due to the change in apparent density.

The sorption isotherms for group V were not measured, no specific change to the sorption isotherm is expected as all samples in group V were prepared with same properties.

From this study it appears as if the reduction in MBV is because of an increase in μ indicating the denser materials will react slower to moisture change.

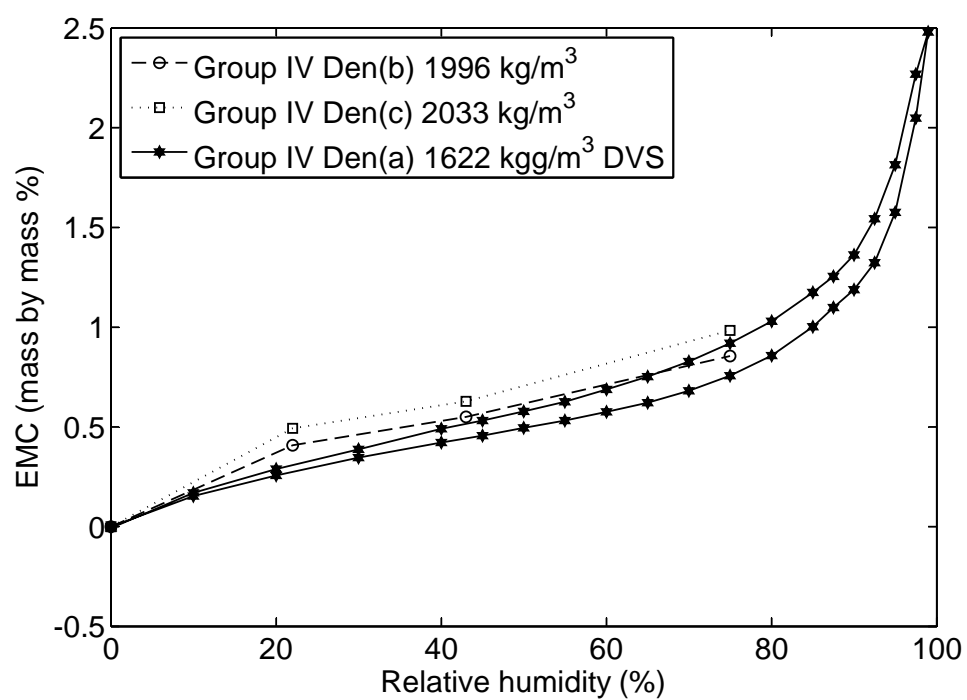


Figure 5.9: Salt solution and DVS sorption isotherms from samples in group IV

5.2.4 Group VI : Mineralogy

Samples in group VI were tested to investigate the influence of the addition of swelling 2:1 clay minerals. The particle size distribution in terms of percent of sand, silt and clay was the same as for samples in group V with a variation of the clay mineralogy. Added swelling clays were either Bentonite or Pillared Bentonite with a total percentage varying from 1% to 10%. The water vapour resistance and moisture buffering results are given in Figure 5.10. The usual trend of an increasing vapour resistance and decreasing moisture buffering is contradicted, in this case both have a tendency to increase. The μ factor increases from about 7 to 10 at maximum and the MBV also increases from about 1.6 to 2.3 g/(m²%RH).

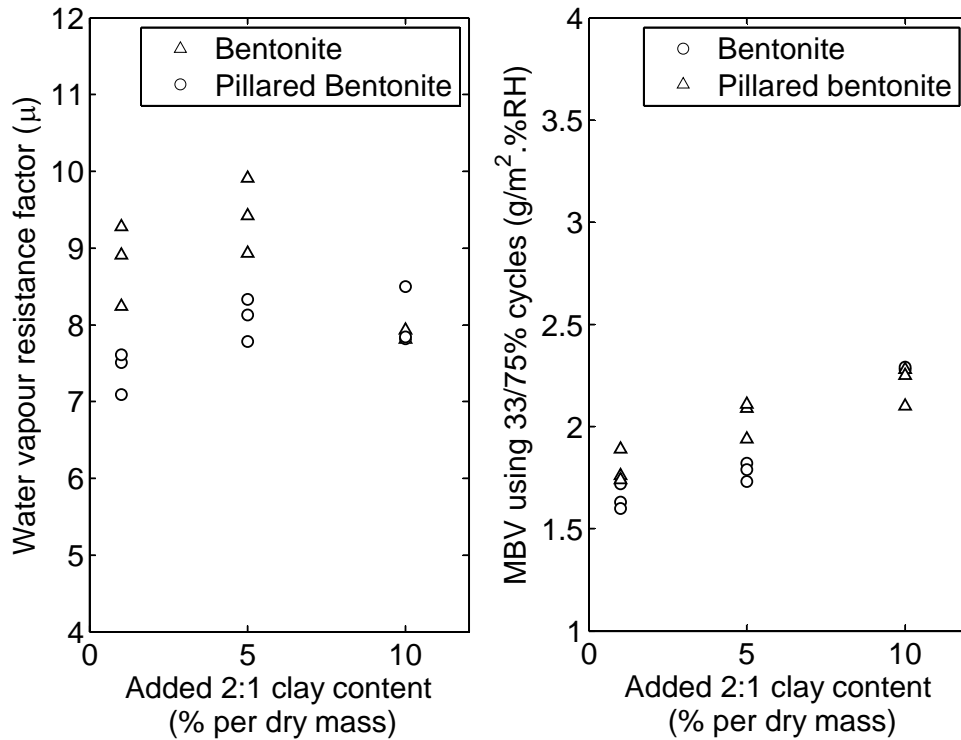


Figure 5.10: Water vapour permeability and moisture buffering results for samples in group VI

This effect was somehow expected, the moisture buffering capacity is influenced by the addition of particles with larger surface area and higher surface charge. It is well documented in the literature that 2:1 clay minerals due to their crystal

structure have a stronger binding potential of polar molecules to their surfaces.

Sorption isotherms from salt solution and DVS confirm the large increase of the equilibrium moisture content and hence the moisture capacity of the material, see Figure 5.11. Figure 5.11 shows the sorption isotherms obtained from salt solutions for samples in group VI for which Bentonite was added. With a greater difference in the equilibrium moisture content the average results for three identical samples from the salt solution method does this time show the variation. The average for samples with 1% of Bentonite is close to the sample with 1% measured with the DVS.

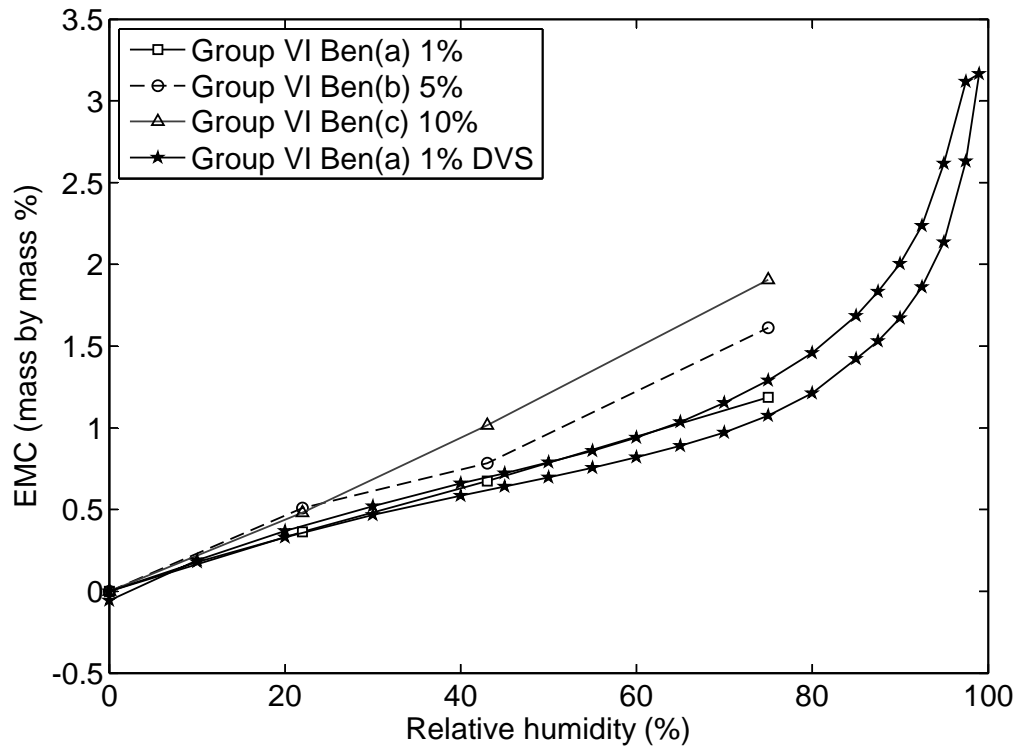


Figure 5.11: Salt solution sorption isotherms for samples 1 to 9 in group VI

A better comparison is made when comparing two samples measured with the DVS. In Figure 5.12 sample Ben(a) with a Bentonite content of 1% is compared to sample Ben(c) with a Bentonite content of 10%. There is a clear difference in equilibrium moisture content. The hysteresis also increases with the addition of Bentonite, the difference between the adsorption and desorption curve from a sample 10% is more than double the one from a sample with only 1%. The

implication of the hysteresis on the moisture adsorption is further investigated in Chapter 6.

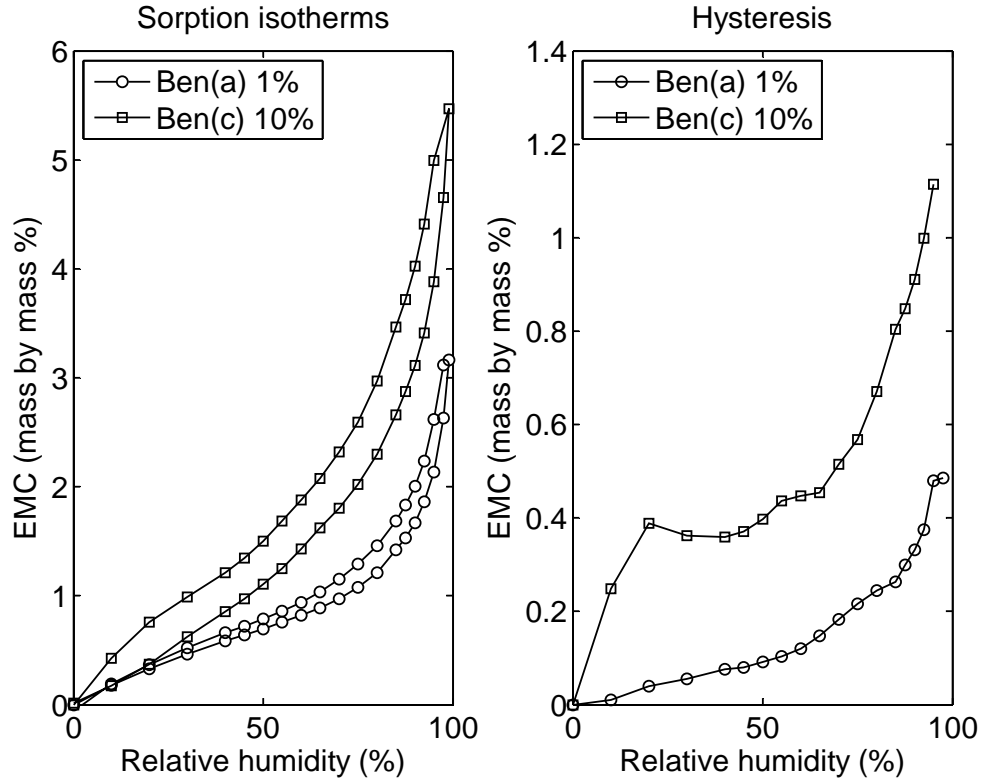


Figure 5.12: Compared sorption isotherms and hysteresis with different Bentonite contents from group VI

5.2.5 Group VII : Natural brick soils

Group VII was prepared with different brick soils used around the UK, the soils varied in particle size distribution and mineralogy. The correlation between each particle size and the hygric properties given in Table 5.2 show that silt content has the best correlation with hygric parameters. Clay plays an important role on the moisture capacity. As it is difficult even with x-ray diffraction to get a precise quantification of the different minerals, especially the clay minerals, the particle size distribution rather than mineralogy was plotted with the results of water vapour resistance and the moisture buffering value in Figure 5.13. The combined content of clay and silt were used in abscissa as both are important size fractions.

Table 5.2: Linear correlation coefficients between size fraction and hygric parameters for samples in group VII

Particle size	Coefficients of linear correlation with		
	μ factor	Moisture capacity	MBV
Clay	-0.21	0.75	0.38
Silt	-0.57	0.58	0.82
Clay + Silt	-0.50	0.81	0.77

The amount of clay and silt seems to affect both the water vapour permeability and the moisture buffering value. It seems to have a stronger effect on the moisture buffering, which is expected as changing the particle size distribution affects the surface area of the material and the mesoporosity, this will be further discussed in Chapter 6 when combining particle size data for all groups.

The μ factor varies between 4.3 to 8.4 and the moisture buffering value varies between 1.6 to 3.7 g/m² .%RH. Most of samples have a closer agreement within the triplicates, only the st samples have a strong variation in the vapour resistance which ranges from 6.1 to 8.4. This is because the “St” samples have the largest maximum particle size (see Table 3.1, in Chapter 3) and these may affect the consistency of the results.

Sorption isotherms of the brick soils clearly show a difference in the adsorption properties. Figure 5.14 gives the sorption isotherm for all the brick soils measured with the DVS and the salt solution method. Both methods provide similar outcomes and the result from the salt solution method is hidden by the curve of the DVS method. The salt solution data is represented with dotted line and the square points whereas the DVS is represented with the solid line and the round points. The agreement between salt solution and DVS method is rather good, for a same material both methods fall in the same range of EMC.

Soils with high adsorption capacity such as Ch, Al and Bi also have a high amount of clay and silt. Their mineralogy may also play a role as they have respectively 5% and 6% of Illite-Smectite content which is a highly adsorbing 2:1 clay. The Bi clay although it has a higher adsorption capacity has a lower moisture buffering value than Le and Al, this can be explained by a lower vapour permeability of the material which in turn could be due to a slightly higher bulk density.

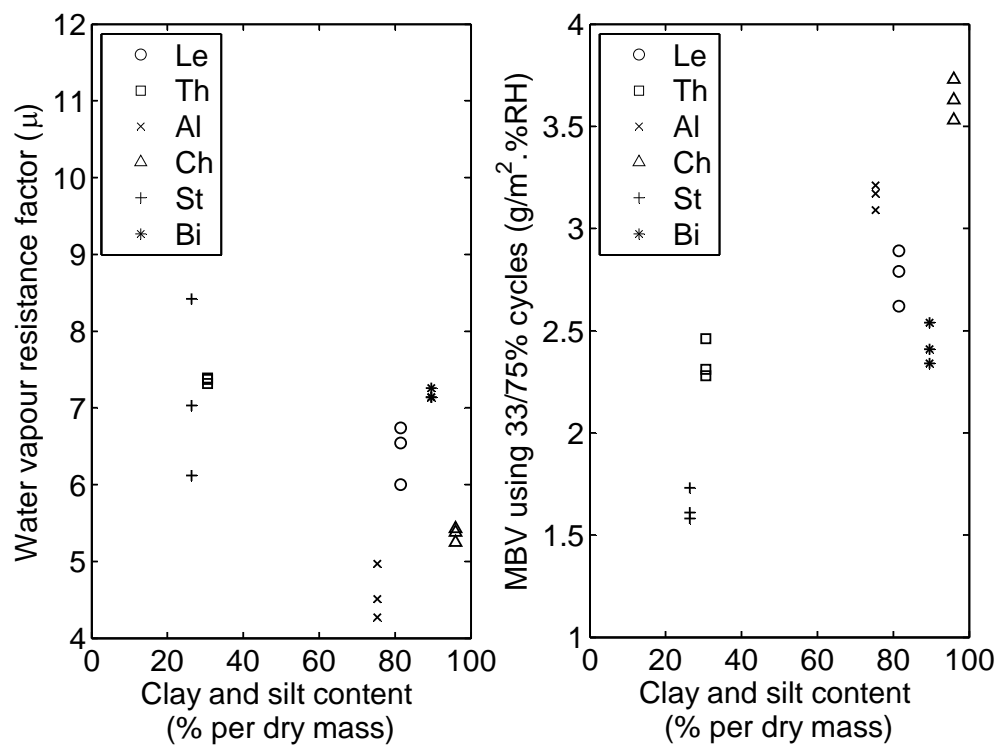


Figure 5.13: Water vapour permeability and moisture buffering results for samples in group VII

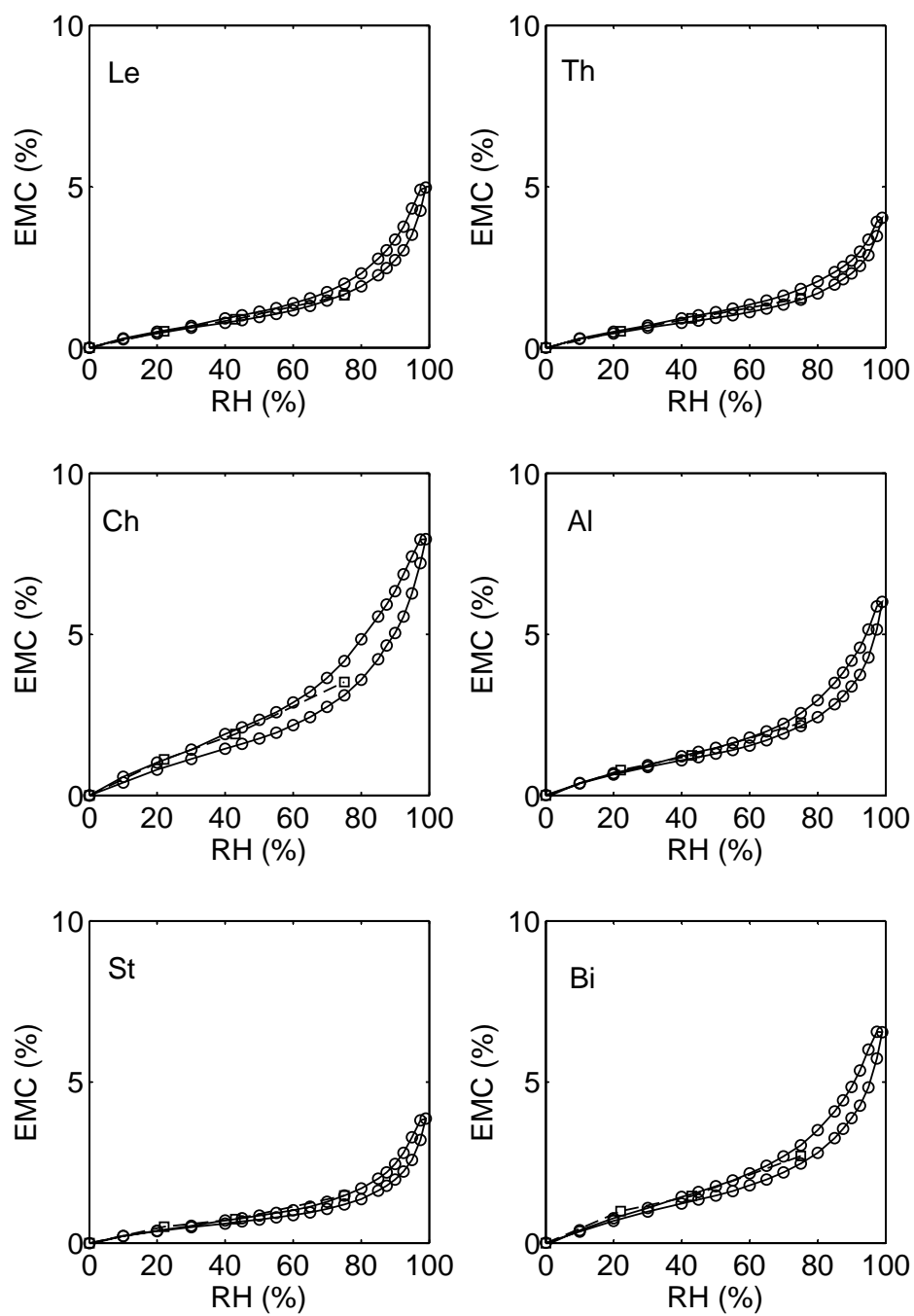


Figure 5.14: Sorption isotherms of different brick soils

5.2.6 Group VIII and IX : commercial plasters

For the plaster samples there wasn't an identified single variable against which the results of water vapour resistance and moisture buffering could be plotted. The results were therefore presented in a bar chart, with the description of the thickness of the sample and the different coats used. The samples were prepared in two different thicknesses, 12 mm as recommended by the manufacturer and 20 mm to compare the performance and confirm experimentally that the penetration depth is not over 12mm. For each thickness three samples were prepared with the addition of a 3mm finishing coat from the same manufacturer. In total four different triplicate sets were made for each plaster.

Results for plaster 1 from group VIII are given in Figure 5.15 for the water vapour resistance and in Figure 5.16 for the moisture buffering capacity. The water vapour resistance for the group VIII varies between 9 to 13 with the thicker samples having a lower resistance factor. In the ISO-12572 (2001) standard, water vapour permeability is the product of the thickness of the sample and the permeance. The thickness is therefore taken into account in the calculation. It is therefore relevant to note that the results show lower vapour resistance for thicker samples which is contrary to what would be expected.

The results of the moisture buffering value for the plasters in group VIII in Figure 5.16 at first seem quite variable, yet the range is actually narrow as it ranges from 1.40 to 1.55 g/m².%RH. The plasters in group VIII perform better than plasters from group IX. The variability in the dynamic performance of both plasters remained relatively small and no significant difference between the thickness or added finishing coat could be observed.

The overall performance of the plasters as a buffering material is situated on the low end of the observed range. It does however perform better even though the clay content is much lower than in the samples from group IV and V. The apparent density is on average 1702 kg/m³ for samples in group VIII and 1704 kg/m³ for samples in group IX.

There is a good agreement within triplicates for the water vapour resistance measured for samples in group IX, see Figure 5.17. It ranges from about 9 to 14 with thicker samples once more having a lower vapour resistance. The moisture buffering value for samples of group IX are given in Figure 5.18, these vary from about 1.20 to 1.40 g/m².%RH which is low compared to most of other groups.

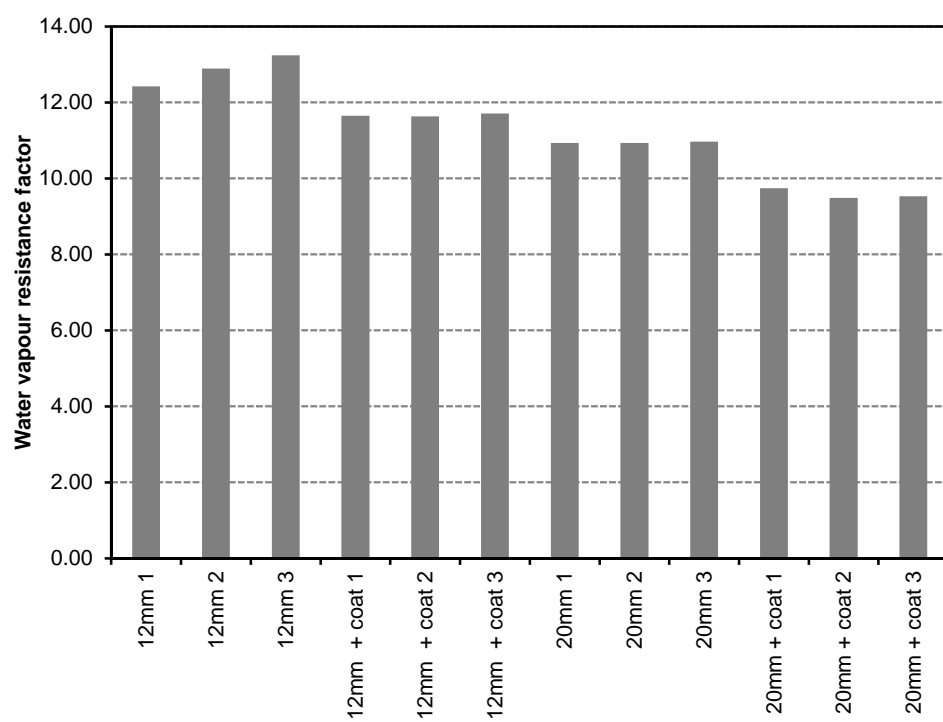


Figure 5.15: Water vapour resistance of plasters from group VIII

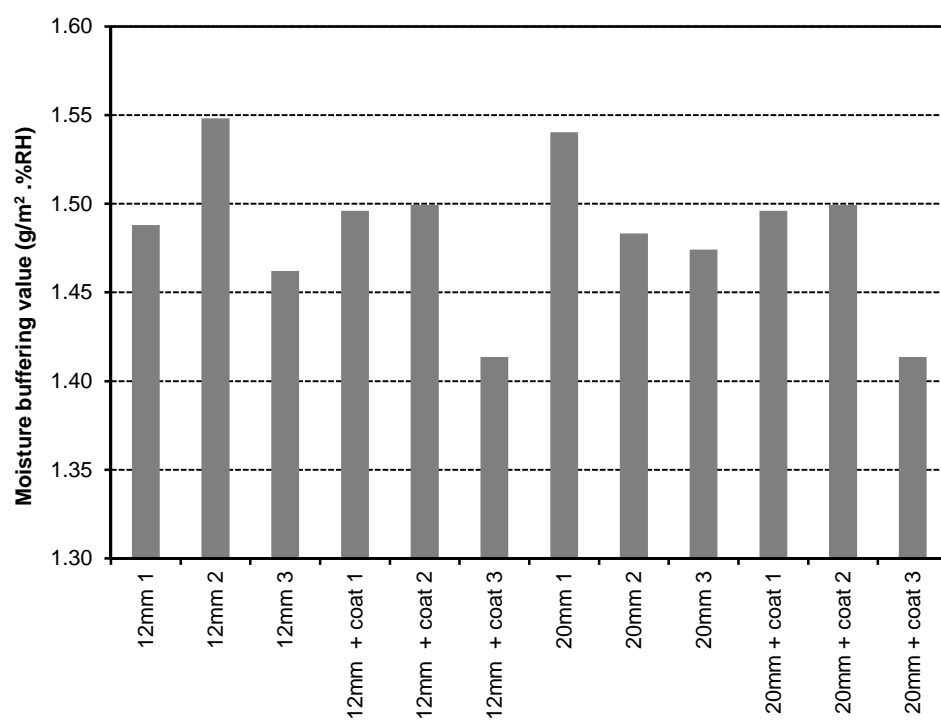


Figure 5.16: Moisture buffering results from plasters in group VIII

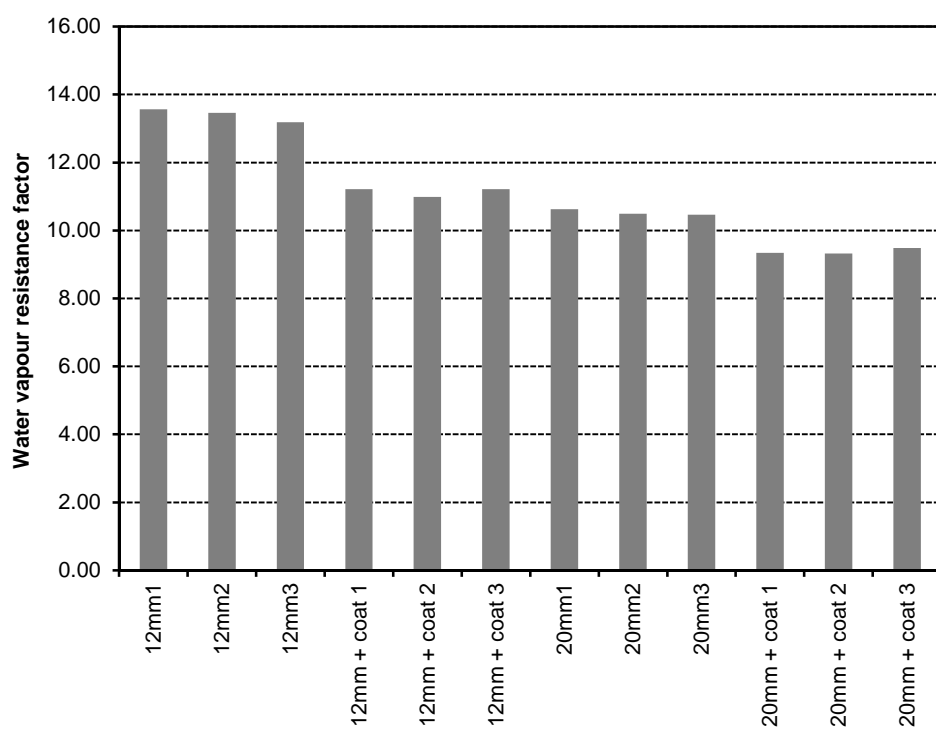


Figure 5.17: Water vapour resistance factor of plaster from group IX

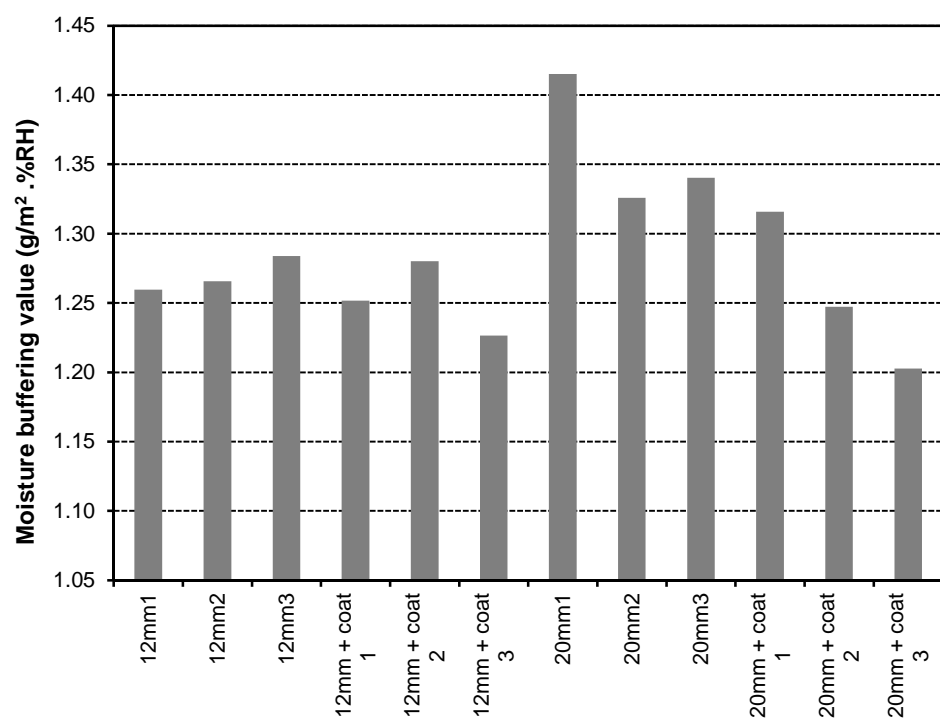


Figure 5.18: Moisture buffering value of plasters from group IX

5.3 Summary

The experimental results show a clear difference in the influence of each modified parameter, some clearly affect the hygric behaviours of the materials. For some changes the material structure is modified which is illustrated by the modification of the water vapour resistance and moisture buffering values without any modification of the sorption isotherms. This results in a reduction in the vapour flow through the material leading to a reduced MBV. In other cases, the nature and availability of the surface adsorption sites is modified and this is illustrated by the loss of correlation between water vapour resistance and moisture buffering and a substantial change in the sorption isotherms.

For all samples presented in this chapter, the water vapour resistance varies between 4.3 and 13.6, the moisture buffering capacity varies between $1.1 \text{ g/m}^2 \cdot \%RH$ and $3.7 \text{ g/m}^2 \cdot \%RH$ and the equilibrium moisture content at 65% RH varies between 0.62% to 2.43%. Further analysis on the entire results will be presented in Chapter 6, but it is important to note that it is difficult to change one parameter (e.g compaction water content) without varying another (e.g. apparent density). The relative importance of the different factors is therefore also discussed in Chapter 6.

6 Discussion

This chapter will look into the trend of all results described in Chapter 5 combined and explain the influence of individual parameters. The experimental moisture buffering results will be compared to theoretical calculated results using the steady-state hygrothermal properties of the material. The investigated properties of the material can be divided into properties that modify the structure of the material or properties that modify the internal surface area or activity.

6.1 Properties affecting the structural organisation of the material

The properties that affect the structure of the material can be identified when the property has an influence on the vapour transmission but the sorption isotherm does not significantly change. This is because the sorption isotherm is not significantly influenced by the structural organisation of the material in the range of humidity levels used in the MBV test (see Chapter 5)

6.1.1 Apparent density

The apparent density represents the dry mass of the sample per bulk volume of the sample. This can affect the porosity and permeability of soils. The dry mass was determined after placing the samples for 24 hours in an oven at 105°C. The volume was calculated by measuring the size of the samples to a precision of 0.01 mm using a digital caliper.

From the results observed in Chapter 5, the apparent density does not have a significant influence on the sorption isotherm of the material but has a rather important influence on the water vapour transmission. The correlation between water vapour permeability and apparent density was calculated using a correla-

Table 6.1: Correlation between apparent density and water vapour resistance factor for all groups

	Parameter	Linear Correlation coefficient
Group I	Stabilisation	0.003
Group II	Water content	0.908
Group III	Water content	0.941
Group IV	Density	0.979
Group V	Mixing method	0.776
Group VI	Mineralogy	0.847
Group VII	Particle size distribution, mineralogy	-0.267
Group VIII	Plaster	-0.557
Group IX	Plaster	0.293

tion coefficient and the results are given in Table 6.1. These results show that groups in which the changed parameter had a direct influence on the apparent density such as groups II, III and IV had a strong correlation coefficient over 0.9. Group V has a low correlation coefficient of 0.77, the range of water vapour resistance between 10.16 and 11.2 may be too narrow to establish a good correlation where the experimental error may play as much of a role as the apparent density.

Group VI presents a rather high correlation coefficient of 0.85 however from the obtained results it cannot be confirmed that the addition of Bentonite will directly affect the apparent density. It is more likely that the apparent density was affected by the modification of the material plasticity and therefore the water needed for compaction. The addition of stabiliser in group I has an influence on the porosity and the water vapour resistance factor without affecting the apparent density this confirms that the reduction in vapour transmission can be explained by crystallization products blocking pores rather than a change in apparent density. Figure 6.1 shows the water vapour resistance factor plotted against the apparent density for all samples including the results from Lustig-Rössler (1992) in group X. As shown by the poorly defined correlation, factors other than density don't appear to have a significant effect on μ .

The variation of the water vapour resistance factor in groups VIII and IX cannot be explained by the variation of apparent density because the correlation is very low. Neither can it be explained by the variation in the thickness or a variation in the materials nature as this was not modified. The remaining hypothesis rests on the preparation process, the water content was not precisely

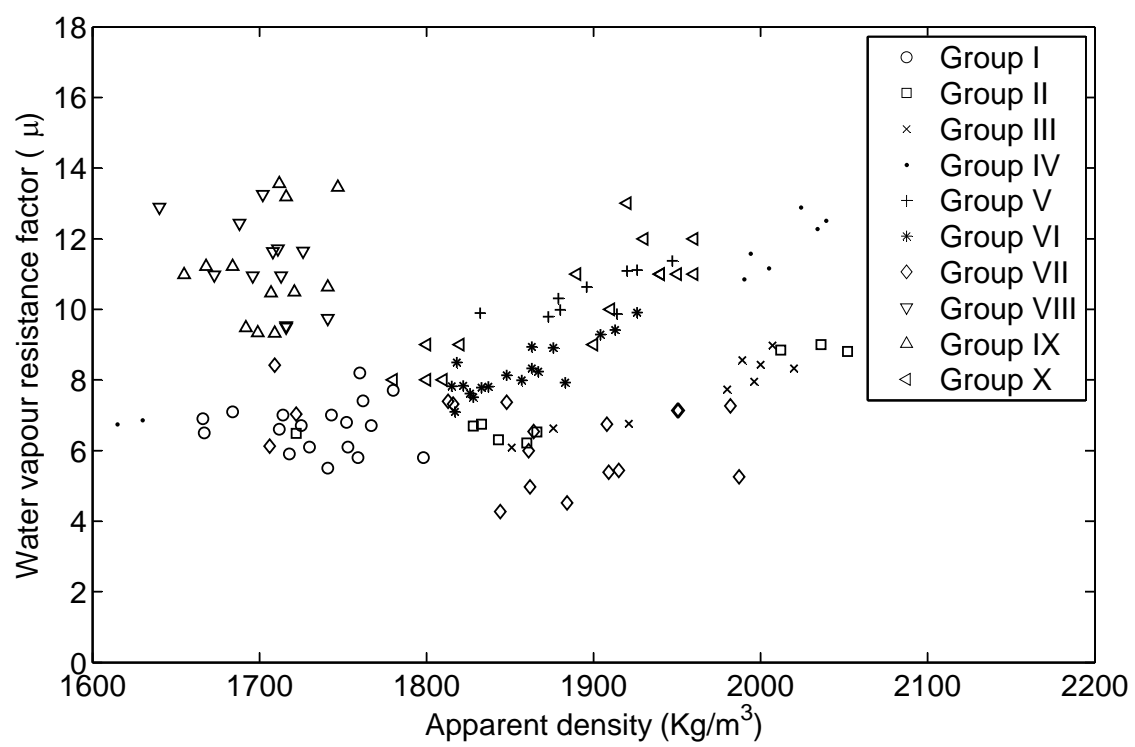


Figure 6.1: Correlation between apparent density and water vapour permeability

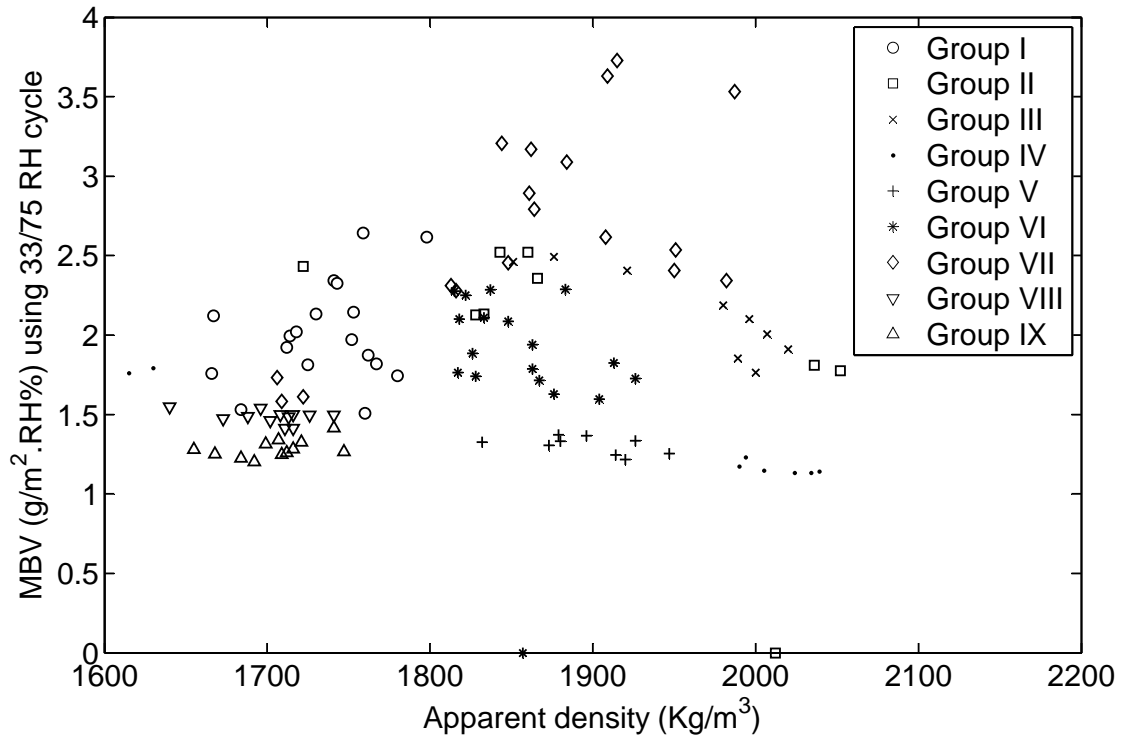


Figure 6.2: Influence of apparent density on the moisture buffering value

controlled during this stage and some cracks appeared on certain samples, this would however result in more variation within identical samples.

Based on observed results it is clear that modifying the apparent density will influence the moisture transmission if no other parameters are changed. On the other side there is no direct correlation between the apparent density and the dynamic moisture adsorption. In Figure 6.2 it can be seen that there is a large variation of the moisture buffering value on a relatively small range of apparent density indicating other factors are influencing the MBV.

As seen in the previous chapter the apparent density doesn't have a significant influence on sorption isotherms which indicates that the modification of the dynamic performance is due to a change in the structural organisation of the material which can mainly be described by the pore network. Because apparent density has little effect on moisture storage it can be deduced that the apparent density mainly modifies the pore network and the macroporosity.

The porosity can be estimated based on the apparent density and using an

average particle density, but this calculation turns out to give little more information as it is directly related to the apparent density. The porosity would have to be measured independently with a method that can also give a good estimation of the microporosity. The mercury intrusion method currently available at the University of Bath was not considered as a suitable method because of the problem occurring in weaker strength materials, where the pressure of the mercury may induce increase of the porosity, but further research into the pore size distribution and the effect this has on the MBV is required.

6.1.2 Water content

The water content used during manufacturing of the samples has a strong influence on the force needed for compaction. It has been shown through the results presented in Chapter 5 that the initial water content had an effect on the apparent density of the material, this is due to an increase of the shrinkage during drying. Indirectly through the change of apparent density the water content influenced the vapour transmission, it is also possible that the water content during compaction has an influence on the structural organisation of particles in the material and would also affect the vapour transmission. To determine this any possible influence of only the water content without the influence of the apparent density had to be estimated.

This was done by estimating the relative increase due to apparent density which then could be subtracted to the variation of the vapour transmission observed in samples where water content and apparent density have a combined influence. The slope of the linear trend described by the following equation $y = 0.013x$ obtained from the results in group IV and V in Figure 6.3 was subtracted to the results of group II and III. This remains however an estimation as the samples in group IV and V were tested with different material as for the water content.

The Figure 6.4 shows the water vapour resistance factors of group II and III corrected by the estimated increase due to the apparent density from groups IV and V. It shows that without the increase of resistance due to the apparent density the water content has a very little effect on vapour transmission properties.

The comparison of sorption isotherms in Figure 6.5 shows that there is no influence on the equilibrium moisture content as both sorption curves are similar. To summarize the initial water content shows to have an influence on the vapour

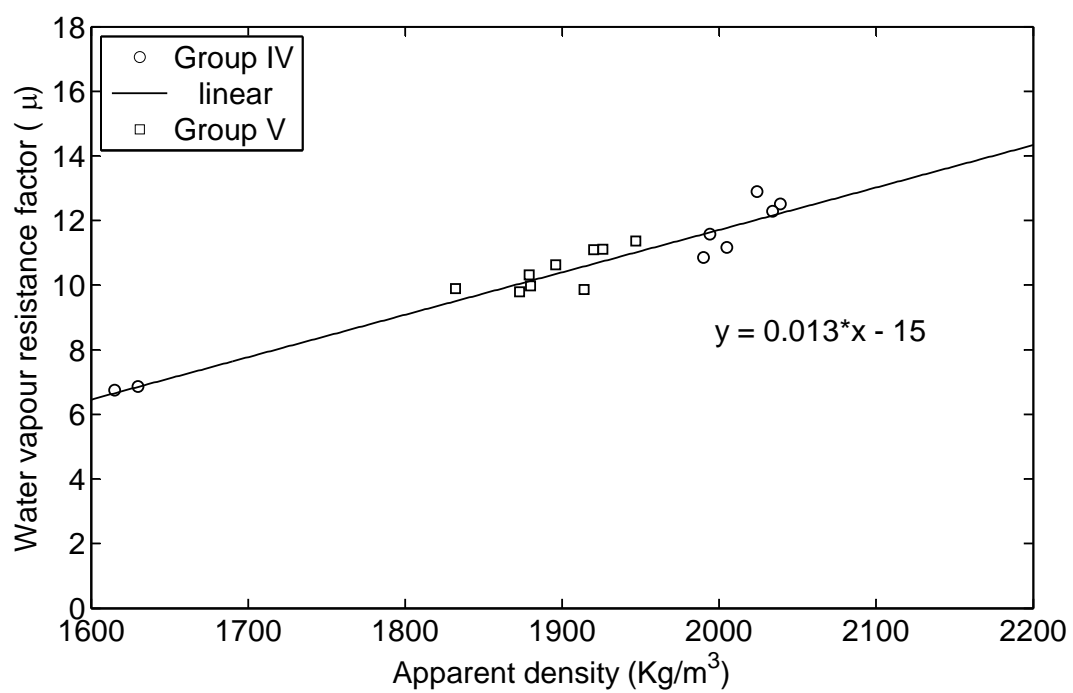


Figure 6.3: Influence of apparent density on water vapour factor in group IV and V

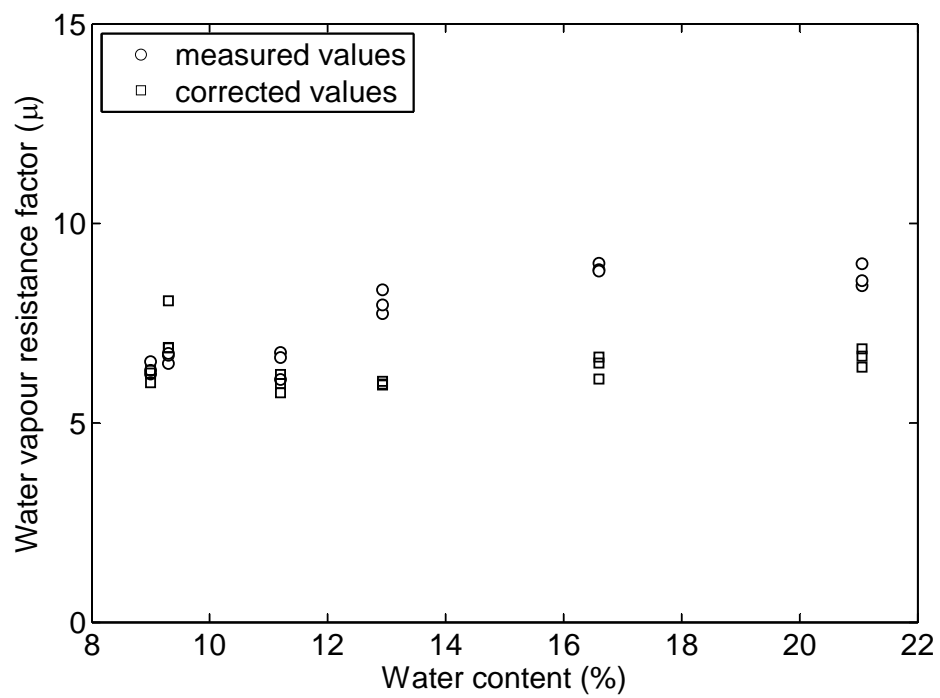


Figure 6.4: Corrected water vapour resistance values of group II and III

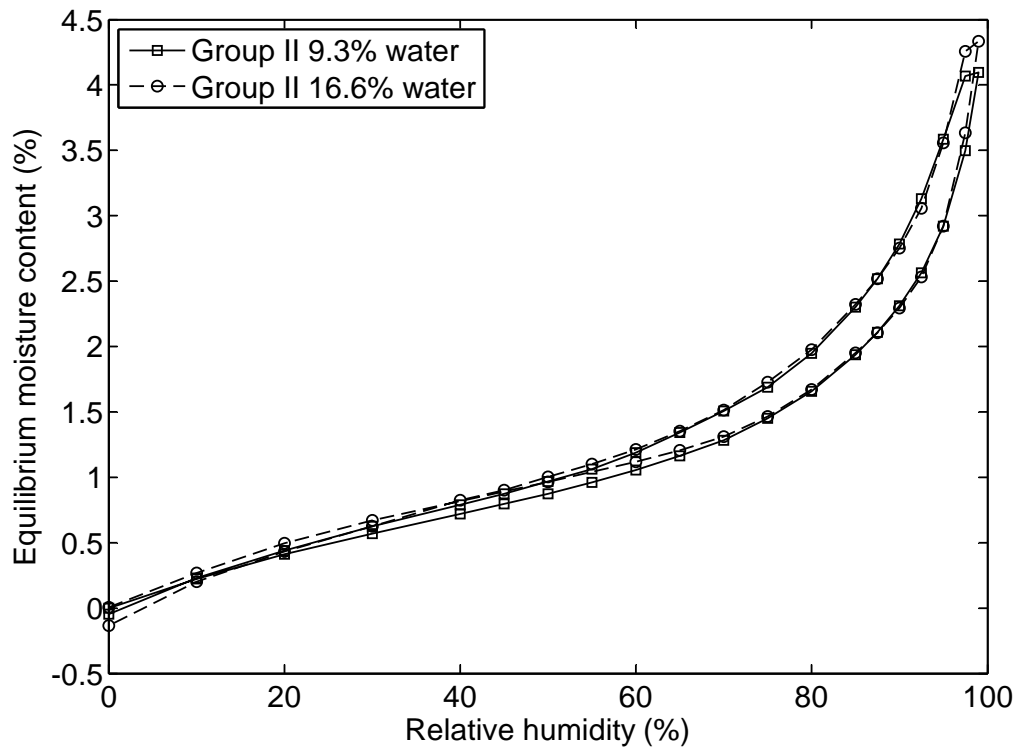


Figure 6.5: Influence of water content on sorption isotherms

resistance but this seems to be due to the increase of apparent density caused by a higher shrinkage after compaction.

6.1.3 Influence of a modified structure on the dynamic adsorption

Plotting apparent density and MBV of all samples in Figure 6.2 does not show any correlation between them. From the previous discussion it is clear that modifying the structure of the material primarily modifies the moisture transmission rate.

It can be seen in Figure 6.9 that there seems to be a negative correlation between moisture buffering and the water vapour resistance factor which would be expected as a lower resistance increases penetration depth. The linear correlation coefficient was used to estimate the correlation of the data between the μ factor and the MBV. It was applied on the data as it is, see Figure 6.6, on the relation between $\log(\mu)$ and MBV to characterise an exponential regression with a linear

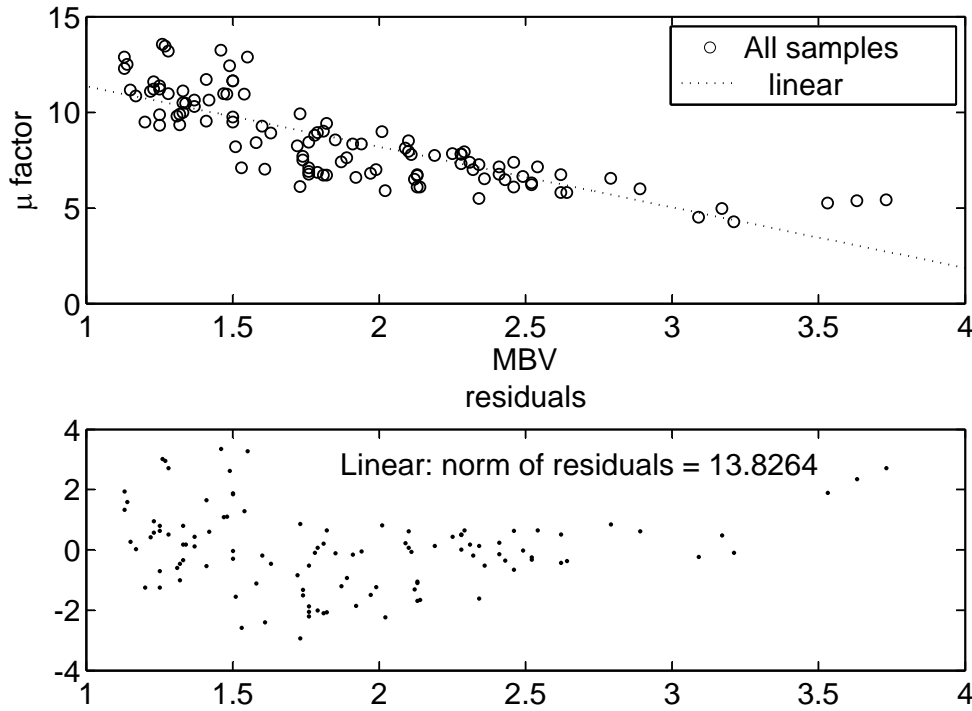


Figure 6.6: Linear fit between μ factor and MBV

fit and on the relation between $\text{Log}(\mu)$ and $\text{Log}(\text{MBV})$ to characterise a power regression with a linear fit, see table 6.2. The norm of residuals was also calculated and is given for a linear fit in Figure 6.6, for an exponential fit in Figure 6.7 and for a power fit in Figure 6.8. The lowest norm of residuals is also given by the power fit which confirms the results of the correlation coefficients.

The power correlation gave a slightly better result with a total correlation coefficient for all groups of -0.87, details are given in table 6.2. When taking into account the data from the materials tested for the Nordtest project, the linear correlation coefficient drops to -0.62 and the correlation if an exponential function is considered drops to -0.72 and -0.71 with a power function.

The strongest correlations are observed for groups II, III and IV which are also the groups where apparent density had the strongest influence. In these groups the change in MBV is therefore clearly only due to a change in structure which affects the vapour resistance.

The water vapour resistance plays a significant role in the moisture buffering

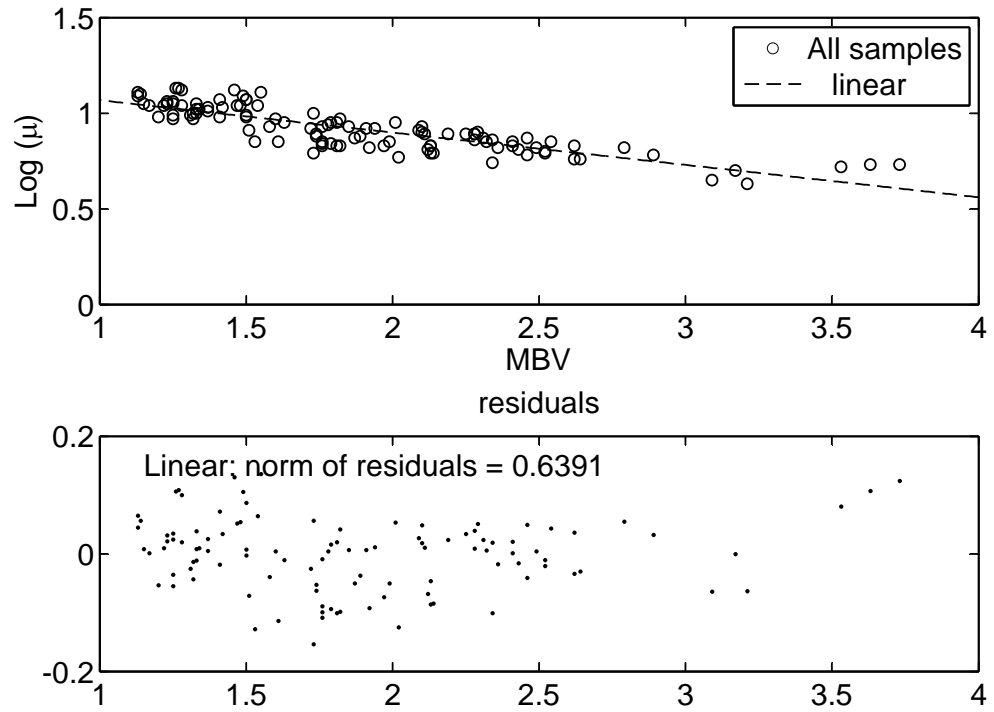


Figure 6.7: Exponential fit between μ factor and MBV

Table 6.2: Lineat correlation coefficients for water vapour resistance and moisture buffering

Group	Linear correlation	Exponential correlation	Power correlation
Group I	-0.76	-0.77	-0.78
Group II	-0.92	-0.93	-0.95
Group III	-0.91	-0.91	-0.90
Group IV	-0.97	-0.98	-0.98
Group V	-0.27	-0.26	-0.27
Group VI	-0.46	-0.44	-0.45
Group VII	-0.76	-0.75	-0.72
Group VIII	0.19	0.19	0.19
Group IX	-0.10	-0.08	-0.08
All groups	-0.81	-0.84	-0.87

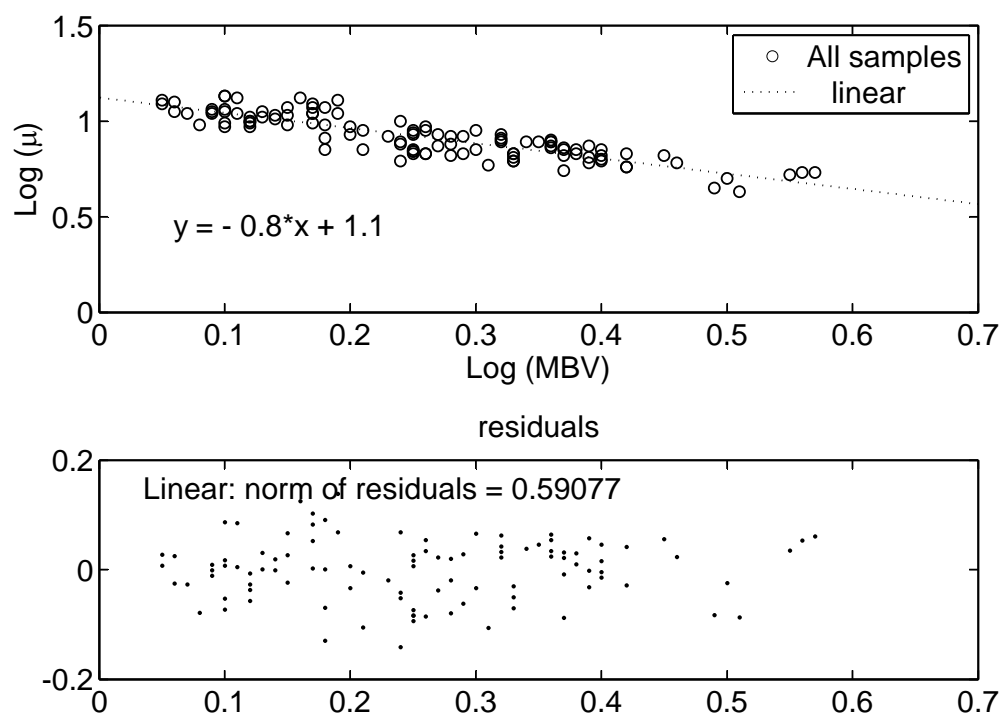


Figure 6.8: Power fit between μ factor and MBV

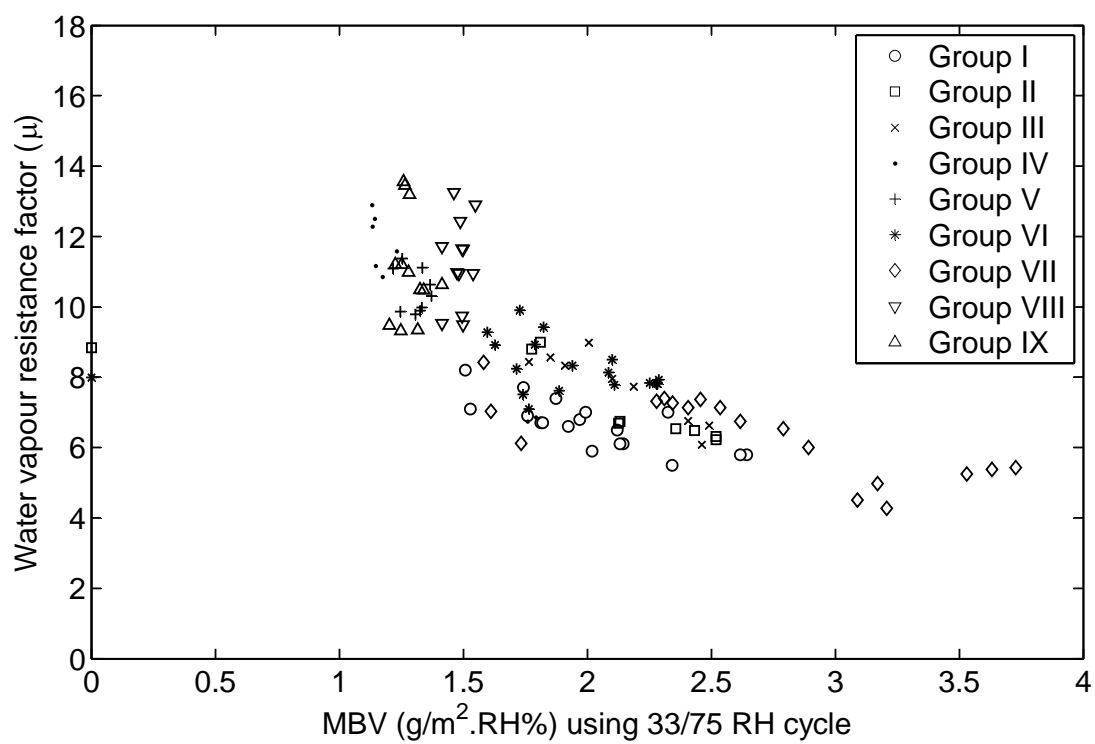


Figure 6.9: Water vapour resistance factor and moisture buffering value

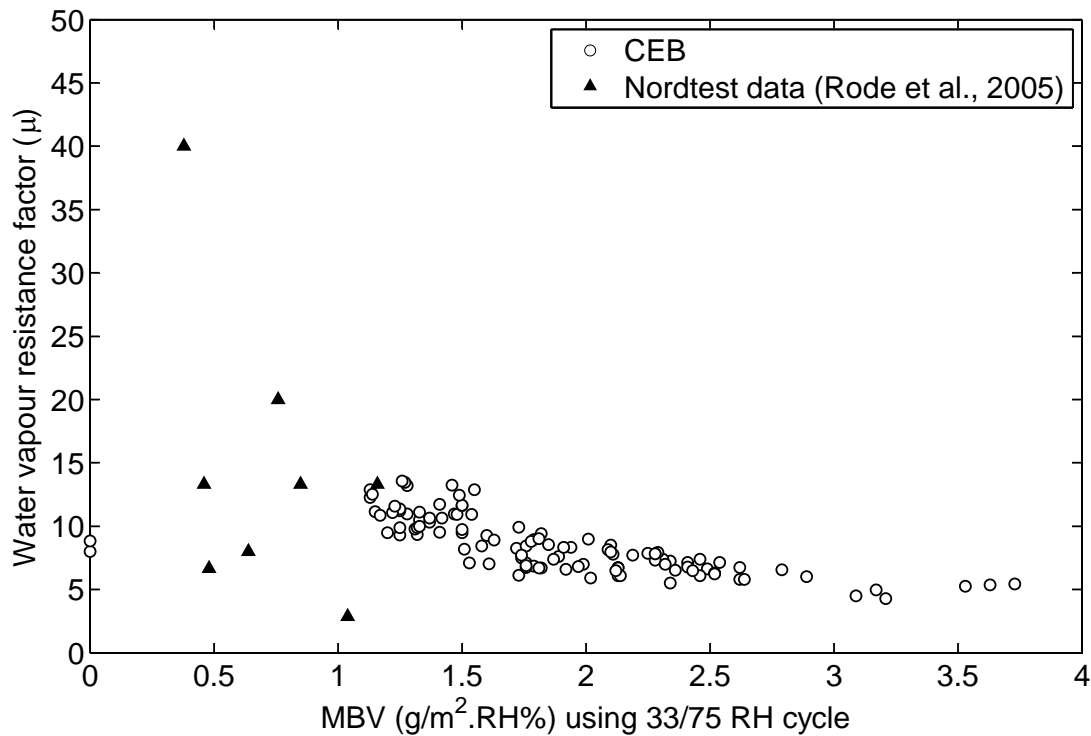


Figure 6.10: Experimental results compared with the results from (Rode et al., 2005)

capacity of unfired clay masonry. As shown, there is a rather good correlation between the MBV and the water vapour resistance factor. Figure 6.9 also shows that there is a large variability within the unfired clay materials. The vapour resistance factor varies between 4.3 and 13.6 and the MBV varies between 1.13 and 3.73 g/(m².%RH). These results can be put in perspective with the average values obtained from the Nordtest project (Rode et al., 2005) of conventional building materials as shown in Figure 6.10. There appears to be a lower value around 5 where a further reduction in vapour resistance is not responsible for the improving MBV, which suggests that the MBV is then improved by other material properties such as the moisture capacity.

6.2 Properties affecting the internal surface activity of the material

The properties having an influence on the internal surface activity of the material were identified by the significant change these have on sorption isotherms. Among the investigated properties are those identified as having a relevant influence : the particle size distribution, the mineralogy and the addition of a stabiliser.

6.2.1 Particle size distribution

To simplify characterisation, the particle size distribution is often expressed in percentages of clay, silt, sand and gravels. The same simplification was used during this study, whereas in reality even the silt or clay fraction could be divided into several sub-fractions. It is also the case that clay minerals vary in size, for example a Smectite type clay is typically smaller than a Kaolinite, they also differ in surface activity which is why mineralogy will be treated as an individual section. The main difference resulting from a change in particle size distribution are the internal surface area and the pore size distribution. The clay content should largely affect the surface area and therefore the multilayer adsorption. Silt is expected to have a limited effect on capillary condensation depending on the size of the silt.

Comparing sorption isotherms in Figure 6.11 of soil “Le” with a silt content of 66.7% and soil “St” with a silt content of 10.3% but a similar clay content respectively of 14.8% and 16%, the main difference can be observed above 20% RH. The lower section below 20% RH is hardly affected and this zone is related to the surface area. For a major contrast in silt content, 66.7% and 10.3%, sorption isotherms are only slightly affected. This seems to indicate that the silt content has a very limited influence on the equilibrium moisture content.

Conversely a soil with a very high clay content of 50.1% (Bi) shows a greater difference on the initial stage and the rest of the sorption isotherm compared to a soil with a low clay content of 5.5% (Th). In Figure 6.12 the sorption isotherms show a higher EMC for the “Bi” sample on the whole range of RH.

Additionally different size fractions do not present much variation in the water vapour resistance factor, see Figure 6.13. Only a slight decrease of vapour resis-

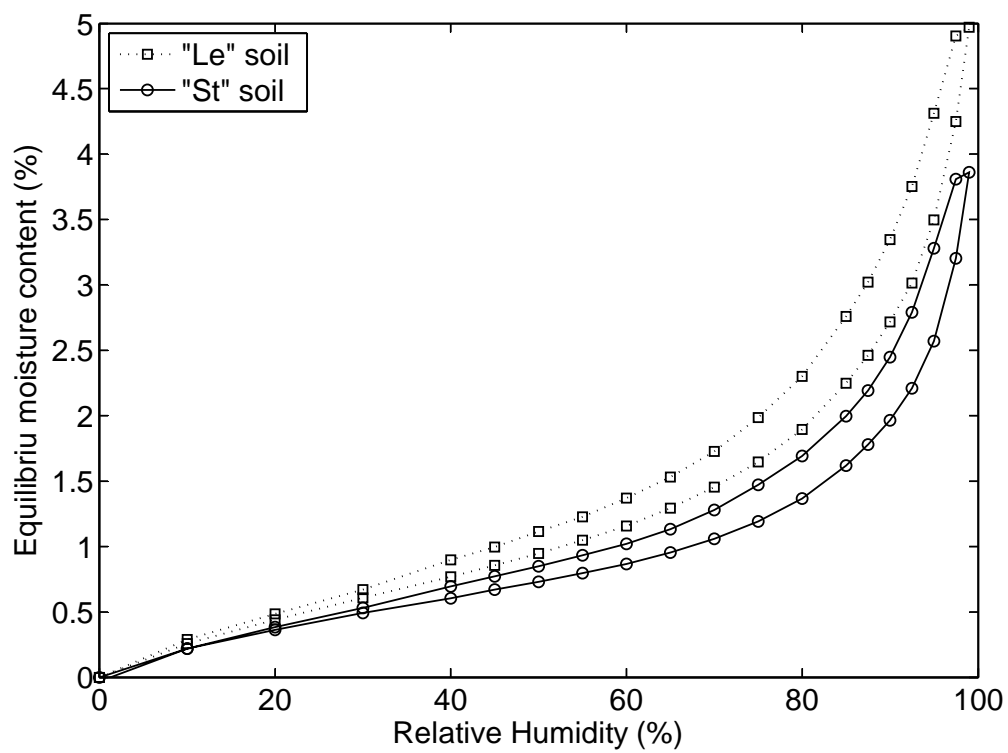


Figure 6.11: Compared sorption isotherms of Le and St soils

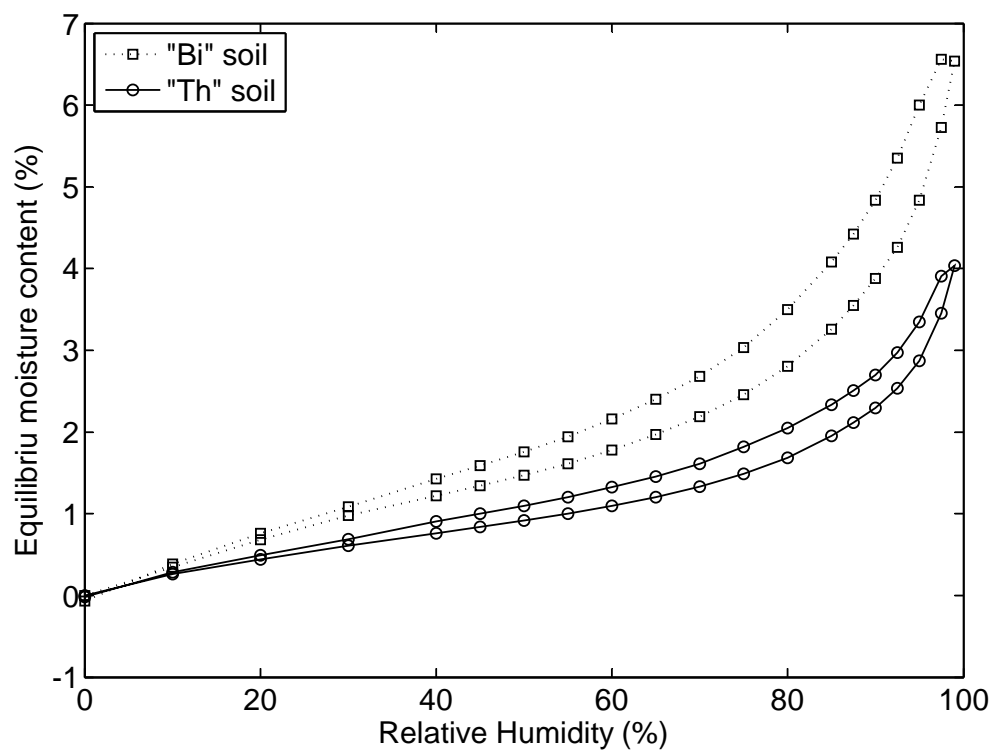


Figure 6.12: Compared sorption isotherms of Bi and Th soils

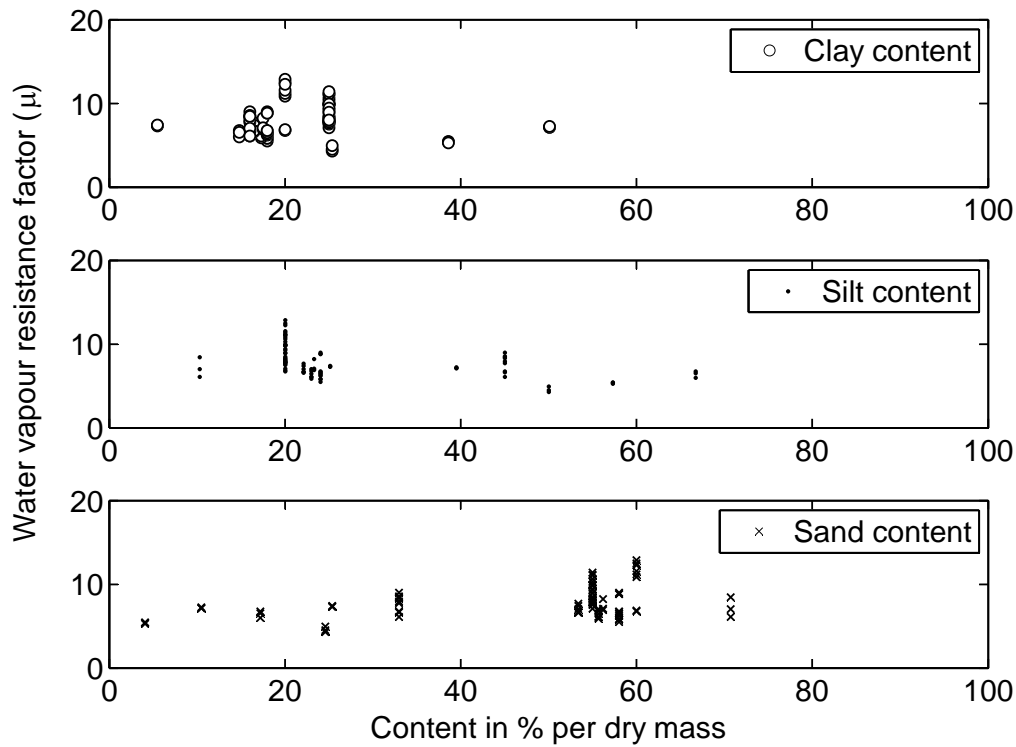


Figure 6.13: The influence of particle size fractions on the water vapour resistance factor

tance with an increase of silt and a slight increase in vapour resistance with an increase in sand content can be observed, this trend is confirmed by the correlation factors in Table 6.3 who remain however rather poor.

The particle size distribution has more effect on the dynamic adsorption. Figure 6.14 shows the influence of the different particle fractions on the moisture buffering value. A negative correlation coefficient of -0.75 between sand content and MBV shows that there is a relation and there is therefore a positive correlation of 0.75 between the combined clay and silt content with the moisture buffering value.

Correlations between particle sizes and hygric properties are presented in Table 6.3. The strongest correlation is seen between the MBV and silt content, which can be explained by the fact that silt also has a strong effect on vapour permeability. Clay presents no correlation with vapour permeability in these results. Equal correlation factor is obtained between clay and moisture capacity

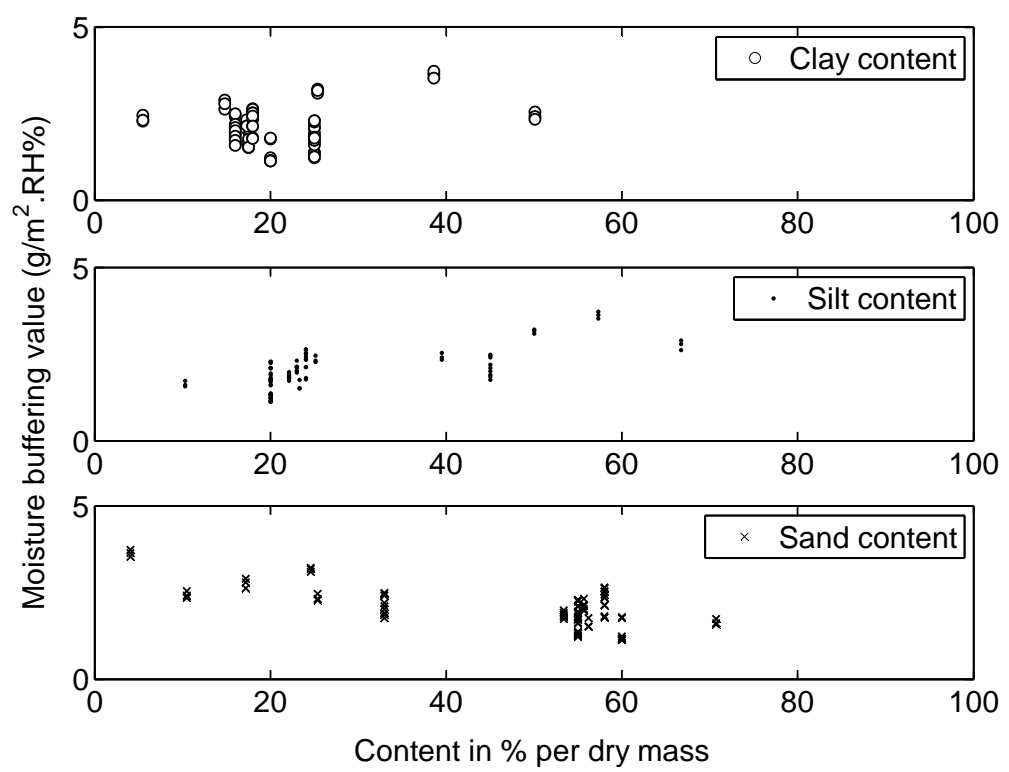


Figure 6.14: The influence of particle size fractions on the moisture buffering value

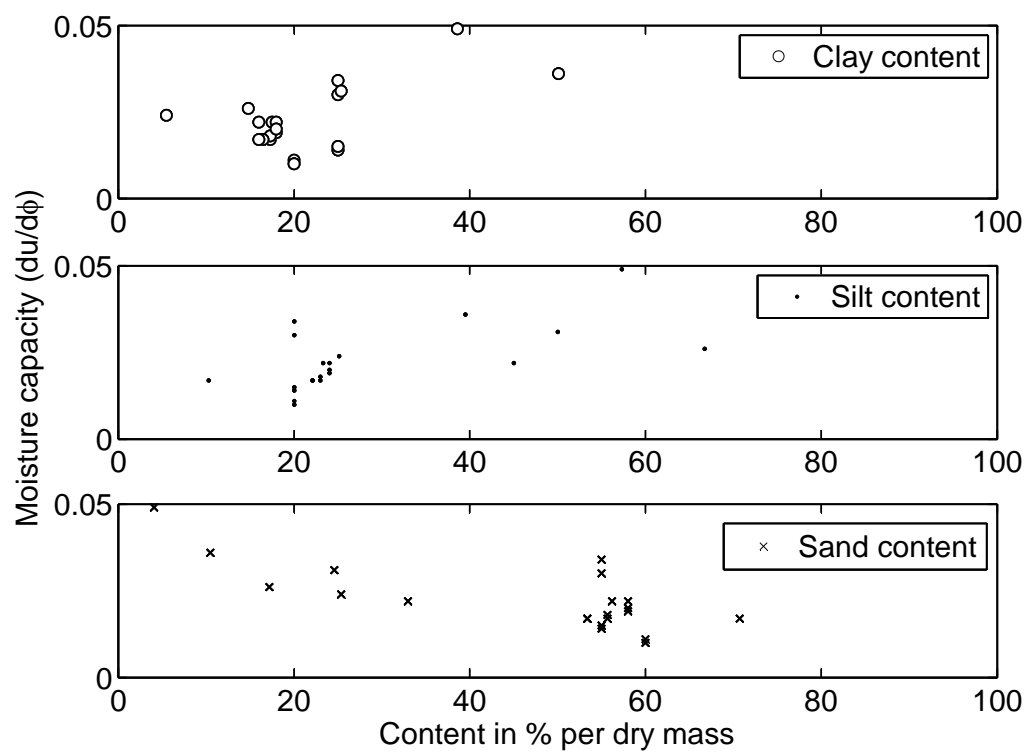


Figure 6.15: The influence of particle size fractions on the moisture capacity

Table 6.3: Linear correlation coefficients between size fraction and hygric parameters for samples from group I to VII

Particle size	Linear correlation with		
	μ factor	Moisture capacity	MBV
Clay	0.02	0.61	0.20
Silt	-0.42	0.61	0.69
Clay + Silt	-0.33	0.75	0.65

and silt and moisture capacity. Based on sorption isotherm results the clay fraction seems to have a stronger effect on moisture capacity. This similar correlation might be because in many samples the clay and silt content are similar. However the best correlation with the moisture capacity is found with the combined clay and silt content so both fractions have a positive influence while sand content has a negative influence on moisture capacity.

To summarise, presented results shows that silt has an influence on all hygric properties and therefore has a stronger influence on MBV then clay alone. Clay plays an important role on moisture capacity whereas it has no correlation with the μ factor. This means that silt plays as much of a role then clay. This is however based on correlation factors that remain all relatively weak, below 0.90, this illustrates that a multitude of parameters influence moisture buffering. It would be interesting in a future study to further refine the particle size distribution as there might be a huge difference if the silt is actually composed of particles of 3 μm or 60 μm .

The pore size distribution is directly related to particle size distribution. An increase of clay and fine silt particles should lead to an increase of microporosity (< 2 nm) and mesoporosity (2 nm - 50 nm) which would be beneficial to the moisture buffering potential if it does not reduce the vapour permeability. Pore size distribution was not measured during this study, yet if the microporosity and mesoporosity can accurately be measured it would allow to find an optimal pore size distribution to allow sufficient vapour permeability and a maximum of moisture storage but this is beyond the scope of this initial research program.

The mineralogy is an important parameter that is rarely taken into account in civil engineering applications using unfired clay. The clay minerals are most often just referred to in terms of particle size, the clay fraction, yet a variation in hygroscopicity between clay types plays an important role in moisture buffering. At

the best, the Atterberg limits are used as an indirect indicator of mineral behavior. Padfield (1998) mentioned in his thesis that the Montmorillonite type clay should have the highest potential to regulate moisture, this can easily be demonstrated when measuring the sorption isotherms for a Kaolinite and a Montmorillonite, see Figure 6.16. The difference between the two clay minerals is very clear, but most of the soils that were measured during this study had sorption isotherms closer to the Kaolinite sorption isotherm and reach a maximum EMC around 5% whereas the montmorillonite reaches levels above 25%. The inconvenience with a Bentonite type clay in engineering applications is the swelling and shrinkage. Too high a Bentonite content would drastically increase the amount of water needed for compaction and therefore also the shrinkage that would occur during drying which may cause undesirable cracks. Hence only a maximum of 10% of Bentonite was added to a Kaolinite based soil. As mentioned earlier, the exact mineralogy of the Bentonite could not be obtained, but according to the manufacturer it is predominantly Montmorillonite.

6.2.2 Mineralogy

The main difference of these two minerals in terms of water adsorption is explained in Figure 6.17. The crystal structure of a 1:1 and a 2:1 clay mineral was described in Chapter 2 and here it illustrates the water adsorption. The Montmorillonite type clay is composed of layers separated by an interlayer space which will with an increase of partial vapour pressure adsorb water molecules. Clay engineering is now sufficiently advanced that this interlayer space can artificially be increased to adsorb even more, this is for example the case for pillared clays. In the case, of the pillared clay that was tested for this study, no major difference to the normal Bentonite was observed.

When comparing the tested samples with different mineralogy in Figure 6.18, it is interesting to note that a sample with 25% of clay content of which 24% Kaolinite and 1% Bentonite has similar adsorption capacity to pure Kaolinite in the monolayer and multilayer adsorption range (below 70% RH). The pure Kaolinite has more pores available for capillary condensation to occur and this can be seen because the curve has a very sharp increase at higher RH levels. The sample with 10% Bentonite shows a significant increase in equilibrium surface adsorption and this is also reflected in the dynamic adsorption. Results in Chapter

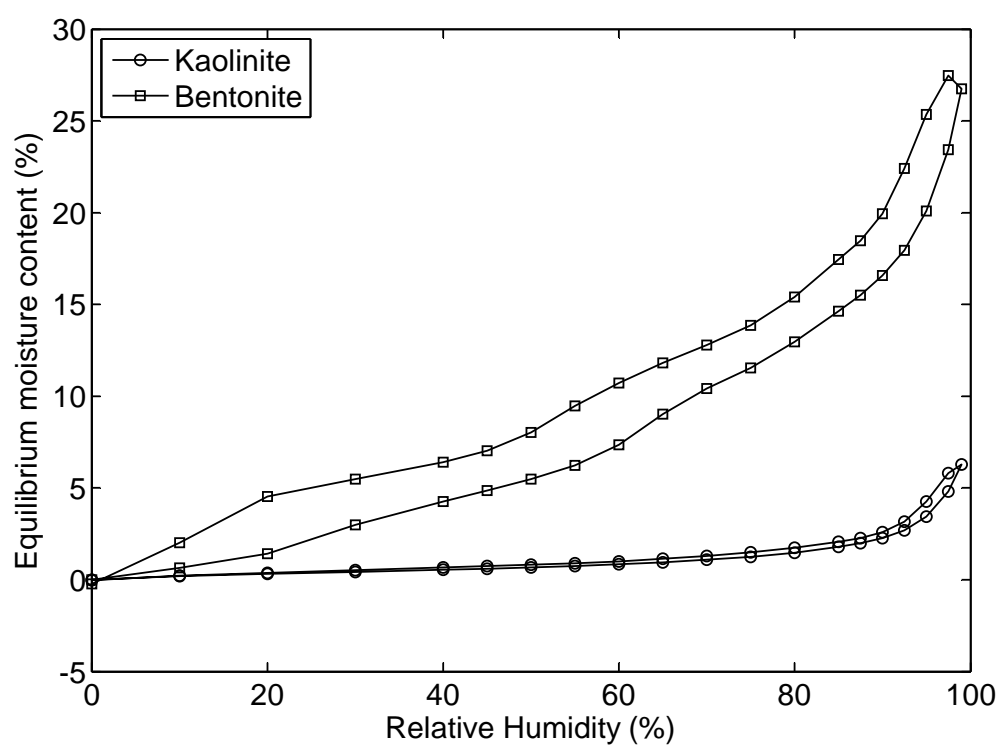


Figure 6.16: Sorption isotherms of the Kaolinite and the Bentonite used during this study

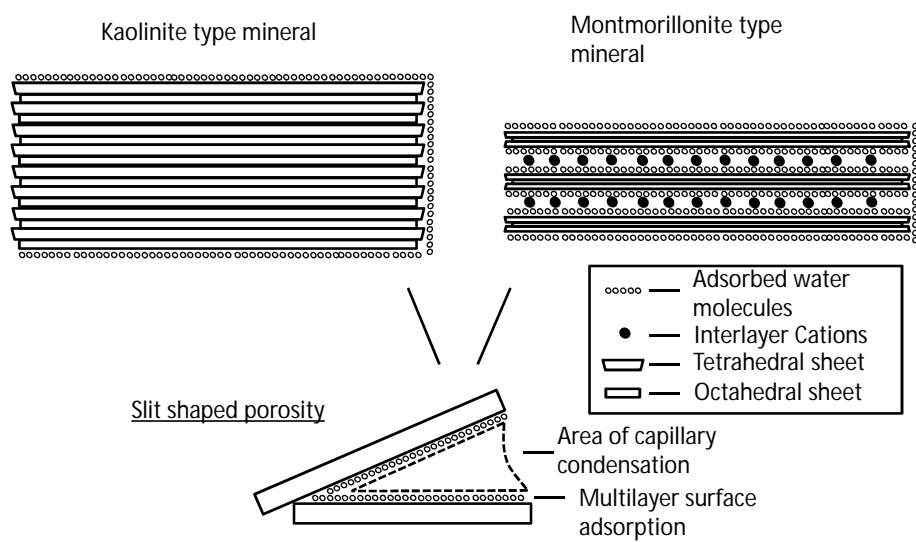


Figure 6.17: Schematic representation of a Kaolinite and a Montmorillonite type mineral and the associated porosity

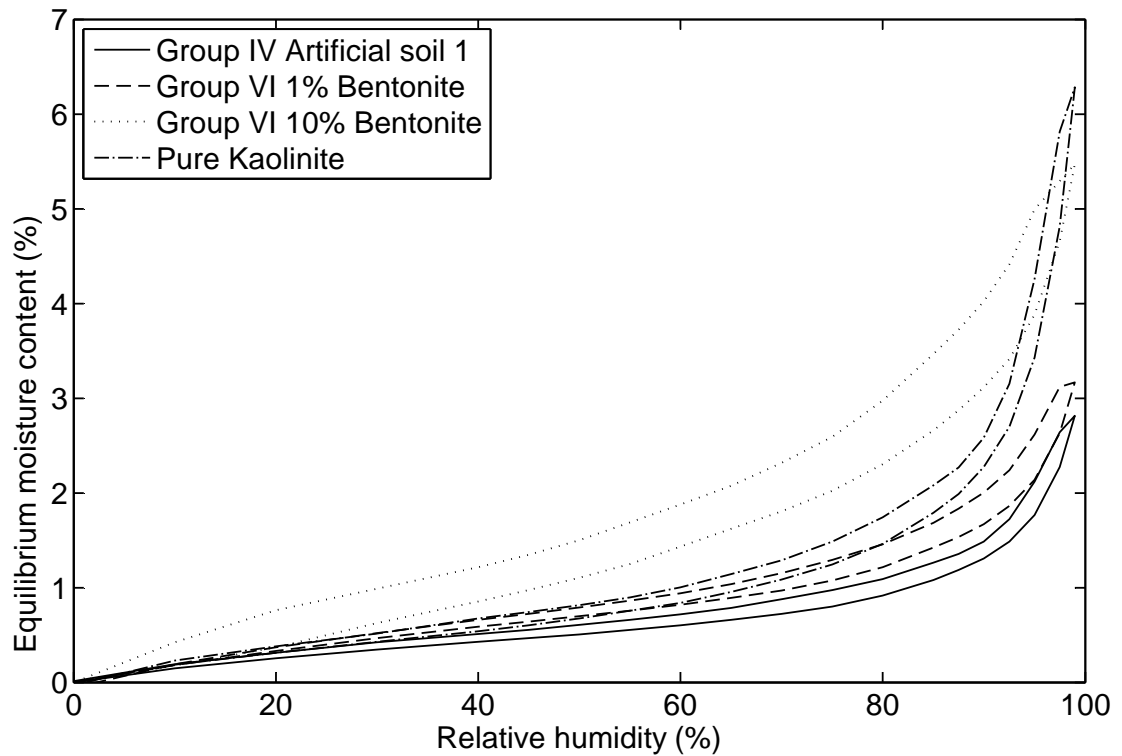


Figure 6.18: Sorption isotherms comparison of tested mineralogy contents, the pure Kaolinite was tested in the form of a powder as a reference.

5 showed that the addition of Bentonite improved the moisture buffering value from about 1.5 to 2.3 g/(m².%Rh). The improvement in the MBV is due to the increase in moisture capacity with the change of surface activity as the water vapour resistance factor has actually increased.

A 100% Bentonite sample is probably the extreme upper limit of possible sorption isotherms for natural soils, as most soils are closer to the kaolinite sorption isotherms and this leaves a large field to improve the dynamic sorption of soils which must be considered along with other engineering properties.

6.2.3 Addition of stabiliser

The addition of stabiliser has been a source of debate, some authors suggest that the addition of stabiliser increases the dynamic adsorption (Liuzzi et al., 2012), whereas other publications suggest the opposite (Eckermann and Ziegert, 2006).

Similarly results in this present study suggest that stabilisation decreases the moisture buffering capacity for the soil studied. It decreases the moisture capacity and increases the water vapour resistance therefore the dynamic adsorption is reduced, see results in Chapter 5. This aspect was investigated for a conference paper (Mcgregor et al., 2012). Several additional analytical methods were used, such as the Scanning Electron Microscope to visualise the potential hydration products from the added stabiliser (mainly cement and lime), also Fourier Transform Infrared Spectroscopy (FTIR) was also used to determine any influence of the stabiliser on the crystal structure of the clay minerals.

Mitchell and El Jack (1966) describes the soil-cement interaction where over time the stabilisers, notably lime, chemically attacks the clay minerals. Similar observations were made by Venkatarama Reddy (2012) who describes the cement as interlocking the clay particles and the lime reacting with the clay minerals. The geopolymer stabilisation behaves in a similar way to lime. In general it is understood that high pH (found in lime or geopolymer stabilisation) dissolves clay minerals and this can be confirmed through the investigation on the infrared spectra of the material. As the infrared spectra were acquired 10 months after the samples were compacted, most of the reactions within the samples are expected to have occurred. For the measurement, the samples were crushed and sieved and only portion smaller than the under $63\mu m$ was used.

Spectras for cement stabilisation are shown in Figure 6.19, lime stabilisation spectras are shown in Figure 6.20 and geopolymer stabilisation is shown in Figure 6.21. Peaks observed in the spectra corresponds to particular vibrational modes of different bonds and the results inform on the interaction of the stabiliser with the soil minerals as some peaks appear and some disappear. As noted by Venkatarama Reddy (2012) the cement stabilisation has little effect on the spectra, and the major influence is an increase of the peak around 1500 cm^{-1} and a decrease of the peak at 1620 cm^{-1} .

The same influence is visible for lime stabilisation, only more pronounced. It can also be noted that the peak around 2524 cm^{-1} is gradually increasing with an increase of stabiliser. The exact interpretation of each peak would lie beyond the scope of this research as it would have to be coupled with further analytical techniques.

The geopolymer spectra shows that there is more interaction with the clay min-

erals as many of the peaks are reduced or disappear, the crystal structure of the clay mineral is degraded which can be seen by the decrease of the peaks around 3600cm^{-1} which usually correspond to the Hydroxyl stretching bands for Kaolinites. Overall this observation agrees with observations made by Venkatarama Reddy (2012).

The fact that the geopolymer stabilisation modifies the structure of the minerals is equally confirmed with the results of the sorption isotherms, see Chapter 5, where the surface adsorption has been decreased but the capillary condensation has significantly increased. This would be expected with a significant change of particle size distribution and is expected as the geopolymer is reported to dissolve clay minerals.

6.2.4 Influence of a modified internal surface activity on the dynamic adsorption

The modification of the internal surface activity can be characterised by the moisture capacity obtained from the sorption isotherms. The moisture capacity obtained from DVS measurements on the section between 30% RH and 80% RH can be compared with the results obtained for the MBV with the climate chamber. Figure 6.22 shows the results of the moisture capacity obtained for all soil mixes that were measured with the DVS. Measurements with the DVS were performed on small samples (less than 1 g) with all surfaces of the samples exposed except that in contact with the balance, unlike the samples in the climate chamber where only one surface was exposed. A clear trend is visible, the comparison yields a linear correlation coefficient of 0.82, which indicates that the moisture capacity is to a certain extent influencing the MBV variation observed at lower water vapour resistance values for unfired clay masonry. The higher the moisture capacity (slope of the sorption isotherm) the higher seems to be dynamic adsorption of the experimentally measured samples.

6.3 Classification of results

According to the classification given by the Nordtest project, all the materials tested classify as good or excellent buffering materials. It would be useful to

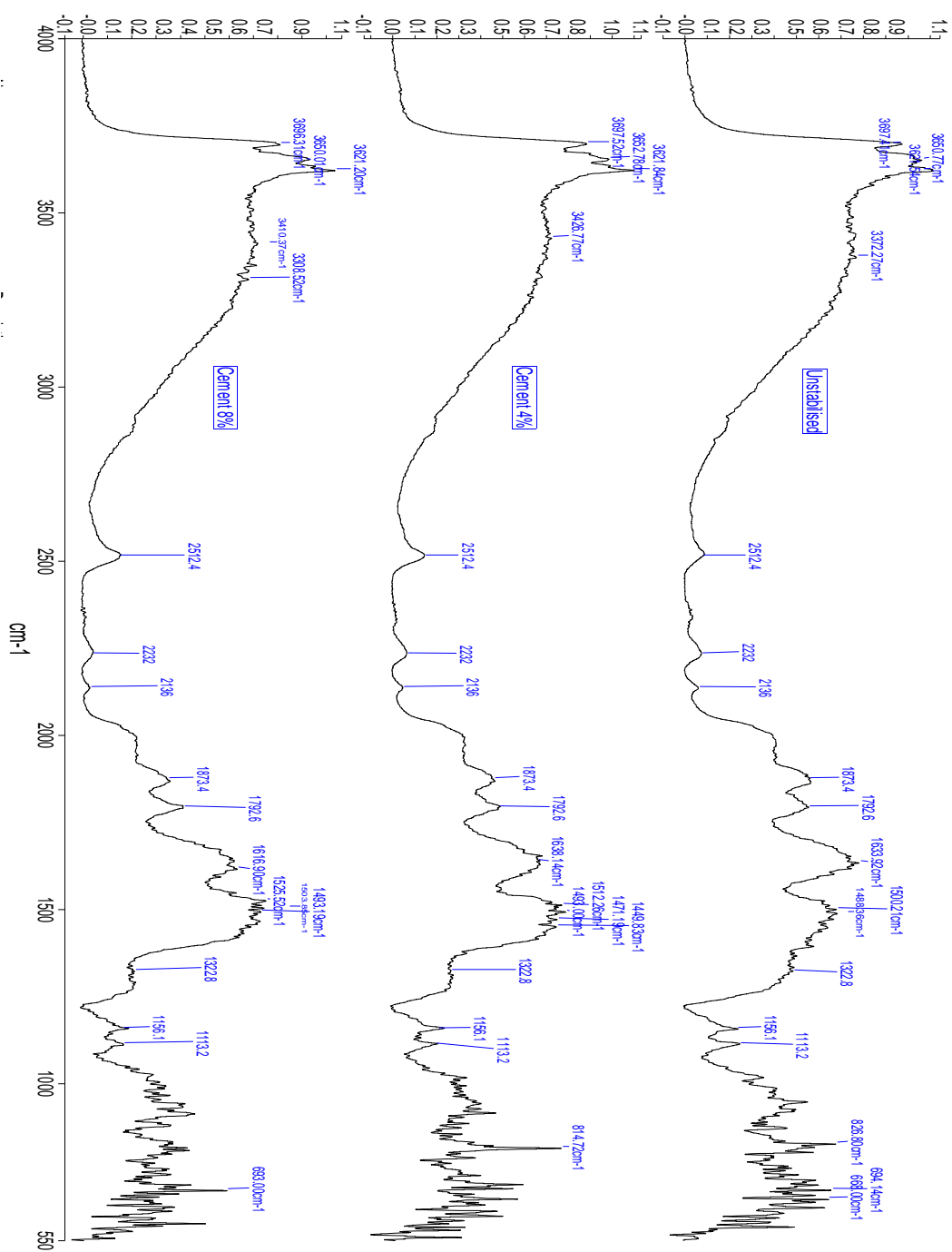


Figure 6.19: FTIR spectra of cement stabilised samples

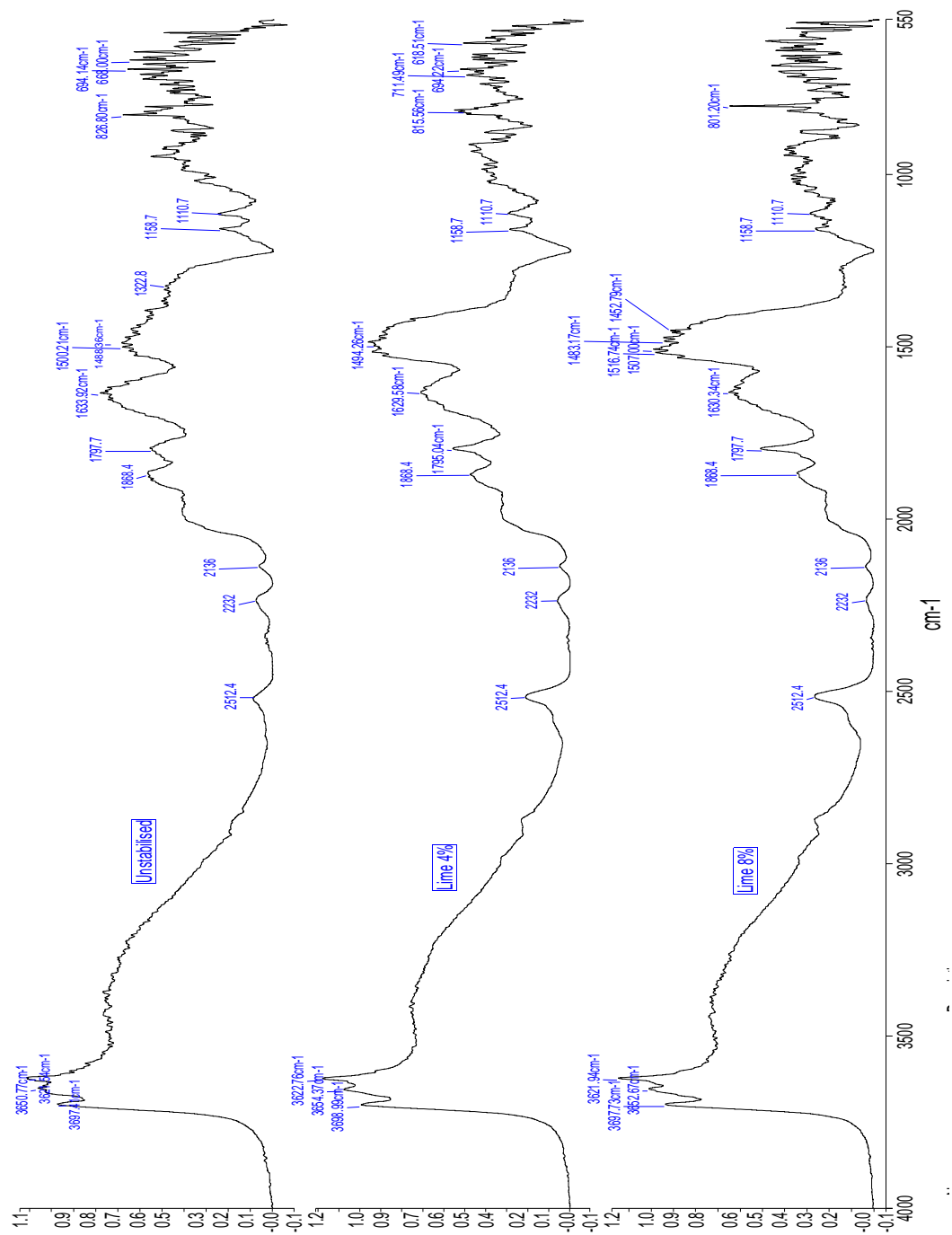


Figure 6.20: FTIR spectra of lime stabilised samples

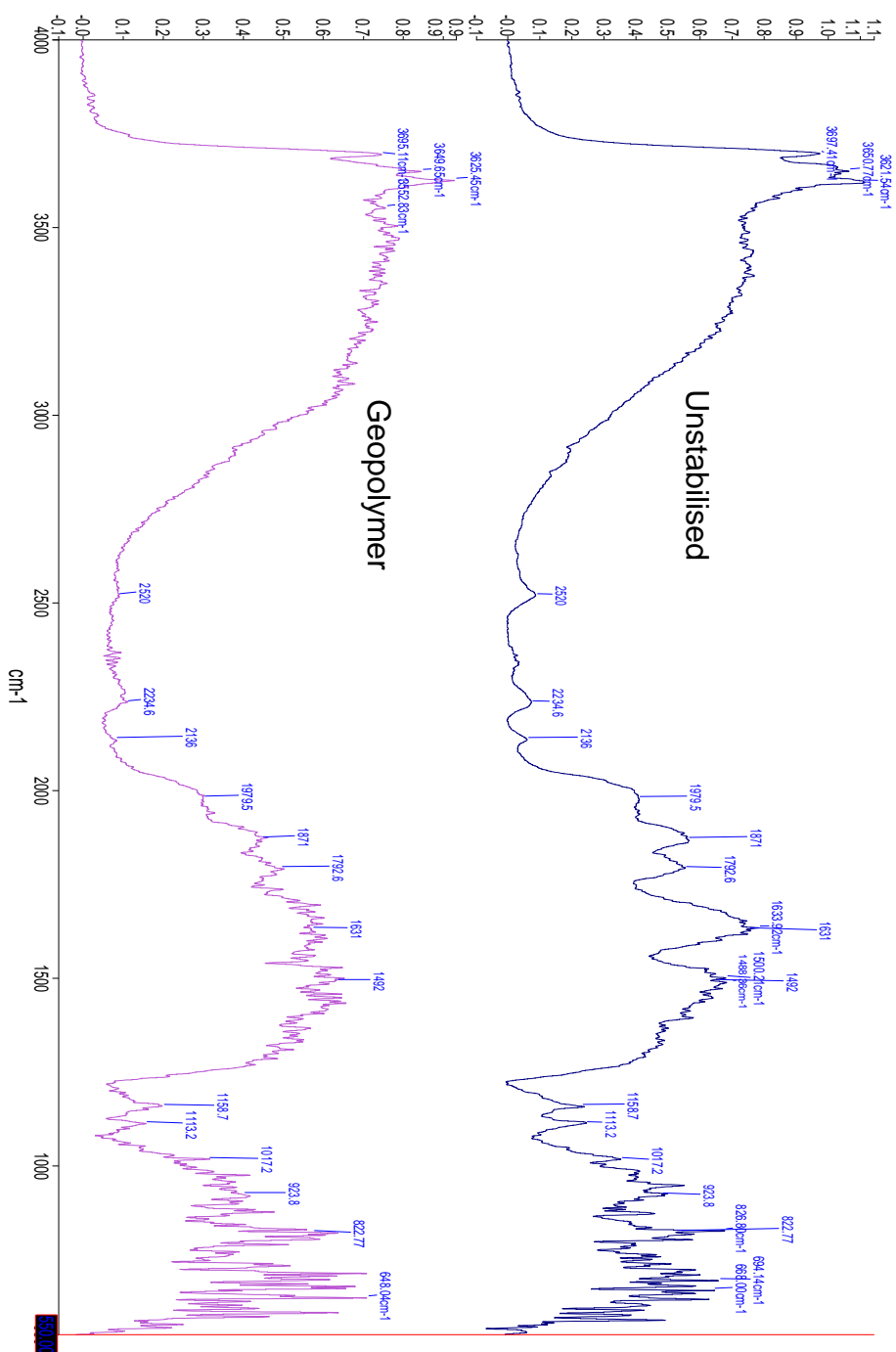


Figure 6.21: FTIR spectra of geopolymer stabilised sample

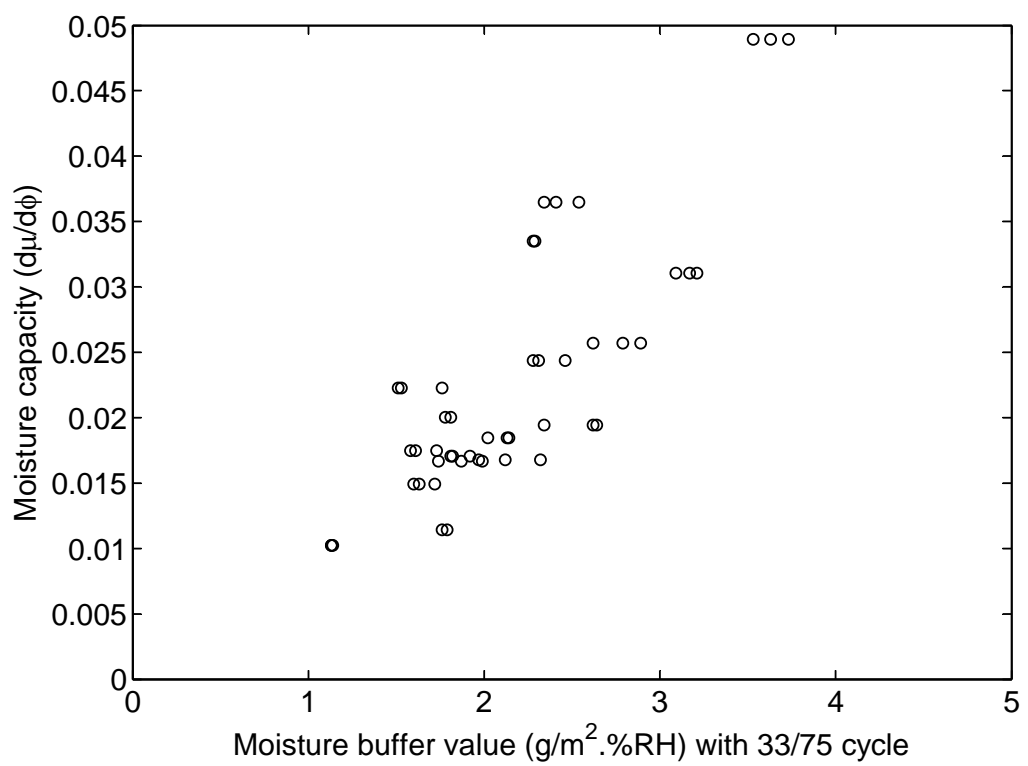


Figure 6.22: Influence of the moisture capacity on the MBV

determine a classification specifically for clay, similar to what has been done in Germany for clay plasters.

The German test determines the water vapour sorption after leaving the sample to reach equilibrium at 50% RH and then increasing to 80% RH for a period of 12 hours. The moisture uptake (g/m²) is measured at 0.5, 1, 3, 6 and 12h. The results are classified in 3 groups WS I, WS II and WS III (Wasserdampf adsorptionsklasse) (Schroeder, 2010), see Figure 6.23. The last class (WS III) is for materials with a moisture adsorption of more than 60 g per m² after 12h.

Materials tested in this study have a much wider range and the maximum adsorption after 8h ranges from 47 g/m² to 157 g/m² in the 33/75% RH cycle and from 54 g/m² to 170 g/m² in the 50/85% RH cycle. Most materials would therefore classify as WS III in the German classification.

For both classifications, additional groups would be needed to better characterise the highly adsorbing materials used for this study. It should be noted that the MBV obtained from different RH cycles should not be compared directly with the WS classes or with each other. However the correlation between the MBV from a 33/75% RH cycle to a 50/85% RH for example has been found in previous work to have a linear trend (McGregor et al., 2014), this was described in Chapter 4. The slope from the trend line can be used as a good estimation of the MBV for these materials from one cycle to another. It can be noted that cycles with a smaller interval, from 50% RH to 85% RH have higher MBVs than samples with a larger interval, between 33% RH to 75% RH, most likely because of the increase in isotherm gradient at higher humidity levels. For the case of the WS classes, a same material would be expected to have a higher adsorption with the German test than with the MBV test because of the chosen boundary conditions. The results obtained in this study from the MBV are compared exceptionally with the WS classification to demonstrate that it does not satisfy the whole range of adsorption capacities for earth building materials.

The German classification could be extended to take into account materials with a very high buffering potential.

Comparing the results obtained in this study with the German classification is shown in Figure 6.24. According to this classification all results even the earth plasters classify in the category WS III. Therefore, the WS III could be divided into further categories including WS IV, WS V and WS VI. Based on the initial

Nr.	Wasserdampf adsorptionsklasse	Wasserdampfadsorption [g/m ²] nach x[h]				
		0,5	1	3	6	12
1	WS I	≥ 3,5	≥ 7,0	≥ 13,5	≥ 20,0	≥ 35,0
2	WS II	≥ 5,0	≥ 10,0	≥ 20,0	≥ 30,0	≥ 47,5
3	WS III	≥ 6,0	≥ 13,0	≥ 26,5	≥ 40,0	≥ 60,0

Figure 6.23: Water vapour sorption classification from Schroeder (2010)

Table 6.4: Proposed extended classification

Water vapour adsorption category	Water vapour adsorption (g/m ²) after x (h)					
	0.5	1	3	6	8	12
WS I	≥ 3.5	≥ 7.0	≥ 13.5	≥ 20.0	≥ 25.0	≥ 35.0
WS II	≥ 5.0	≥ 10.0	≥ 20.0	≥ 30.0	≥ 36.0	≥ 47.5
WS III	≥ 6.0	≥ 13.0	≥ 26.5	≥ 40.0	≥ 47.0	≥ 60.0
WS IV	≥ 12.0	≥ 24.0	≥ 44.0	≥ 60.0	≥ 67.0	≥ 80.0
WS V	≥ 14.0	≥ 29.0	≥ 56.0	≥ 80.0	≥ 87.0	≥ 102.0
WS VI	≥ 18.0	≥ 36.0	≥ 68.0	≥ 100.0	≥ 107.0	≥ 122.0

German classification, the following values in extension are proposed in Table 6.4 and Figure 6.25

6.4 Prediction of MBV based on steady-state properties

In the Nordtest project report (Rode et al., 2005), a mathematical model is given to calculate the MBV which is called MBV_{ideal}. This is meant to complement the MBV_{practical} which is based on experimental results. The MBV for a RH

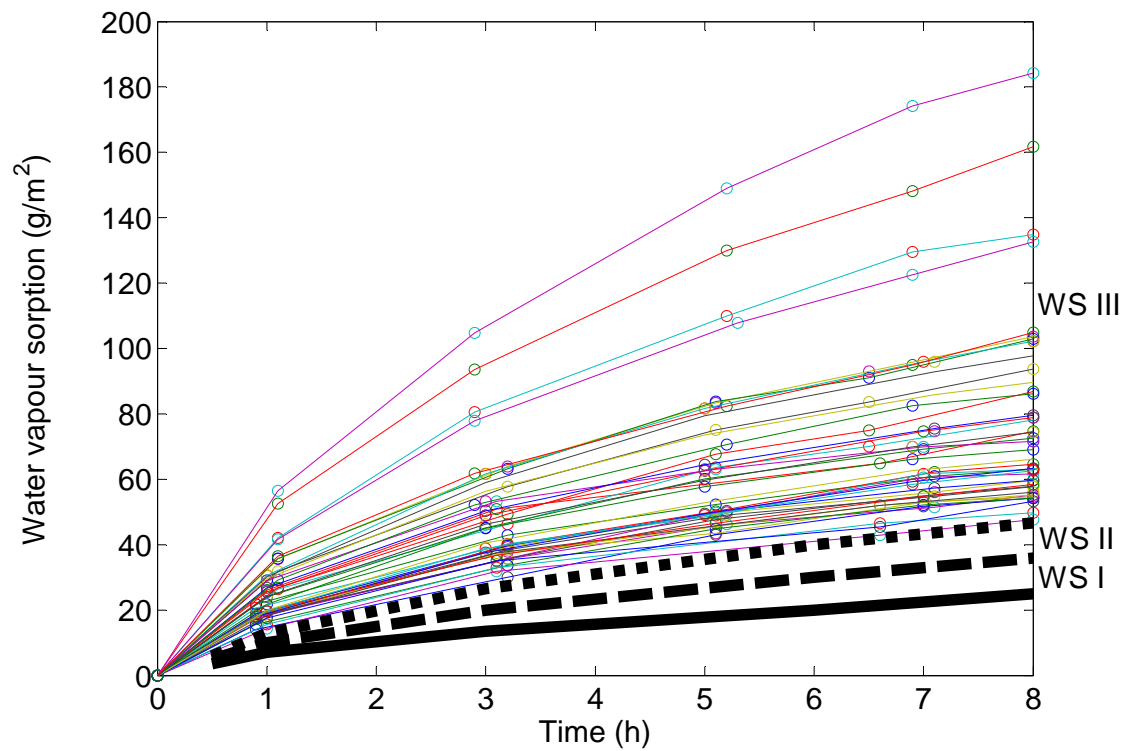


Figure 6.24: Experimental results and the German classification limits for earth plasters, WS I between the full line and large dotted line, WS II between the large dotted and small dotted line and WS III is anything above the small dotted line

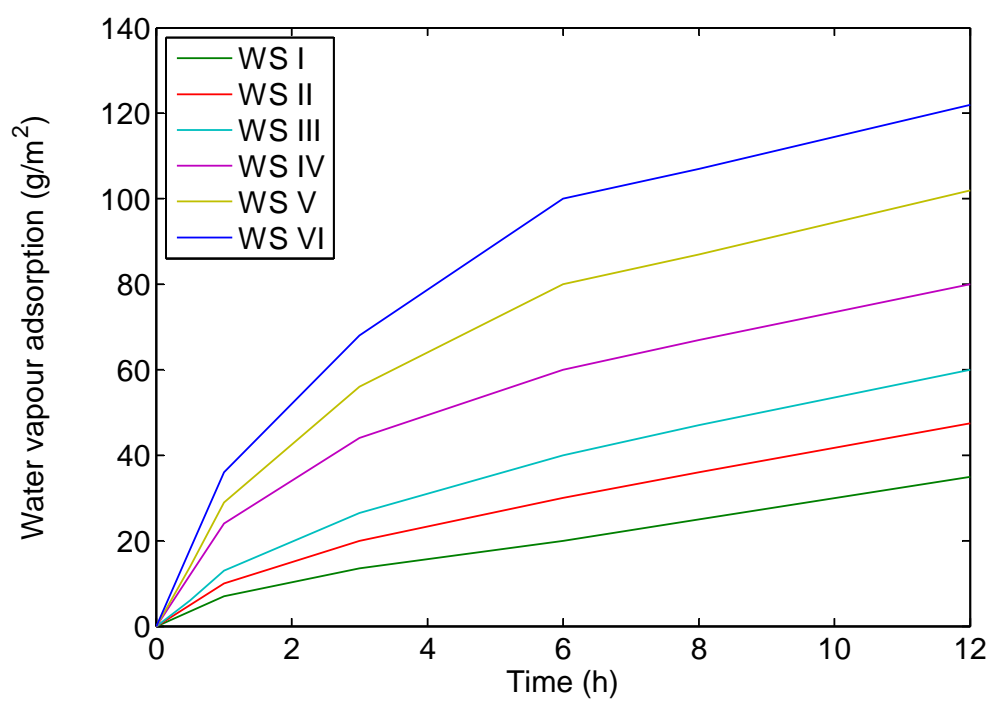


Figure 6.25: Proposed classifications subdivisions based on experimental results

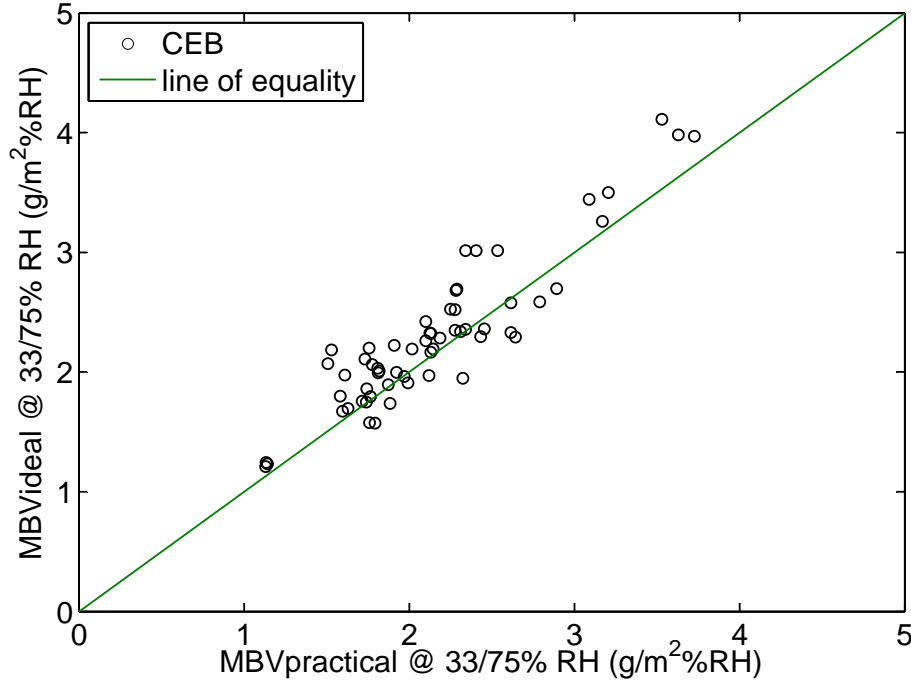


Figure 6.26: Experimental and calculated results compared

cycle of 33% RH to 75% RH and time variation of 8 h and 16h can be calculated using the equation 6.1:

$$MBV_{ideal} = 0.00568 \cdot p_s \cdot b_m \cdot \sqrt{t_p} \quad (6.1)$$

Where p_s (Pa) is the saturation water vapour pressure at 23°C, b_m is the moisture effusivity described in Chapter 2 and t_p (s) is the time period. The moisture effusivity is calculated based on the water vapour permeability, the apparent density and the moisture capacity. Based on the samples for which the sorption isotherms were measured in the DVS, a liner correlation of 0.92 between the calculated MBV_{ideal} and the experimental $MBV_{practical}$ is obtained, see Figure 6.26

This presents a rather good agreement, it should be noted that the agreement is close because the surface film resistance was kept to a minimum by using a high air velocity in the chamber during the experiment. The MBV_{ideal} does

not include the surface film resistance, therefore it was named “ideal” as it only considers the adsorption.

6.4.1 Penetration depth

Similar to the MBVideal, the penetration depth was calculated based on steady-state properties. The penetration depth was calculated according to the formula 6.2 from the Nordtest project report (Rode et al., 2005) and using the 1/e moisture variation limit rather than the 1% limit as it was described in Roels and Janssen (2006) to be more appropriate :

$$\frac{\Delta u_x}{\Delta u_s} = e^{-x\sqrt{\frac{\pi}{D_w t_p}}} \quad (6.2)$$

Where Δu_x is the moisture variation within the material and Δu_s is a sinusoidal moisture variation on the material surface. The term $\frac{\Delta u_x}{\Delta u_s}$ can be replaced by the designed value describing the penetration depth, if the 1/e limit is used then the penetration depth is the depth where the moisture variation within the material is less than the moisture variation on the surface. In this case the penetration depth is defined by 1/e therefore the equation becomes :

$$d_{1/e} = \sqrt{\frac{D_w t_p}{\pi}} \quad (6.3)$$

The calculated penetration depths using equation 6.3 based on the moisture capacity results from the DVS and the Salt solutions isotherms are given in Figure 6.27. The penetration depth varies for these samples between 3 mm and 7 mm. The highest penetration depth was observed on samples from Den_a which had a the lowest density for the compressed earth blocks without any additional fibers added.

Even on samples with high MBV the penetration depth remains below 10 mm which confirms the experimental sample thickness of 30 mm was sufficient (Chapter3).

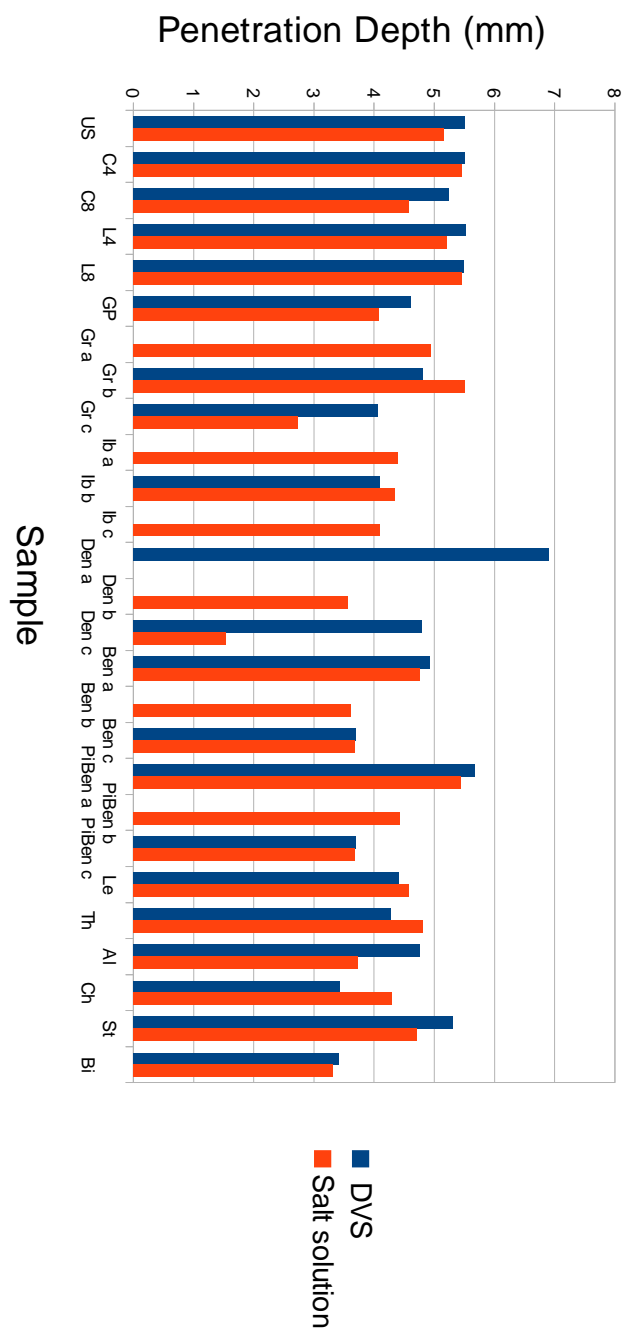


Figure 6.27: Penetration depth values based on DVS or salt solution moisture capacity

6.4.2 Prediction of steady-state properties based on the results from the moisture buffering test

Based on the results obtained from the moisture buffering test, a method was developed to predict steady-state parameters by Samuel Dubois from Gembloux Agro-Bio Tech. A joint publication was produced (Dubois et al., 2014) based on the results from a moisture buffering test performed during this study on unfired clay masonry.

The moisture buffering test undertaken for this paper was slightly different than those for the rest of the study. As the aim was to use the results in a model, only one sample was measured at a time in a climate chamber with continuous logging on a scale and rather than waiting for a dynamic equilibrium. Four consecutive cycles were measured after an initial conditioning to reach stable state of the sample at 55% RH and 20 ± 1 °C (Environment set in the conditioning room). One sample from group II with the Gr unstabilised soil and the artificial soil 3 from group VI were used for the paper.

The proposed inverse modeling approach that was followed is described in Figure 6.28. The simulated mass variation was obtained with a moisture model using COMSOL whereas the parameter optimisation was done using the DREAM program.

The steady-state parameters obtained through the inverse modeling approach deviated slightly from the experimental results but the relation between the two samples were respected. The deviation was described as resulting either from the many source of error that can occur in maintaining stable environmental conditions in the experimental procedure or that those values correspond to the average of environmental conditions met during a dynamic moisture buffering test. This is a similar remark to that by Roels and Janssen (2006) where simulation indicated that the most accurate calculated MBV were obtained when the steady-state water vapour permeability was measured close to the average RH conditions of the dynamic test.

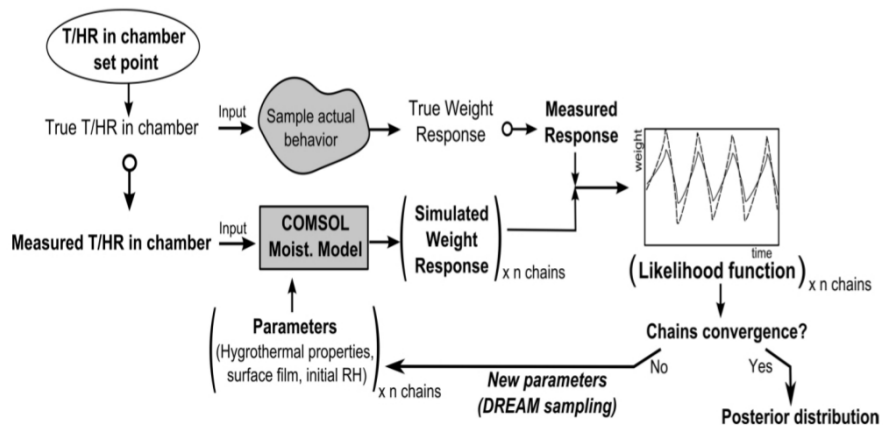


Figure 6.28: Inverse modeling procedure (Dubois et al., 2014)

6.5 Summary

The parameters that can vary in soils used for preparing building materials are numerous and the main parameters that can influence the moisture buffering capacity of a soil were discussed here. These can be divided in properties that affect the internal structure or the internal surface activity of the material. These are directly reflected by two main properties which are the water vapour permeability and the moisture capacity. Material properties such as apparent density or water content don't significantly influence the moisture capacity, but they can modify the permeability. A lower bound value for the water vapour resistance factor of about 5 seems to exist for unfired clay masonry. A further improvement can be found by looking at the mineralogy and the particle size distribution of the material. To have a significant impact the particle size distribution needs to be focused on clay and silt content. The stabilisation of the soil influences MBV by altering clay minerals and affecting vapour permeability.

From the observed results a new classification could be proposed to better characterise highly adsorbing materials. An extension of the German classification seemed the most appropriate.

Based on existing mathematical models that connect steady-state hygric properties to dynamic properties, good agreements were found between calculated MBV values and experimental values. The penetration depth could thereafter be estimated based on steady-state properties.

An international collaboration was undertaken applying inverse modeling and parameter optimisation algorithms to retrieve steady-state properties based on the dynamic moisture buffering test undertaken during this study.

7 Further investigation on the sorption properties and the addition of natural fibres

7.1 Investigation of dynamic adsorption properties with the DVS equipment.

The DVS equipment was primarily used to measure sorption isotherms, but as the test procedure can be entirely programmed, several tests were attempted to further characterise the dynamic sorption behaviour. The system uses a microscale to precisely record every minute the mass change of a sample placed within a chamber where RH and temperature can precisely be controlled and pre-programmed therefore more information could be retrieved than solely the sorption isotherms. The moisture buffering could be reproduced which provides information on the role of the hysteresis during the moisture buffering test. From the measurement of sorption isotherms, information on the adsorption rates in between RH levels could be further analysed. The dynamic data obtained could be compared to the dynamic data from the moisture buffering test.

7.1.1 DVS moisture buffering test, influence of hysteresis

The moisture buffering test was simulated with the DVS using the same time and RH levels used for this research but the sample was much smaller. In Figure 7.1 it can be seen that with the DVS test, the sample reaches equilibrium moisture content (EMC) within the time normally allowed for adsorption and desorption during the moisture buffering test. During this test the sample is first allowed to reach its dry state at 0% RH. This is to make sure the sample follows the

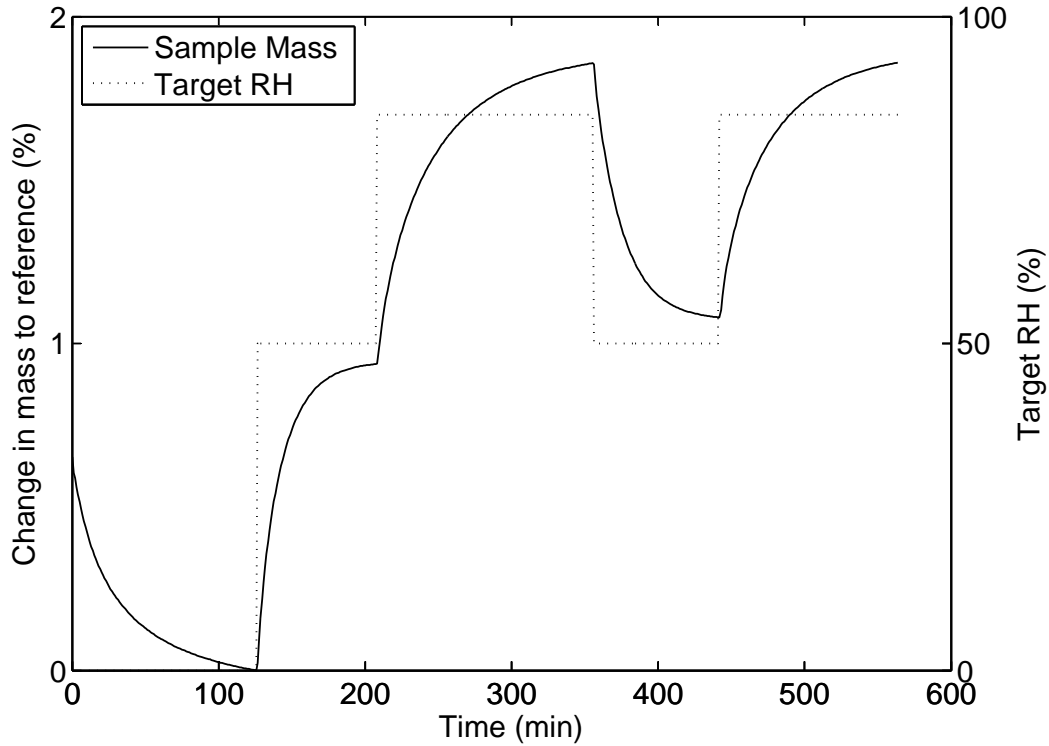


Figure 7.1: DVS moisture buffering test

adsorption path of the sorption isotherm. It then reaches equilibrium at 50% RH, the RH is then increased to 85%, once the sample has reached the EMC it is again lowered to 50% RH. The EMC reached during the second phase at 50% RH is higher than the previous one because it corresponds to a point on the desorption curve of the sorption isotherm. This is expected to occur in transient levels in the moisture buffering test.

Therefore a more accurate determination of the linearised moisture capacity that is active during the moisture buffering test would be to calculate the slope between the EMC on the desorption curve (for the low RH) and the EMC on the adsorption curve (for high RH), see Figure 7.2. A different slope would be used to determine the moisture capacity if taken into account the hysteresis, $du1$ is the difference in EMC on the adsorption curve which is normally used whereas $du2$ is the difference when taking into account the hysteresis.

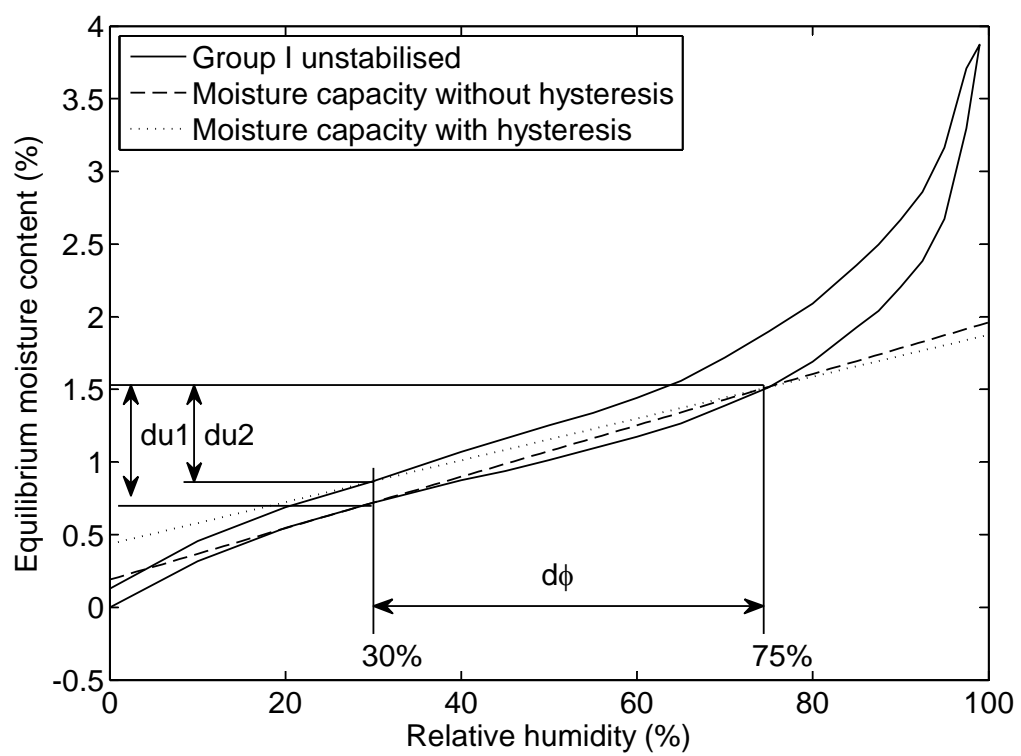


Figure 7.2: The active moisture capacity during a moisture buffering test

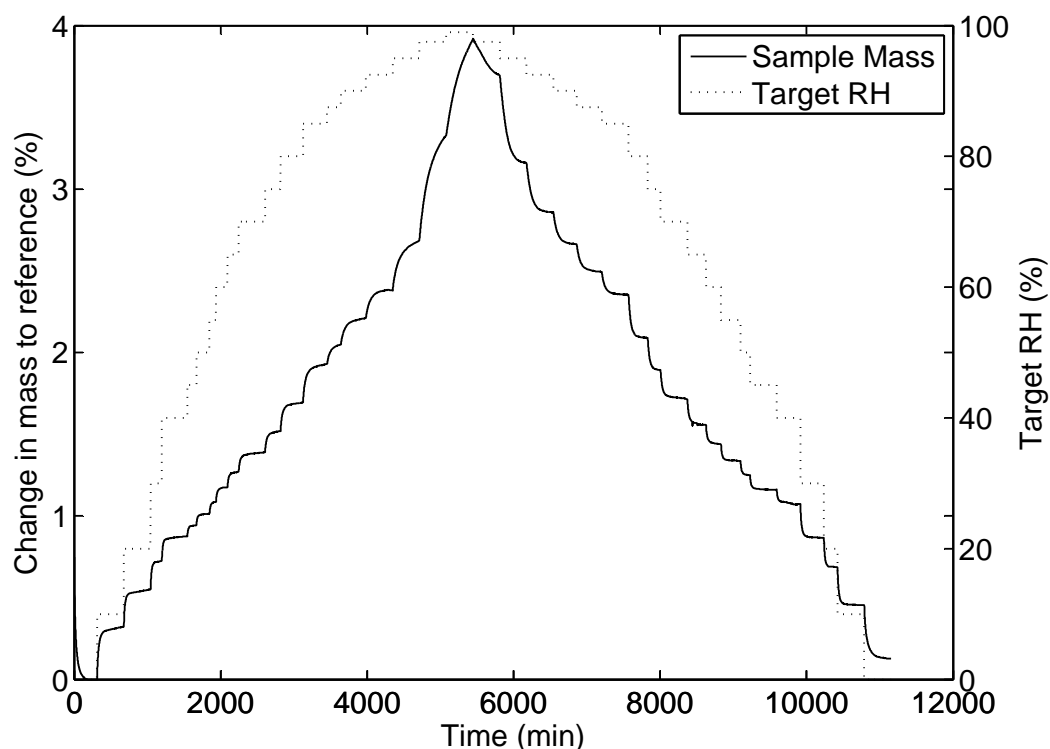


Figure 7.3: Data from sorption isotherm measurement

7.1.2 Variation in adsorption rate

During the measurement of the sorption isotherm the RH is gradually increased, for each RH step the sample reaches EMC before the next RH step, see Figure 7.3 which presents the typical mass change for adsorption and desorption dynamics for RH% steps. The DVS records the mass of the sample every minute and can therefore give precise indication on the adsorption rates between each RH step.

Figure 7.4 shows the adsorption rates for variable % RH step from 0% RH to 100% RH. The particular interest is in the range between 45% RH to 85% RH where the size of the steps are constant but the initial adsorption rate is slightly increasing towards higher RH and the overall average adsorption rate which can be seen in Figure 7.4 by the area below the curve is also increasing.

The change in mass as seen in Figure 7.3 can be represented by an asymptotic curve between each RH increment where the asymptote is represented by the EMC for the RH level. In an identical way, the adsorption rate is at first very

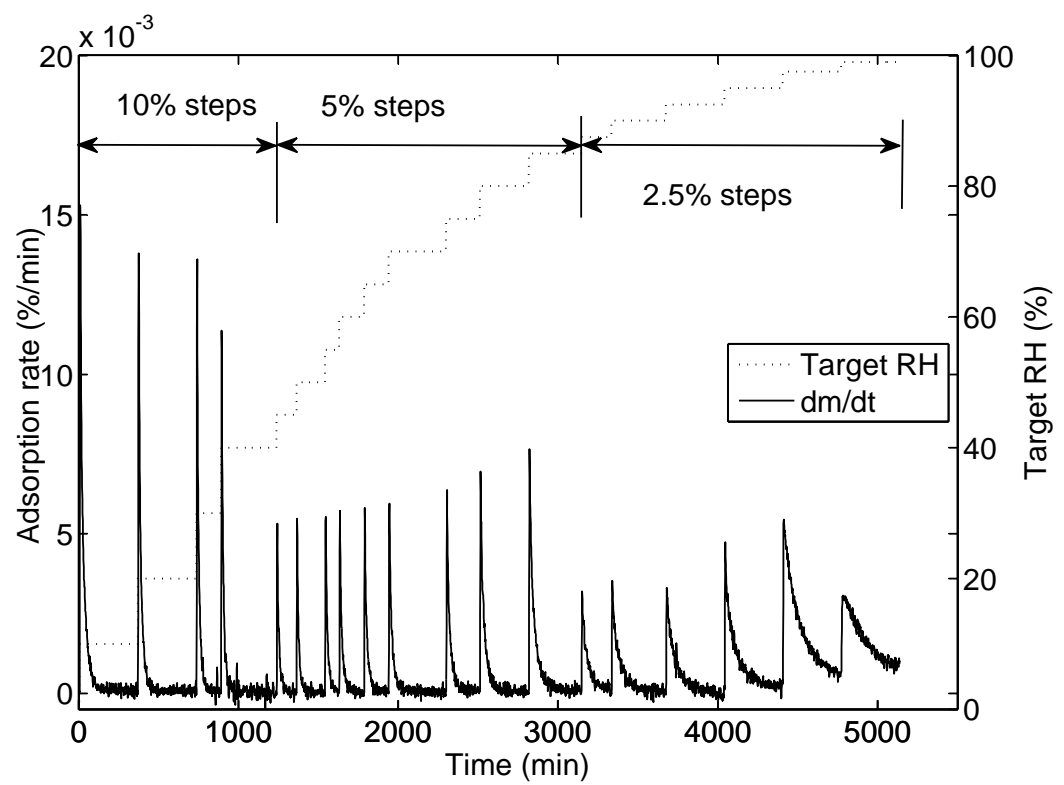


Figure 7.4: Variable adsorption rates on the RH range

strong and then gradually approaches zero closer to the EMC. The adsorption rate is stronger at steps occurring at higher RH which also indicates that the moisture capacity is non-linear over the RH range.

7.1.3 Comparison between small and large scale moisture buffering test

In Figure 7.5 a comparison is made between the moisture buffering tests performed with the DVS on a small sample with no sides of the sample being sealed and the moisture buffering test performed in the climate chamber on. The two test were undertaken on the same material, it is therefore expected that they have equal equilibrium moisture content at 85% RH. The adsorption rate to reach EMC is however very different. Because the size is the only varying parameter it means the reduction of adsorption rate in the larger samples is primarily due to the delay in the vapour transmission through the material and this is related to the exposed surface area per unit volume. This indicates that the buffering potential of this material is largely unused, and only the layers close to the surface of the material are active. The calculation of the $1/e$ penetration in Chapter 6 depth confirms this.

7.2 Addition of organic fibres

7.2.1 Introduction

A common practice in earth building is to add natural fibres to the soil. For example in the south-west of England a traditional building method is cob. Cob is still used in some new construction, with this method the soil is mixed with fibres wet and is directly used to shape the walls, slightly being compacted by hand (Watson and McCabe, 2011). In many plasters, fibres are added for strength and to improve the insulation or reduce thermal conductivity (Ashour et al., 2010). The addition of barley straw has shown to reduce thermal conductivity by about 50% but it has also an influence on the equilibrium moisture content (EMC). In the study conducted by (Ashour et al., 2011) three different fibres were added to a soil for the preparation of earth plasters. The fibres consisted of wood shavings, wheat straw and barley straw. The barley straw showed the strongest influence

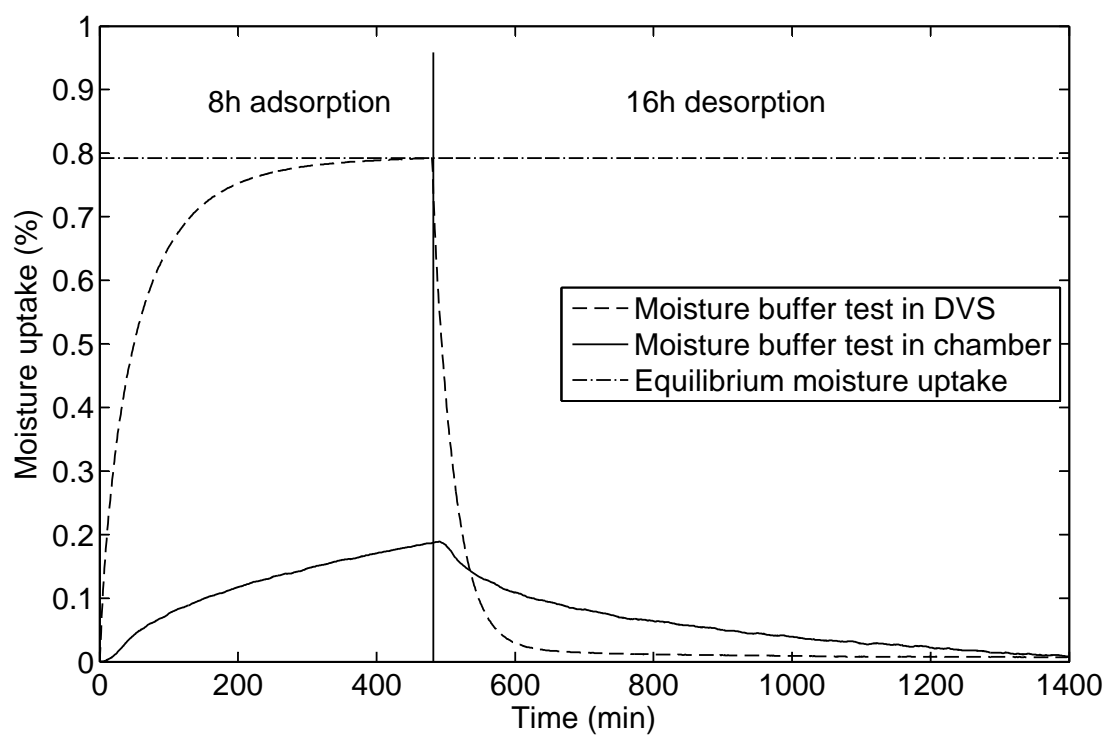


Figure 7.5: Relative moisture uptake to mass for small and large scale sample



Figure 7.6: Chopped Barley straw ($\simeq 2$ cm)

on the equilibrium moisture content. The improvement for a relative humidity (RH) between 40% to 80% was in order of 1% to 3% towards the higher RH levels.

This increase in EMC which in turn modifies the moisture capacity of the material could have a beneficial influence on the dynamic moisture adsorption or moisture buffering capacity. This was investigated by the preparation of series of compressed earth blocks with variable contents of barley straw. Additionally, earth plasters were also prepared with the addition of a varying content of three different fibres, barley straw in Figure 7.6, barley wool in Figure 7.7 and corn stalk in Figure 7.8. It is possible that the fibres will increase vapour permeability as well as moisture capacity by transferring moisture along fibres on the soil/fibre interface.

Only the dynamic MBV results are presented in this section, the work was done in cooperation with Mariana Palumbo from the Spanish Universitat Politècnica de Catalunya in Barcelona. Samples were initially prepared in the University of Bath. The moisture buffering capacity was measured in the University of Bath but the rest of hygric properties such as the sorption isotherms and the vapour permeability will further be tested in the Spain at a later date.



Figure 7.7: Barley wool



Figure 7.8: Chopped Corn stalk (0.5 cm max)

7.2.2 Sample preparation

The compressed earth blocks were prepared with artificial soil 2 (see Chapter 3) which had a content of 25% of Kaolinite clay, 25 % of silt and 55% of sand. The blocks were prepared as 100 mm diameter and 30 mm thickness in a sewage pipe used a formwork and compacted with an adapted Wykeham Farrance 50kN triaxial frame. Six samples were compacted with the same compaction force of 0.5 T and six were compacted to a determined density of 1800 kg/m³ this was because the addition of straw would change compaction behaviour. From each of these six sample sets three were prepared with 1% per dry mass of barley straw and three others were prepared with 2% per dry mass of barley straw. This means for each mix three identical triplicates were used for the testing.

As a basis for the earth plasters, the commercial plaster 2 was used (see Chapter 3) having previously removed the fibres that the plaster already contained. The plasters were mixed until a sufficient workability was achieved. Depending on the fibre, a variable water content had to be added.

Samples and material properties are summarized in Table 7.1.

From the material data in Table 7.1, it can be seen that the addition of fibres changes the apparent density of the samples. The plasters which were prepared without compaction in a form of 100 mm diameter and 20 mm thickness achieved a consistent size, with an average of sample thickness of 20.7 mm, a minimum of 19.4 mm and a maximum of 21.9 mm. Their apparent density is however largely modified, the plaster without fibres achieves an apparent density of 1848 kg/m³ on average whereas the plaster with 2% of corn stalk only reaches an apparent density of 948 kg/m³ on average. This is expected to greatly influence hygric properties and therefore the moisture buffering value.

No significant difference is observed between the CEB compacted with an equal compaction force or prepared to reach equal apparent density, in fact only the samples with 2% of fibres had lower apparent density.

7.2.3 Testing and results

The moisture buffering test described in Chapter 3 was used for all samples.

Table 7.1: Sample description

Sample mix	Fibre content	Apparent density (kg/m ³)	Mixing water (% per dry mass)
CEB 0%	0%	1896	14
CEB 1% same compaction	1 % barley straw	1818	n.a
CEB 2% same compaction	2 % barley straw	1682	n.a
CEB 1% same density	1 % barley straw	1770	n.a
CEB 2% same density	2 % barley straw	1669	n.a
Plaster 0%	no fibres	1848	17
Plaster 1% b.s	1 % barley straw	1613	n.a
Plaster 1% b.w	1 % barley wool	1541	25.7
Plaster 1% c	1% corn stalk	1229	39
Plaster 2% b.s	2 % barley straw	1400	28.8
Plaster 2% b.w	2 % barley wool	1439	30.4
Plaster 2% c	2% corn stalk	948	57

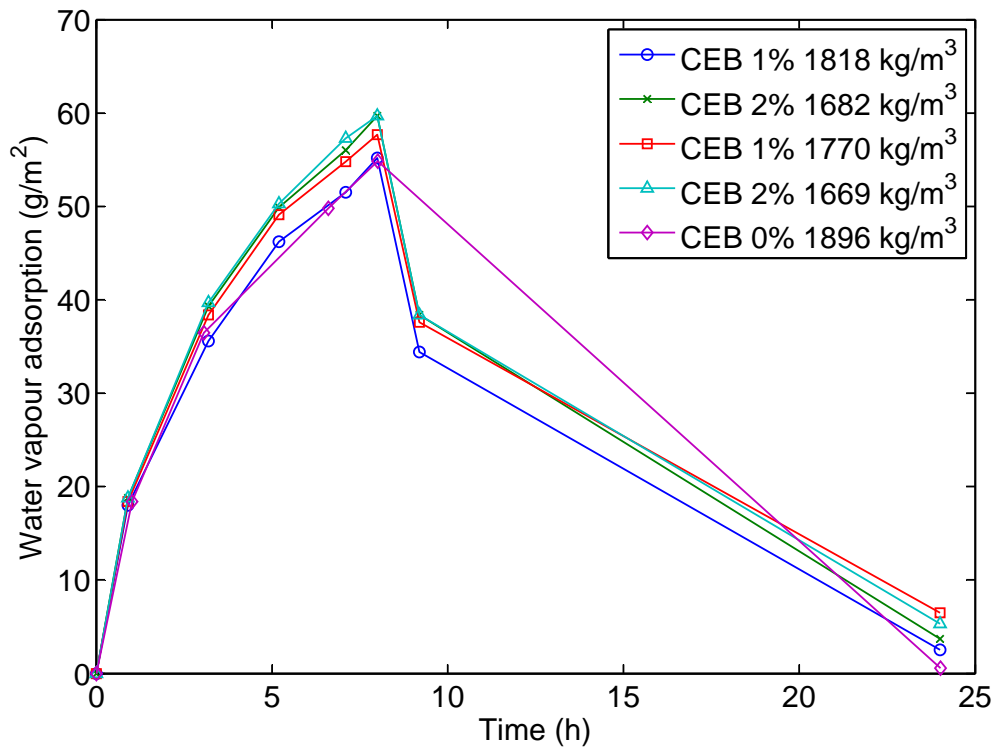


Figure 7.9: Results from the moisture buffering test of CEB with barley straw fibres and CEB without fibres from group V

7.2.3.1 CEB moisture buffering results

The results of the dynamic adsorption and desorption of a 24 h cycle with 8h high RH at 75% and 16h low RH at 33% given in Figure 7.9.

The results of these tests are compared with the compressed earth blocks from group V which were prepared with the same soil but without fibres. The dynamic adsorption is very similar for all samples and the maximum at 8h varies from 54.5 g/m² to 59.7 g/m². The two mixes with 2% of fibres have increased their maximum adsorption by 10% compared with the mix from group V.

7.2.3.2 Plasters moisture buffering results

The results of the moisture buffering test for the plasters are shown in Figure 7.10.

The addition of fibres considerably alters the water vapour adsorption. Plasters

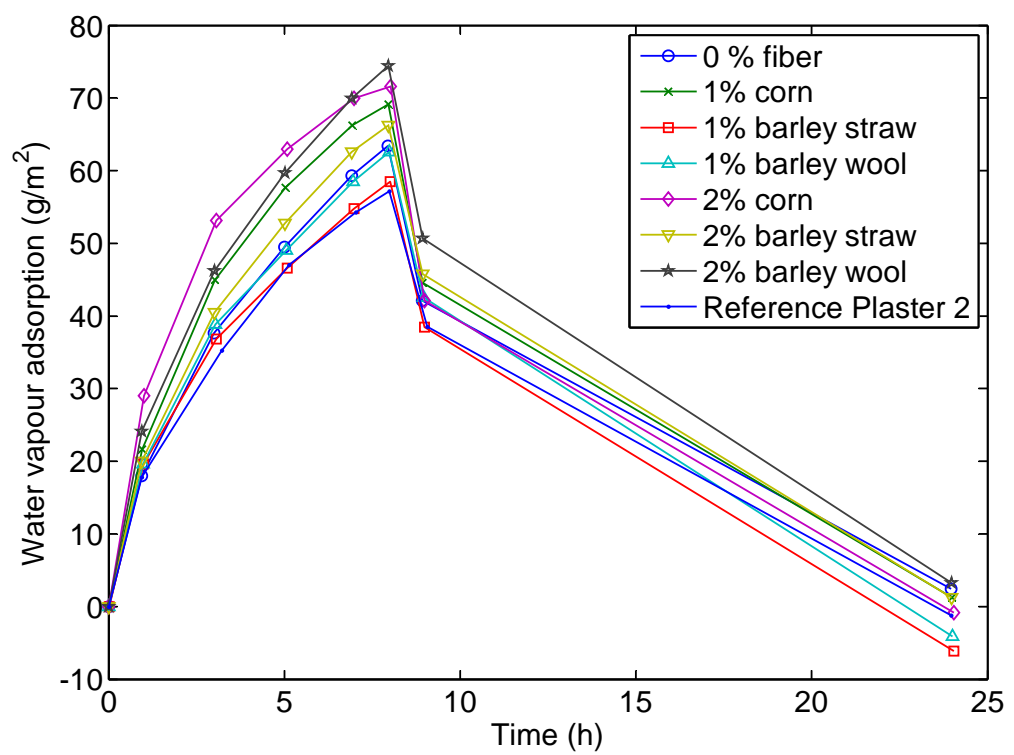


Figure 7.10: Results from the moisture buffering test of plasters with fibres

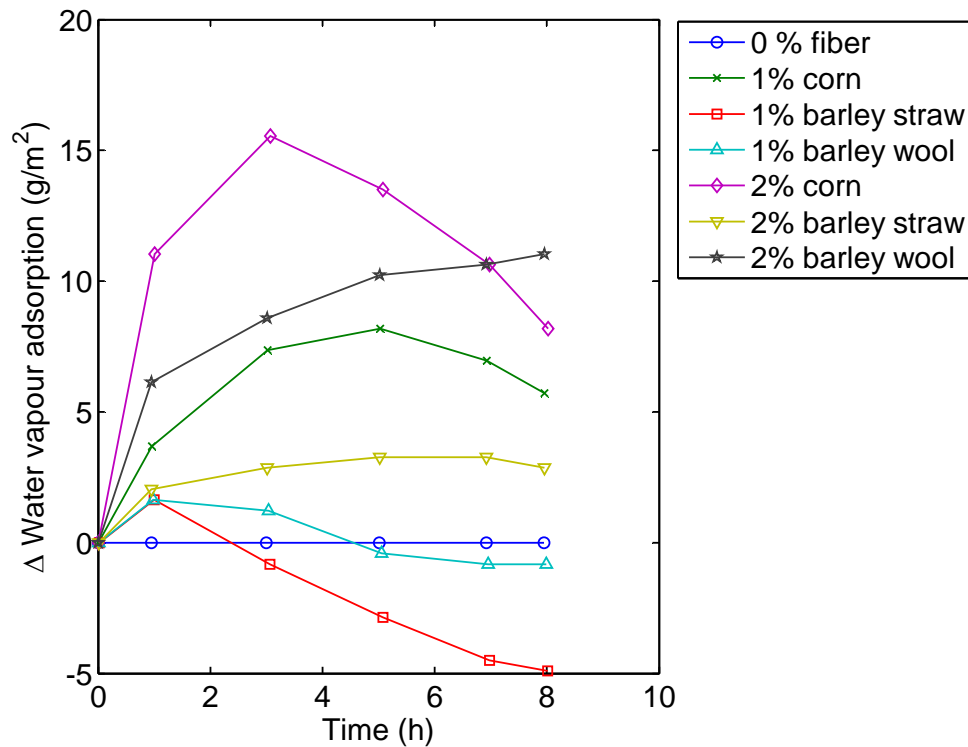


Figure 7.11: Difference of water vapour adsorption compared to 0% fibres

with 1% of barley straw or barley wool have a maximum adsorption that is close or below the mix with 0% of fibres, all other mixes perform better than the 0% mix and even as the reference plaster which is the original plaster 2 from group IX without any modification. The modification is not consistent for all times, this is the case for the mix with 2% of corn who was the strongest adsorption capacity until 7h and then is below the capacity of the 2% barley wool. The effect of fibres can be seen in Figure 7.11. The effect is compared in terms of difference to the 0% fibres samples.

All samples show an improved vapour adsorption at 1h which could indicate that there is an improvement in vapour permeability therefore samples react faster to moisture change. The final adsorption can be lower than for the 0% mix in some cases which suggests that the equilibrium moisture content is probably lower for these mixes. The same remark can be made for the 2% corn and 2% barley wool. The 2% corn has a stronger adsorption rate until 3h and then starts to decrease whereas the 2% barley wool has a steady adsorption rate until 8h

Table 7.2: MBV for all tested mixes

Sample mix	Δ_m (g)	MBV (g/m ² .%RH)
CEB 0%	54.8	1.31
CEB 1% same compaction	54.8	1.30
CEB 2% same compaction	58.7	1.40
CEB 1% same density	57.1	1.36
CEB 2% same density	58.5	1.40
Plaster 0%	63.4	1.51
Plaster 1% b.s	58.5	1.39
Plaster 1% b.w	62.6	1.49
Plaster 1% c	69.1	1.65
Plaster 2% b.s	66.2	1.57
Plaster 2% b.w	74.4	1.77
Plaster 2% c	71.6	1.70

when the mix has finally adsorbed more water vapour than the 2% corn mix.

It has explained in Chapter 6 that the apparent density can modify the moisture buffering through the effect it has on water vapour permeability. The fibres therefore increase the moisture buffering as they have a significant affect on the apparent density, the apparent density was determined in the same way than for the compressed earth blocks in this study by a precise determination of the volume of the sample and the dry weight. However, the addition of fibres also seem to reduce the moisture capacity.

7.2.4 Moisture buffering value

From the results of the moisture buffering test the moisture buffering value (MBV_{practical}) can be calculated. Based on the description in Chapter 2, the MBV_{practical} can be calculated by equation 7.1:

$$MBV = \frac{\Delta_m}{A \cdot \Delta RH} \quad (7.1)$$

Where Δ_m is the difference in mass at 8h, A is the surface area exposed which is approximately 0.008 m², ΔRH is the RH variation. The average of three samples for each mix is given in Table 7.2.

7.2.5 Discussion

This study is beyond the original scope of the research and remains incomplete as to fully understand the changes observed in the dynamic adsorption, the water vapour permeability and the sorption isotherms have to be determined. Interesting information can, however, be observed with the results from the moisture buffering test.

The compacted samples only undergo a slight improvement with the addition of barley straw. The adsorbed water vapour after 8h of RH increases by 10% for the samples with 2% fibres. It would not be practical to add more fibres than 2% per dry mass as 2% represents a very large volume of fibres. More fibres would create issues for compaction.

In conclusion, the addition of fibres to earth plasters seems to have a two fold effect which would need to be confirmed with further testing. On one side the fibres improve the adsorption rate compared to the 0% fibre samples during an initial phase. This initial phase depends on the fibre and is more or less pronounced, but all fibres have higher adsorbed water vapour than the 0% after 1h. The other side is that the adsorption then decreases compared to the 0% samples. Two sample mixes, the 1% barley wool and 1% barley straw, have final adsorbed water vapour content lower than the 0%.

An explanation for this effect can be that the addition of fibres lowers the water vapour resistance and therefore the samples react faster to a change in RH but the equilibrium moisture content is also lower and therefore the maximum moisture the sample can reach is reached faster. This implies the addition of fibres would not significantly improve moisture buffering on long term cycles.

8 Conclusions

8.1 Summary

The first stage of this study consisted of understanding the measuring process of dynamic water vapour adsorption. The moisture buffering test is not a test that was routinely undertaken and the influence of the testing equipment, the environmental conditions and the time frames had to be determined.

This was described through experimental results using two different climatic chambers which modified the results. The effect was explained by the influence of the air velocity on the surface film resistance and therefore the dynamic adsorption. It was demonstrated that the greater the air velocity, the higher the consequent vapour adsorption during the moisture buffering test.

The influence of the boundary conditions on the test results were shown to be crucial. However, it could be shown that results from one set of environmental conditions could be converted to results from another. If the relation between the two sets of values is known, the moisture buffering value from a material can be determined for one set based on the experimental results from another. This still remains an approximation and testing is required to confirm it. It can be noted that the moisture buffering value for three identical samples were close but always had some variation because the dynamic moisture adsorption cannot be an exact value as there is some natural variation involved in the process and materials.

The time frame used showed to have only a limited influence on final result. Samples reach a dynamic equilibrium in both symmetrical (12h/12h) and asymmetrical cycles (8h/16h). In the dynamic equilibrium state the material adsorbs as much as it can release. In the 12h/12h cycle the material is already slightly more saturated as it only has a 12h low humidity compared to the 16h low humidity phase this has for effect to reduce the adsorption rate during the high humidity phase.

The size of the sample affected the results and it was hypothesized that the size has an effect on the surface film resistance in the chamber. But this would need further investigation to be confirmed and is relevant to all materials, not only earth.

Different thicknesses were tested and all had similar results.

Based to these initial results, series of samples with different material properties were prepared as 100 mm discs, 30 mm thick.

The second phase of the study consisted of undertaking series of measurements on a variety of soil blocks and plasters. The water vapour permeability, sorption isotherms and the moisture buffering were consistently measured. In total 146 samples were prepared and measured of which there were 37 triplicates of compressed earth blocks and 15 triplicates of plasters.

The variability of these soils was investigated through a parametric study consisting of varying individual parameters if possible. These parameters were apparent density, mixing method, mixing water content, stabiliser content, mineralogy, particle size distribution and the natural variability of brick soils.

Each parameter modified either or both the moisture storage capacity or the water vapour resistance of the sample. Through a combined analysis of the measured sorption isotherms, vapour permeability and moisture buffering, it could be determined how these parameters modify the hygric properties of the soils.

Soil parameters that influence the water vapour resistance were the apparent density (subsequently the porosity), stabiliser content and the particle size distribution. Soil parameters that influence the moisture capacity were mainly the mineralogy and the particle size distribution.

The moisture buffering test method used allowed the Moisture Buffering Value (MBV) of the bricks and plasters to be determined. The MBV in 33%/75% RH cycles at 8h ranged from 1.13 g/m².%RH to 3.73 g/m².%RH. The variation of the MBV was documented for each group and could be explained by the variation of the steady-state properties. The experimental MBV_{practical} could be compared to the MBV_{ideal} calculated from the steady-state properties a reasonable correlation of 0.92 could be found between the two set of values. Theoretical analysis could therefore be used as a good estimation of the dynamic adsorption characteristics of soils as long as the steady-state properties are accurately measured in similar environmental conditions to the moisture buffering test. These conditions

include similar ranges of RH which means using the “wet cup” test rather than the “dry cup” test, isothermal conditions at 23°C and similar air velocity.

The range of results obtained showed that existing classification for moisture buffering capacity was poorly defined as these are not adapted for highly adsorbing materials such as unfired clay masonry. A new classification was proposed extending the existing German DIN classification. The DIN uses a different measuring method which starts from a steady-state initial condition and does not reach dynamic equilibrium but can be adapted to the MBV tests.

Two commercial plasters were tested and could be classified in the lower end of moisture buffering capacities measured during this study. The potential to improve their capacity by the addition of natural fibers was investigated in a joint research project with the Universitat Politècnica de Catalunya. Those results showed the potential to modify the adsorption rates in a way that either brings a fast buffering response within a few hours but with a low total adsorption capacity, or to obtain a more steady adsorption rate over 8h with a higher final adsorption capacity.

The current characterisation of earth as buffering materials mainly understates their potential. Existing commercial products do not necessarily provide this data but it seems that these could be largely improved and that their current performance is rather low.

8.2 Future work

- In terms of application, the use of earth as a buffering material is currently underused. A complementary study of this work would be to provide an inventory of MBV of existing commercial products which would provide a good overview of the performance of the materials on the market. Currently insufficient data is available for commercial products, therefore when values are provided they can't really be compared to other products.
- The adsorption process on soil particles is complex. Through existing research in other scientific fields it has been shown that clay minerals can adsorb many polar molecules and not only water molecules. This can have potential benefit in the built environment for the control of indoor pollutants. Volatile Organic Compounds (VOCs) are, for example, major pol-

lutants in the indoor environment and these molecules can be adsorbed by clay minerals. The buffering potential of unfired clay masonry could be extended from regulating the indoor humidity levels to indoor pollutant concentrations.

- Further work on modelling the response of the whole building to changes in moisture is required. While some research is being conducted, the effect has not been fully quantified.
- On the material side, more investigation could be done on the relation of the pore size distribution and its tortuosity with the dynamic adsorption properties.

Bibliography

- Abadie, M. and Mendonça, K. (2009), ‘Moisture performance of building materials: From material characterization to building simulation using the moisture buffer value concept’, *Building and Environment* **44**, pp.388–401.
- Allinson, D. and Hall, M. (2010), ‘Hygrothermal analysis of a stabilised rammed earth test building in the uk’, *Energy and Buildings* **42**, pp.845–852.
- Allinson, D. and Hall, M. (2012), ‘Humidity buffering using stabilised rammed earth materials’, *Construction Materials Proceedings of the institution of Civil Engineers* **165**, pp.335–344.
- Arundel, A., Sterling, E., Biggin, J. and Sterling, T. (1986), ‘Indirect health effects of relative humidity in indoor environments’, *Environmental Health Perspectives* **65**, pp.351.
- Ashour, T., Georg, H. and Wu, W. (2011), ‘An experimental investigation on equilibrium moisture content of earth plaster with natural reinforcement fibres for straw bale buildings’, *Applied thermal engineering* **31**, pp.293–303.
- Ashour, T., Wieland, H., Georg, H., Bockisch, F.-J. and Wu, W. (2010), ‘The influence of natural reinforcement fibres on insulation values of earth plaster for straw bale buildings’, *Materials and Design* **31**(10), pp.4676–4685.
- Bergaya, F. and Lagaly, G. (2006), ‘General introduction: Clays, clay minerals, and clay science’, *Developments in Clay Science* **1**, pp.1–18.
- Braman, S. S. (2006), ‘The global burden of asthma’, *CHEST Journal* **130**, pp.4–12.
- BS1377-2 (1990), ‘Bs 1377-2:1990 methods of test for soils for civil engineering purposes. part 2: Classification tests’.

- Chabriac, P.-A., Fabbri, A., Morel, J.-C., Laurent, J.-P. and Blanc-Gonnet, J. (2014), ‘A procedure to measure the in-situ hygrothermal behavior of earth walls’, *Materials* **7**(4), pp.3002–3020.
- Darling, E., Cros, C., Wargocki, P., Kolarik, J., Morrison, G. and Corsi, R. (2012), ‘Impacts of a clay plaster on indoor air quality assessed using chemical and sensory measurements’, *Building and Environment* .
- Davidovits, J. (1991), ‘Geopolymers: Inorganic polymeric new materials’, *Journal of thermal analysis* **37**, pp.1633–1656.
- Dontsova, K., Norton, L., Johnston, C. and Bigham, J. (2004), ‘Influence of exchangeable cations on water adsorption by soil clays’, *Soil Science Society of America Journal* **68**, pp.1218–1227.
- Dubois, S., McGregor, F., Evrard, A., Heath, A. and Lebeau, F. (2014), ‘An inverse modelling approach to estimate the hygric parameters of clay-based masonry during a moisture buffer value test’, *Building and Environment* **81**(0), pp.192 – 203.
- Eckermann, W. and Ziegert, C. (2006), Auswirkung von lehmbaustoffen auf die raumluftfeuchte, Technical report, Unpublished report.
- Engelund, E. T., Klammer, M. and Venås, T. M. (2010), Acquisition of sorption isotherms for modified woods by the use of dynamic vapour sorption instrumentation. principles and practice, in ‘IRG 41 Annual Meeting’.
- Eshoj, B. and Padfield, T. (1993), The use of porous building materials to provide a stable relative humidity, in ‘Preprints of the ICOM-CC Conference’, James and James, pp. pp. 605–609.
- Fang, L., Clausen, G. and Fanger, P. (1999), ‘Impact of temperature and humidity on chemical and sensory emissions from building materials’, *Indoor Air* **9**, pp.193–201.
- Fredlund, D. G. (2006), ‘Unsaturated soil mechanics in engineering practice’, *Journal of geotechnical and geoenvironmental engineering* **132**(3), pp.286–321.

- Gómez, I., Guths, S., Souza, R., Millan, J., Martín, K. and Sala, J. (2011), 'Moisture buffering performance of a new pozolanic ceramic material: Influence of the film layer resistance', *Energy and Buildings* **43**(4), pp.873–878.
- Hall, M. and Allinson, D. (2009), 'Analysis of the hygrothermal functional properties of stabilised rammed earth materials', *Building and Environment* **44**, pp.1935–1942.
- Hameury, S. (2005), 'Moisture buffering capacity of heavy timber structures directly exposed to an indoor climate: a numerical study', *Building and Environment* **40**, pp.1400–1412.
- Hammond, G. P. and Jones, C. I. (2008), 'Embodied energy and carbon in construction materials', *Proceedings of the Institution of Civil Engineers-Energy* **161**(2), pp.87–98.
- Hansen, E. and Hansen, M. (2002), Unfired clay bricks-moisture properties and compressive strength, *in* 'Proceedings of the 6th Symposium on Building Physics in the Nordic Countries', Norwegian University of Science and Technology, Trondheim, Norway.
- Harderup, L.-E. (2005), A pc-model to predict moisture buffer capacity in building materials according to a nordtest method, *in* '7th Nordic Symposium on Building Physics', pp. 1155–1162.
- Harvey, C. and Lagaly, G. (2006), 'Hanbook of clay science. conventional applications', *Developments in Clay Science* **1**, pp.501–540.
- Heath, A., Walker, P., Fourie, C. and Lawrence, M. (2009), 'Compressive strength of extruded unfired clay masonry units.', *Proceedings of the Institution of Civil Engineers: Construction Materials and Structures* **162** (3), pp.105–112.
- Holm, A., Kuenzel, H. and Sedlbauer, K. (2003), 'The hygrothermal behaviour of rooms: combining thermal building simulation and hygrothermal envelope calculation', *IBPSA Proceedings Building Simulation Eindhoven* .
- Houben, H. and Guillaud, H. (1994), *Earth construction: a comprehensive guide*, Intermediate Technology Publications.

- IGT, L. C. C. (2010), Final report, Technical report, HM Government.
- IPCC (2013), Climate change 2013 : Summary for policymakers, Technical report.
- ISO-12571 (2000), ‘Hygrothermal performance of building materials and products-determination of hygroscopic sorption properties’.
- ISO-12572 (2001), ‘Determination of water vapour transmission properties’.
- ISO-24353 (2008), ‘Hygrothermal performance of building materials and products-determination of moisture adsorption/desorption properties in response to humidity variation’.
- Janssen, H. and Roels, S. (2009), ‘Qualitative and quantitative assessment of interior moisture buffering by enclosures’, *Energy and Buildings* **41**, pp.382–394.
- JIS-A1470 (2002), ‘Test method of adsorption/desorption efficiency for building materials to regulate an indoor humidity-part 1: Response method of humidity.’.
- Jones, A. (1998), ‘Asthma and domestic air quality’, *Social Science and Medicine* **47**, pp.755–764.
- Künzel, H. M. (1995), *Simultaneous heat and moisture transport in building components*, IRB-Verlag.
- Kunzel, H. (1965), ‘Die feuchtigkeitsabsorption von innenoberflächen und inneneinrichtungen’, **42**, pp.102–116.
- Likos, W. and Lu, N. (2002), ‘Water vapor sorption behavior of smectite-kaolinite mixtures’, *Clays and Clay Minerals* **50**, pp.553.
- Liuzzi, S., Hall, M., Stefanizzi, P. and Casey, S. (2012), ‘Hygrothermal behaviour and relative humidity buffering of unfired and hydrated lime-stabilised clay composites in a mediterranean climate’, *Building and Environment* **61**, pp.82–92.

- Lustig-Rössler, U. (1992), Untersuchungen zum feuchterverhalten von Lehm als Baustoff, PhD thesis, Inaugural dissertation, Gesamthochschule Universität Kassel, Kassel.
- Mahdavi, A. and Kumar, S. (1996), ‘Implications of indoor climate control for comfort, energy and environment’, *Energy and Buildings* **24**, pp.167–177.
- Maskell, D., Heath, A. and Walker, P. (2014), ‘Geopolymer stabilisation of unfired earth masonry units’, *Key Engineering Materials* **600**, pp.175–185.
- Mcgregor, F., Heath, A., Ayre, G., Fodde, E. and Walker, P. (2012), The effect of stabilisation on humidity buffering of earth walls, in ‘Proceedings of LEHM 2012: 6th International Conference on Building with Earth’, Dachverband Lehm e.V, Weimar, Germany.
- McGregor, F., Heath, A., Fodde, E. and Shea, A. (2014), ‘Conditions affecting the moisture buffering measurement performed on compressed earth blocks’, *Building and Environment* **75**, pp.11–18.
- Meunier, A. (2005), *Clays*, Springer, Berlin.
- Minke, G. (2012), *Building With Earth: Design and Technology of a Sustainable Architecture*, Birkhäuser Architecture, Basel, Switzerland.
- Mitchell, J. and El Jack, S. (1966), The fabric of soil cement and its formation, fourteenth national conference on clays and clay minerals, in ‘Fourteenth National Conference on Clays and Clay minerals’.
- Morony, J. J. (2005), Adobe and latent heat: A critical connection, in ‘Inproceedings of the Second Annual Conference, Adobe Association of the Southwest, Northern New Mexico Community College, El Rito, New Mexico.’.
- Mortensen, L. H., Peuhkuri, R. and Rode, C. (2005), Full scale tests of moisture buffer capacity of wall materials, in ‘7 th Nordic Symposium on Building Physics, Reykjavík’, pp. 662–669.
- Morton, T., Stevenson, F., Taylor, B. and Smith, N. (2005), ‘Low cost earth brick construction’, *Arc Chartered Architects, Fife* .
- Novikov, V. (2003), *Concise Dictionary of Materials Science*, CRC Press, USA.

- Padfield, T. (1998), The role of absorbent building materials in moderating changes of relative humidity, PhD thesis, The Technical University of Denmark.
- Peuhkuri, R. (2003), Moisture Dynamics in Building Envelopes, PhD thesis, Denmark Technical University.
- P'KLA, A. (2002), Caractérisation en compression simple des blocs de terre comprimée (BTEC): Application aux maçonnerie, PhD thesis, Ecole Nationale des Travaux Publics de l'Etat (ENTPE), Lyon.
- Redlich, C., Sparer, J. and Cullen, M. (1997), 'Sick-building syndrome', *The Lancet* **349**, pp.1013–1016.
- Rode, C., Holm, A. and Padfield, T. (2004), 'A review of humidity buffering in the interior spaces', *Journal of building physics* **27**, pp.221–226.
- Rode, C., Peuhkuri, R., Mortensen, L., Hansen, K., Time, B., Gustavsen, A., Ojanen, T., Ahonen, J., Svennberg, K. and Arfvidsson, J. (2005), Moisture buffering of building materials, Technical report, Technical University of Denmark (DTU).
- Roels, S., Carmeliet, J., Hens, H., Adan, O., Brocken, H., Cerny, R., Pavlik, Z., Hall, C., Kumaran, K. and Pel, L. (2004), 'Interlaboratory comparison of hygric properties of porous building materials', *Journal of thermal envelope and building science* **27**, pp.307–325.
- Roels, S. and Janssen, H. (2006), 'A comparison of the nordtest and japanese test methods for the moisture buffering performance of building materials', *Journal of building physics* **30**, pp.137–161.
- Rouquérol, F., Rouquerol, J. and Sing, K. (1999), *Adsorption by Powders and Porous Solids: Principles, Methodology and Applications*, Academic Press.
- Ruiz-Hitzky, E. and Van Meerbeek, A. (2006), 'Polymer-clay nanocomposite. in bergaya f, theng bkg, lagaly g, eds. handbook of clay science. chapitre 10.3', *Developments of Clay Science 1* **1**, pp.583–621.

- Ruiz, J., Bilbao, R. and Murillo, M. (1998), 'Adsorption of different voc onto soil minerals from gas phase: Influence of mineral, type of voc, and air humidity', *Environmental science and technology* **32**, pp.1079–1084.
- Salonvaara, M., Ojanen, T., Holm, A., Künzel, H. M. and Karagiozis, A. N. (2004), Moisture buffering effects on indoor air quality-experimental and simulation results, in 'Proceedings of Buildings IX, Clearwater, Florida'.
- Schroeder, H. (2010), *Lehmbau*, Wiesbaden:Vieweg+Teubner.
- Seed, H. B. and Chan, C. K. (1959), 'Structure and strength characteristics of compacted clays', *Journal of the Soil Mechanics and Foundations Division, ASCE* **85**, pp.87–128.
- Sing, K. S. W. (1985), 'Reporting physisorption data for gas/solid systems with special reference to the determination of surface area and porosity (recommendations 1984)', *Pure and Applied Chemistry* **Vol. 57**(Issue 4), pp. 603–619.
- Sundell, J. (2004), 'On the history of indoor air quality and health', *Indoor Air* **14**, pp.51–58.
- Svennberg, K. (2006), Moisture buffering in the indoor environment, PhD thesis, Lund University.
- Svennberg, K., Lengsfeld, K., Harderup, L. and Holm, A. (2007), 'Previous experimental studies and field measurements on moisture buffering by indoor surface materials', *Journal of building physics* **30**, pp.261–274.
- Theng, B. (1979), *Formation and properties of clay-polymer complexes*, Vol. 9, Elsevier.
- Trechsel, H. (1994), *Moisture Control in Buildings*, ASTM.
- Venkatarama Reddy, B. (2012), Status of clay minerals in stabilised soil blocks, in 'LEHM 2012 - 6th International Conference on Building with Earth', Weimar.
- Vereecken, E., Roels, S. and Janssen, H. (2011), 'In situ determination of the moisture buffer potential of room enclosures', *Journal of building physics* **34**, pp.223.

- Walker, P. (2005), *Rammed earth: design and construction guidelines*, BRE Bookshop.
- Watson, L. and McCabe, K. (2011), 'The cob building technique. past, present and future', *Informes de la construccion* **63**(523), pp.59–70.
- Worch, A. (2004), 'The behaviour of vapour transfer on building material surfaces: the vapour transfer resistance', *Journal of Thermal Envelope and Building Science* **28**, pp.187–200.

Appendix

Group I

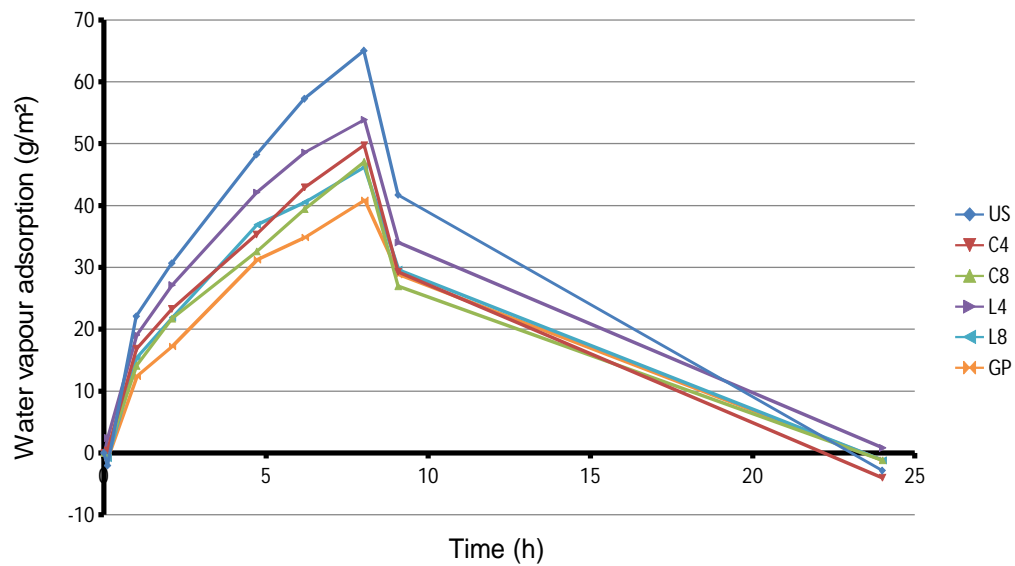


Figure .1: Moisture buffering test under 53/75 % RH cycle, group I

Sample name	Average density (kg/m ³)	Stabiliser	μ Factor	MBV practical 50/85 cycle (g/m ² ·%RH)	MBV practical 53/75 cycle (g/m ² ·%RH)	Predicted 33/75 MBV from 50/85 cycle (g/m ² ·%RH)
US	1766	-	5.70	3.41	2.96	2.53
C4	1721	4% cement	6.77	2.88	2.26	2.14
C8	1752	8% cement	7.37	2.52	2.14	1.87
L4	1734	4% lime	6.03	2.82	2.45	2.10
L8	1735	8% lime	6.67	2.49	2.10	1.85
Gp	1704	3% NaOH	7.40	2.15	1.86	1.60

Table .1: Group I experimental results

Group II and III

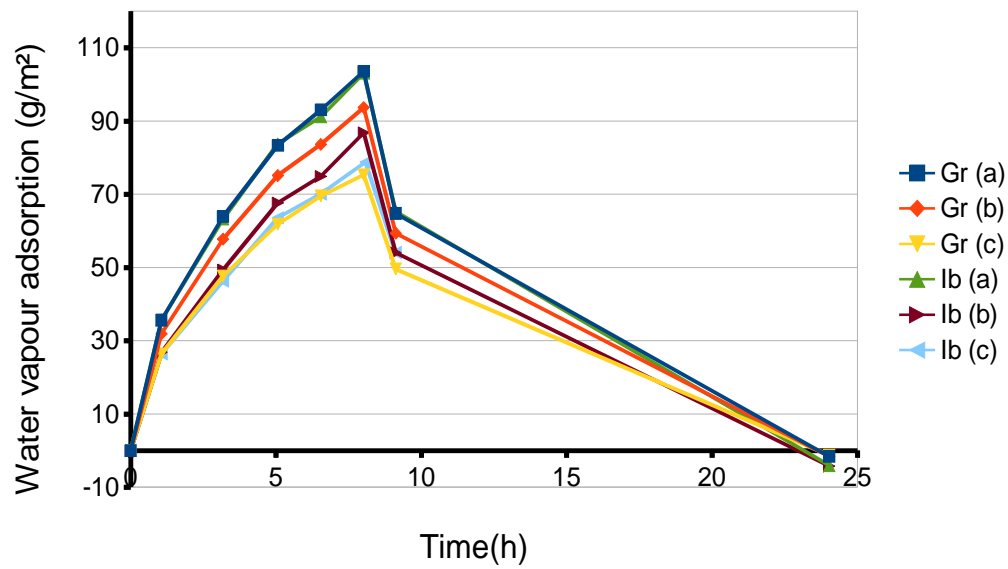


Figure .2: Moisture buffering test 33/75% RH, group II and III

Sample name	Average density (kg/m ³)	Initial water content (% per dry weight)	μ Factor	MBV practical (g/m ² .%RH)
Gr _a	1856	9	6.35	2.47
Gr _b	1794	9.3	6.64	2.23
Gr _c	2033	16.6	8.88	1.79
Ib _a	1882	11.2	6.49	2.45
Ib _b	1999	12.93	8.0	2.07
Ib _c	1999	21.06	8.66	1.87

Table .2: Group II and III experimental results

Group IV

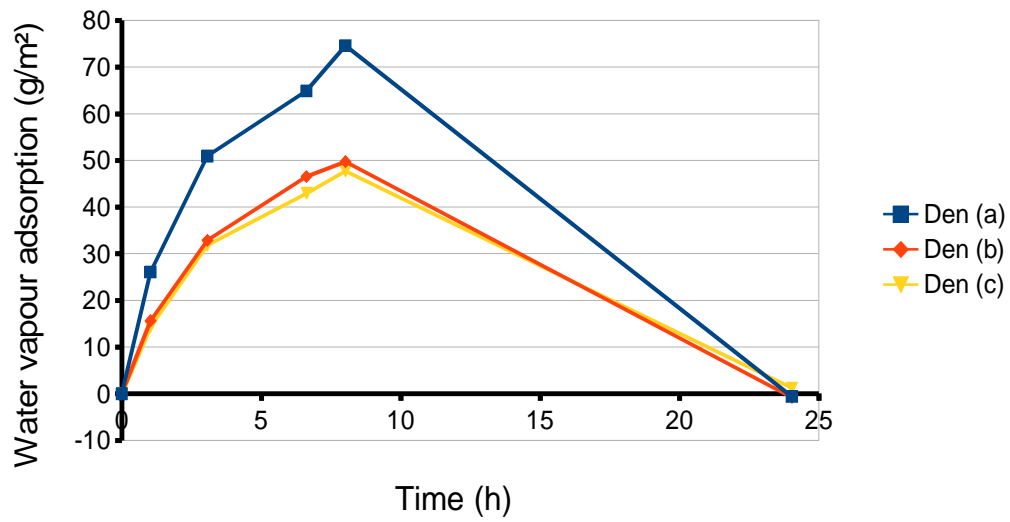


Figure .3: Moisture buffering test 33/75% RH, group IV

Sample name	Average density (kg/m ³)	μ Factor	MBV practical (g/m ² %RH)
Den _a	1622	6.80	1.78
Den _b	1996	11.20	1.18
Den _c	2033	12.56	1.14

Table .3: Group IV experimental results

Group V

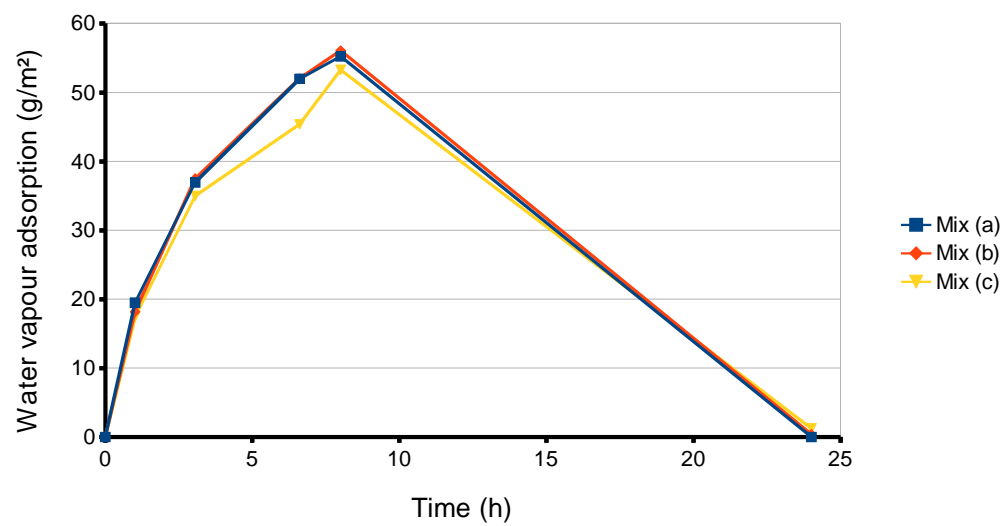


Figure .4: Moisture buffering test 33/75% RH, group V

Sample name	Average density (kg/m ³)	Mixing method	μ Factor	MBV practical (g/m ² . %RH)
Mix _a	1897	Hand	10.16	1.31
Mix _b	1861	Small mortar mixer	10	1.33
Mix _c	1931	Large mortar mixer	11.20	1.27

Table .4: Group V experimental results

Group VI

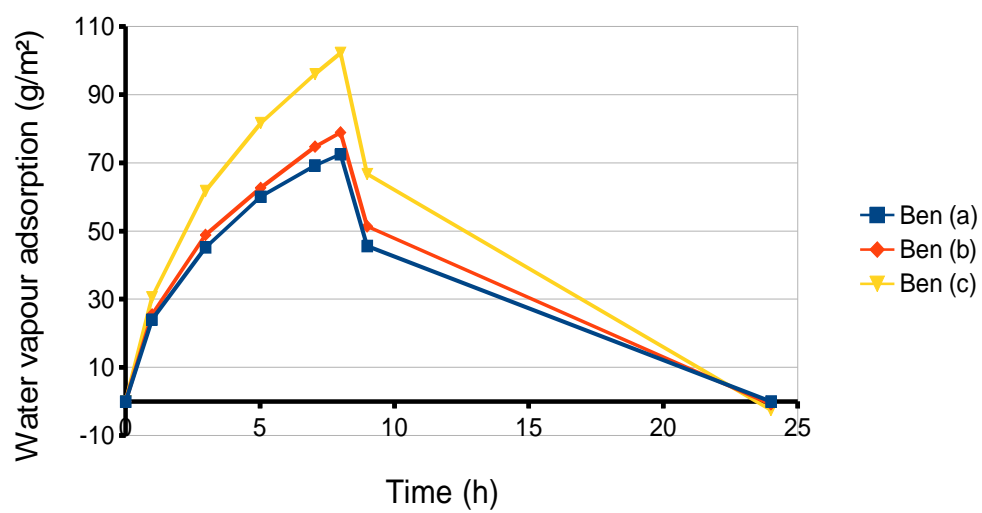


Figure .5: Moisture buffering test 33/75% RH, group VI

Sample name	Average density (kg/m ³)	Bentonite or Pillared Bentonite added	μ Factor	MBV practical (g/m ² .%RH)
Ben _a	1882	1% Bentonite	8.81	1.65
Ben _b	1901	5% Bentonite	9.42	1.78
Ben _c	1818	10% Bentonite	8.05	2.29
PiBen _a	1824	1% Pillared Bentonite	7.40	1.80
PiBen _b	1848	5% Pillared Bentonite	8.08	2.05
PiBen _c	1999	10% Pillared Bentonite	8.66	2.21

Table .5: Group VI experimental results

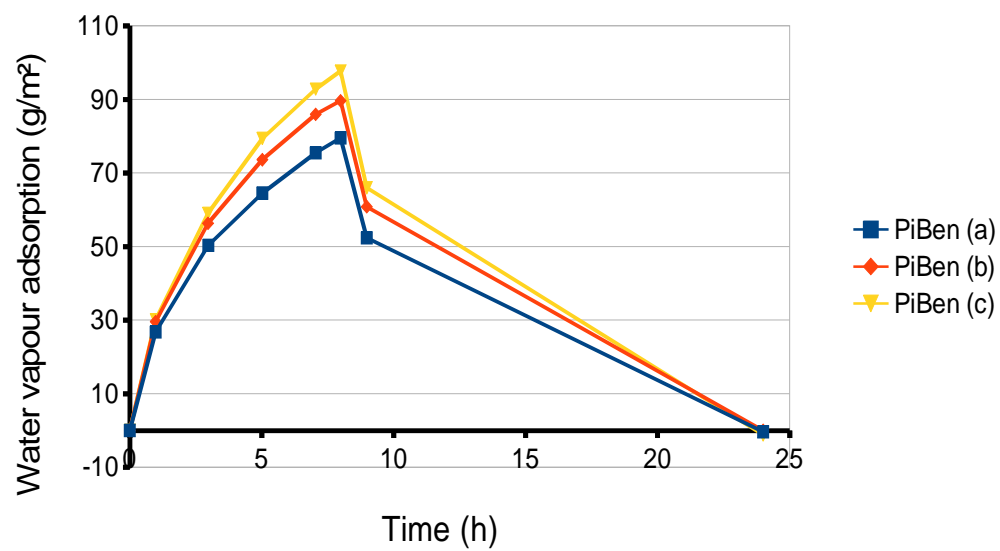


Figure .6: Moisture buffering test 33/75% RH, group VI

Group VII

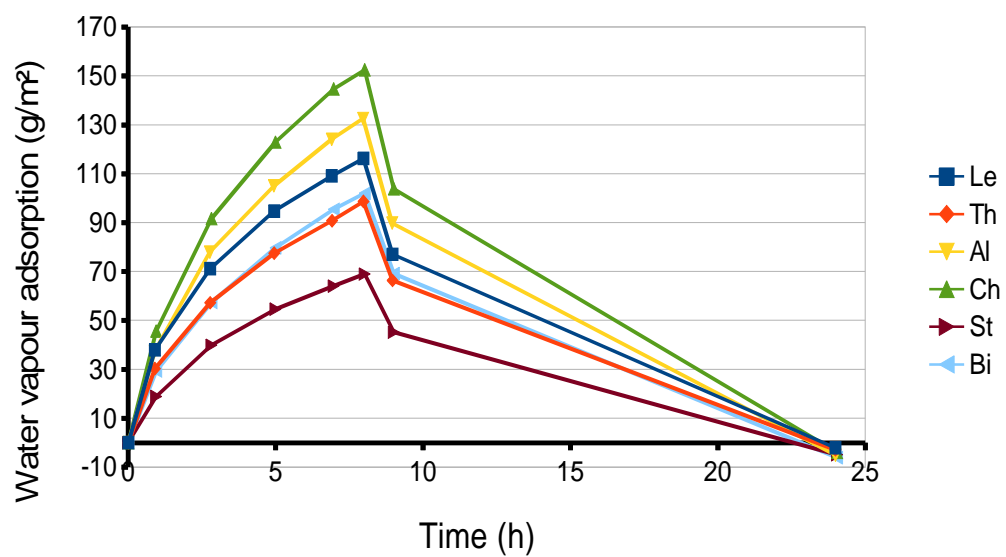


Figure .7: Moisture buffering test 33/75% RH, group VII

Sample name	Average density (kg/m ³)	Clay and silt content (% per dry mass)	μ Factor	MBV practical (g/m ₂ .%RH)
Le	1878	81.49	6.43	2.77
Th	1826	30.60	7.36	2.35
Al	1863	75.38	4.59	3.16
Ch	1937	95.90	5.35	3.63
St	1712	26.30	7.19	1.64
Bi	1961	89.58	7.18	2.43

Table .6: Group VII experimental results

Group VIII

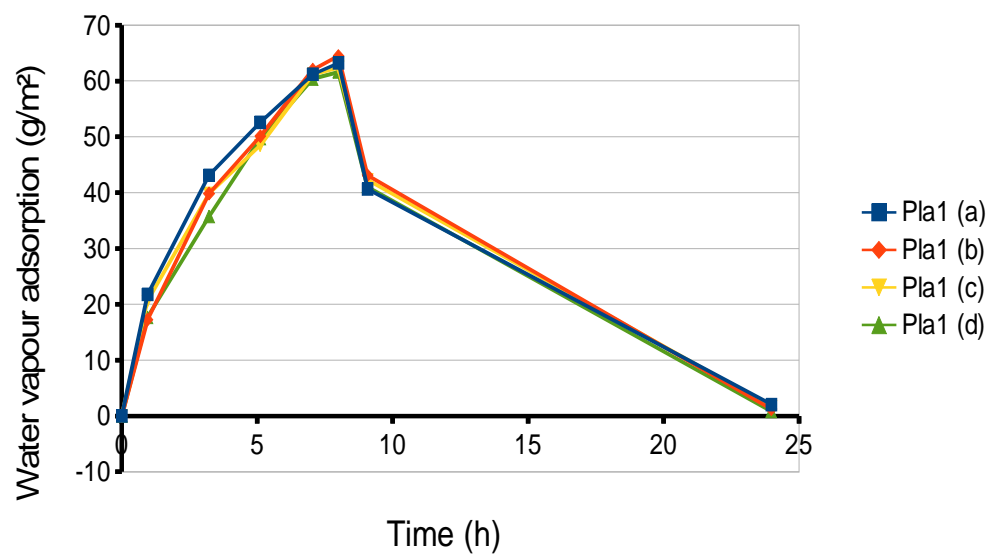


Figure .8: Moisture buffering test 33/75% RH, group VIII

Sample name	Sample numbers	Average density (kg/m ³)	Plaster type and thickness	μ Factor	MBV practical (g/m ² .%RH)
Pla1 _a	1-3	1677	12 mm undercoat	12.86	1.50
Pla1 _b	4-6	1715	12 mm undercoat + 3 mm finish coat	11.66	1.47
Pla1 _c	7-9	1694	20 mm undercoat	10.95	1.50
Pla1 _d	10-12	1724	20 mm undercoat +3 mm finish coat	9.59	1.47

Table .7: Group VIII experimental results

Group IX

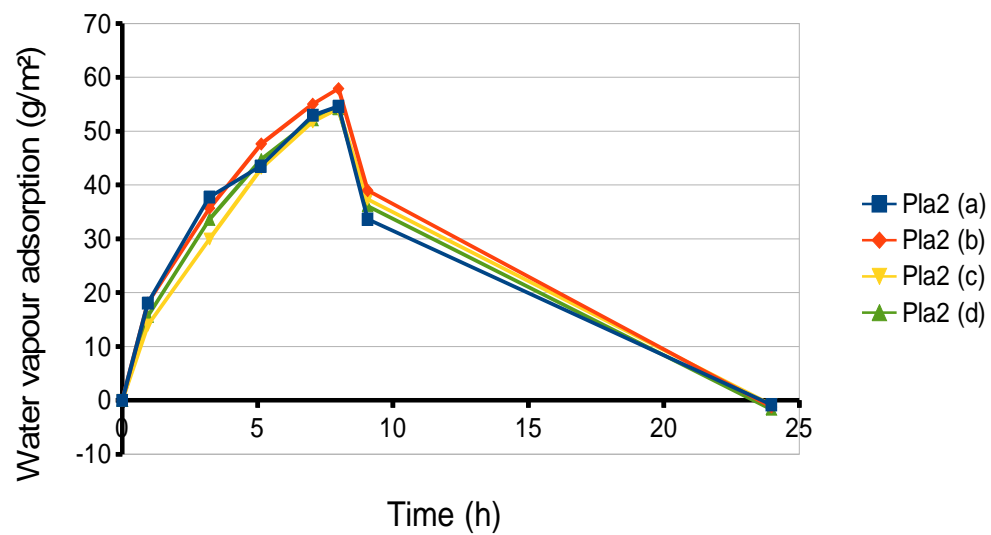


Figure .9: Moisture buffering test 33/75% RH, group IX

Sample name	Sample numbers	Average density (kg/m ³)	Plaster type and thickness	μ Factor	MBV practical (g/m ² .%RH)
Pla2 _a	1-3	1725	12 mm undercoat	13.40	1.27
Pla2 _b	4-6	1669	12 mm undercoat + 3 mm finish coat	11.14	1.25
Pla2 _c	7-9	1723	20 mm undercoat	10.53	1.36
Pla2 _d	10-12	1700	20 mm undercoat +3 mm finish coat	9.38	1.26

Table .8: Group IX experimental results

Articles Published